Factors influencing HSV-1 CD8$^+$ T cell populations and their function during ganglionic latency

by

Benjamin R. Treat

B.S. Biochemistry and Molecular Biology, Penn State University, 2008

Submitted to the Graduate Faculty of the

School of Medicine in partial fulfillment

of the requirements for the degree of

Doctor of Philosophy

University of Pittsburgh

2018

UNIVERSITY OF PITTSBURGH

SCHOOL OF MEDICINE

This dissertation was presented

by

Benjamin R. Treat

It was defended on

March 5, 2018

and approved by

Robert L. Hendricks, Ph.D.
Professor, Department of Ophthalmology

Fred L. Homa, Ph.D.
Associate Professor, Department of Microbiology and Molecular Genetics

Lawrence P. Kane, Ph.D.
Professor, Department of Immunology

John V. Williams, M.D.
Professor, Department of Pediatrics

Dissertation Advisor

Paul (Kip) R. Kinchington, Ph.D.
Professor, Department of Ophthalmology

Factors influencing HSV-1 CD8$^+$ T cell populations and their function during ganglionic latency

Benjamin R. Treat, Ph.D.

University of Pittsburgh, 2018

Herpes simplex virus type 1 (HSV-1) latency in sensory ganglia such as trigeminal ganglia (TG) is associated with a persistent immune infiltrate that includes effector memory CD8$^+$ T cells that can influence HSV-1 reactivation. In C57BL/6 mice, HSV-1 induces a highly skewed CD8$^+$ T cell repertoire, in which half of CD8$^+$ T cells (gB-CD8s) recognize a single epitope on glycoprotein B ($gB_{498\text{-}505}$), while the remainder (non-gB-CD8s) recognize, in varying proportions, 19 subdominant epitopes on 12 viral proteins. The gB-CD8s remain functional in TG throughout latency, while non-gB-CD8s exhibit varying degrees of functional compromise. To understand how dominance hierarchies relate to CD8$^+$ T cell function during latency, we characterized the TG-associated CD8$^+$ T cells following corneal infection with a recombinant HSV-1 lacking the immunodominant $gB_{498\text{-}505}$ epitope (S1L). Instead, there was a general increase of non-gB-CD8s with specific subdominant epitopes arising to codominance. In a latent S1L infection, non-gB-CD8s in the TG showed a hierarchy targeting different epitopes at latency compared to acute times, and these cells retained an increased functionality at latency. These data indicate that loss of the immunodominant $gB_{498\text{-}505}$ epitope alters the dominance hierarchy and reduces functional compromise of CD8$^+$ T cells specific for subdominant HSV-1 epitopes during viral latency. To address how expression from the viral genome influences this CD8$^+$ T hierarchy, we developed recombinant in the S1L background that expressed ectopic $gB_{498\text{-}505}$ copies under the influence of several candidate promoters with different expression kinetics. Ectopic epitope expression from the early or strong promoters restored full gB-CD8

immunodominance. However, epitope expression from candidate viral true late gene promoters resulted in delayed or severely reduced priming efficiency of gB-CD8s, with indications of low levels of late epitope expression in the TG sufficient to retain primed gB-CD8s. Epitope expression from latently active promoters could efficiently attract and expand gB-CD8s in the TG. These data indicate that viral antigen expression during latency will influence the $CD8^+$ T cell hierarchy that is monitoring a latently infected TG.

TABLE OF CONTENTS

LIST OF TABLES

LIST OF FIGURES

1.0 INTRODUCTION

The word ‘herpes’ has been used in medicine for at least 2,600 years, dating back to early descriptions of skin diseases that likely included Herpes Simplex Virus (HSV) lesions, Herpes Zoster rashes, and other similar skin maladies[1]. As one might expect from a virus with such ancient recognition, Herpesviridae is a ubiquitous and wide-ranging virus family. This family also contains a myriad of mollusk, bird, reptile, and mammal hosts throughout the world. In fact, when investigated closely, most animal species harbor at least one herpesvirus, with nearly 200 identified Herpesviridae family members to date, with a large majority unlooked for, and likely undiscovered thus far[2, 3]. In general, most herpesviruses are highly adapted to one or few host species, and severe symptoms often only occur in the very young or immunocompromised. Given the long coevolution of herpesviruses with life on this planet, it is perhaps unsurprising that they have evolved a vast array of complex and varied mechanisms to survive, hide, and spread within their host populations.

1.1 HUMAN HERPESVIRUSES

There are nine currently identified human herpesviruses, that are classified into the subfamilies of alpha-, beta-, or gammaherpesvirinae[2, 4]. These viruses all share similar structural elements and the ability to establish latent infections in humans. Latency within the

broad context of human herpesviruses can be defined as an extended period in which no infectious viral particles are made, yet viral DNA is retained within the host, and the possibility of reactivating to produce infectious virus is retained. Alphaherpesvirus members include Herpes simplex virus type 1 (HSV-1) and 2 (HSV-2), and Varicella-zoster virus (VZV), and typically have a rapid primary lytic cycle that quickly establishes latency within sensory neurons. Betaherpesvirus members include Cytomegalovirus (CMV) and Roseolovirus (including HHV-6A, HHV-6B, and HHV-7) which commonly replicate at a slower rate and establish latency within monocyte-lineage cells. CMV is one of the leading causes of congenital birth defects[5]. Gammaherpesviruses latently infect immune cells such as lymphocytes and include Epstein-Barr virus (EBV) and Kaposi's Sarcoma associated herpesvirus (KSHV). Both EBV and KSHV are also of note due to their oncogenic potential, with EBV linked to lymphomas and nasopharyngeal carcinomas, and KSHV causing Kaposi's sarcoma, a cancer commonly occurring in AIDS patients[6].

1.2 HSV-1 EPIDEMIOLOGYAND DISEASE

Many humans encounter HSV early in life, with asymptomatic primary disease affecting one or more mucosal regions that lead to latent infections within innervating sensory and sympathetic ganglia [7, 8]. Infection rates vary greatly by geographic region, however by the age of 15, more than 40% of humans are seropositive for HSV-1, and by the age of 40, over 80% of people have encountered HSV-1 [9-11]; Seroprevalance is as high as 98% in some regions, and in general this virus is extremely ubiquitous within the adult population worldwide[11]. Most seropositive individuals never experience any outward pathologies associated with reactivation

events, although asymptomatic shedding of infectious virus may be frequent[12]. Additionally, a fraction of those infected will reactivate with symptoms ranging from minor, such as (herpes labialis) cold sores, to major, such as herpetic whitlow, to life-threatening, such as herpes simplex encephalitis (HSE) [10]. Though HSE is rare (about four cases per million people per year), it is a leading cause of fatal viral encephalitis in neonates[13]. Another major consequence of HSV-1 reactivation is Herpes Stromal Keratitis (HSK), a consequence of repeated HSV reactivation events that cause a scarring and progressive loss of clarity of the cornea. HSK is a leading cause of infectious blindness in adults in western societies, with corneal transplants being the only current treatment for restoring vision to opaque corneas[14, 15].

1.3 HSV-1 STRUCTURE AND GENOME ORGANIZATION

Characteristic to all herpesviruses are four highly conserved components of the viral particle. These include 1) The DNA core contains the dsDNA viral genome, which in HSV-1 is about 152,000 base pairs in size and encodes over 80 viral genes; 2) The viral capsid, which consists of an icosahedron composed of at least eight virally-encoded proteins; 3) a tegument layer, which is amorphous and contains at least 23 viral proteins, an unknown number of host proteins, and is instrumental in assembly, egress, and making newly infected host cells permissive to viral infection, with functions including capsid transport, immune evasion, and transcriptional regulation; and 4) the envelope, a lipoprotein layer studded with at least 13 viral glycoproteins vital for binding and entry, which also likely contains several host proteins[16].

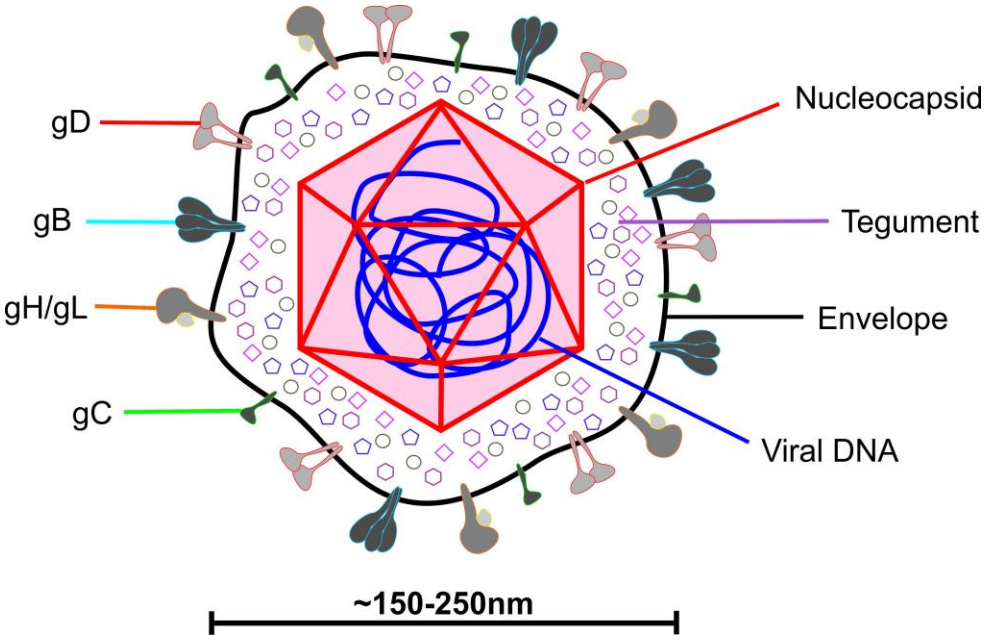

Figure 1. HSV-1 virion structure

HSV-1 consists of an amorphous enveloped particle that is approximately 150-250nm in size, and which contains a proteinaceous tegument composed of mostly viral and some host proteins. Of note, included within the tegument is the viral protein VP16, which transactivates viral immediate early (α) gene expression. The tetrahedral nucleocapsid (which consists of 162 capsomers) contains a single copy of viral DNA consisting of about 152kb. Studded on the outside of the envelope are the viral proteins used for viral attachment and entry: notably, glycoproteins gB, gC, gD, and the complex gH/gL. Image created in CorelDRAW x7.

The HSV-1 genome is encoded in linear dsDNA which circularizes to form an episome upon entry into the nucleus, by use of the homologous short "a" sequences located at either end of the genome[17, 18]. Other notable features of the HSV genome include two repeat regions within the genome— with the ~9kbp long repeat being especially important and containing several immediate early genes and the LAT locus, and the 6.6kb short repeat region containing ICP4, the major viral transactivator[19]. There are also two unique coding regions—the 108kb unique long region (UL), which encodes many important glycoproteins, structural and tegument proteins, and proteins involved in viral DNA replication, and the 13kb unique short region (US), which encodes an important viral kinase and glycoproteins[19].

1.4 HSV-1 LIFE CYCLE

1.4.1 Viral entry

HSV-1 binds to cellular surfaces via interactions between viral glycoproteins and cellular surface receptors. The first interactions are generally with glycoprotein B and C (gB and gC) interacting with heparan sulfate chains, which are a class of glycosaminoglycan found on the surface of the vast majority of mammalian cells[20-22]. Though these initial binding interactions are very advantageous to the virus in the wild, in some experimental models, these heparan sulfate interactions can be dispensable for viral replication. Indeed, gC binding to heparin sulfate has been shown to be vital for infecting apical surfaces in intact skin or ocular surfaces, but is completely dispensable in models where the initial infected region has a disrupted epithelial layer which exposes the basal layer[23, 24].

After initial interactions mediating a close association between the viral particle and the target cell, secondary specific interactions are engaged. Viral glycoprotein D (gD), along with gB, bind to one of at least three major identified cellular surface receptors, depending on the cell type and context of infection. Herpesvirus entry mediator (HVEM), nectin-1 and nectin-2, as well as specific sites within heparan sulfate (characterized by 3-O-sulfated residues) are the identified receptors that HSV-1 uses to gain entry within cells[25]. The actual fusion event is mediated by a protein complex consisting of gB, along with a heterodimer formed by gH-gL. The current model is that tight gD anchoring to specific cellular receptors promote a conformational change within the gB/gH-gL complex, after which this complex undergoes a radical conformational change and pierces the target cell membrane, initiating the viral envelope/cellular membrane fusion process[26, 27]. These entry and membrane fusion events

occur at either the cellular surface, or within endosomal compartments, again depending on the cell type and context of infection[28, 29].

HSV-1 also has a wide variety of putative minor binding and entry receptors that are not discussed here. HSV-1 has been identified as capable of infecting most human cell types *in vitro*, and the ability to bind and enter many animal cell types leads to the broad host range mentioned previously[30]. This broad range of receptors and entry methods in part explains HSV-1's ability to infect many disparate hosts, and is one reason that this virus is ideally suited for use in animal models.

1.4.2 Lytic infection cycle and gene expression

After viral envelope fusion and entry within the cell, the capsid containing the viral genome is transported to the nucleus via microtubules and viral tegument protein interactions with host dynein[31, 32]. Once docked at the nuclear pore complex, the viral DNA enters the nucleus through the pore. The viral tegument contains VP16 (UL48), which enters the nucleus along with host cell factor (HCF) and, once in the nucleus interacts with another host protein, Oct-1, to form a complex that initiates transcription of the viral immediate early (α) genes[33-36]. At this time, the tegument has also delivered other viral products that acclimate the cellular environment for viral replication. Among these are the virion host shutoff (VHS, UL41), which contains RNase activity and is responsible for degrading host messenger RNA to counteract viral innate immune defenses[37, 38]. Also contained within the tegument are the viral serine/threonine kinases encoded by US3 and UL13, which are highly active and promiscuous

viral kinases that regulate a large range of host cellular functions that include regulation of pro/anti-apoptotic proteins and inhibition of type-1 interferon responses[41-43].

Initiation of viral transcription by the VP16 complex results in the production of viral immediate early (α) genes – including ICP0, ICP4, ICP22, ICP27, and ICP47[19]. The first four of these genes are involved in promoting and regulating the transcription and expression of the next wave of genes, the early (β) genes. In particular, ICP0 is an E3 ubiquitin ligase that promotes the degradation of many cellular targets, including promyelocytic leukemia (PML) and SP100 [44, 45]. ICP0 also can transactivate cellular genes promiscuously in part by binding CoREST and dissociating histone deacetylases (HDACs)[46]. ICP4 is the major viral transcription factor required for virtually all viral β and late (γ) gene transcription[19, 47, 48]. ICP47 has a different role – this viral gene encodes a protein that selectively binds to and inhibits human TAP1/TAP2 and blocks the transport of viral peptides into the endoplasmic reticulum where they would be subsequently presented at the cell surface by MHC-I[49, 50]. This has the net effect of hiding presented viral peptides from $CD8^+$ T cell detection.

The β gene products coordinate to replicate viral DNA and alter the cellular environment further to promote γ gene expression[19]. γ genes are divided into two categories, γ1 genes are referred to as "leaky late" genes, and the transcription of these genes are begun concordantly with β gene products, but only at low levels. After the onset of viral DNA replication, these genes are transcribed and make proteins at much higher levels. γ2 genes, or "true late" genes, are only made in any measurable quantity after viral DNA replication has already begun, at a very late stage of viral replication[19, 51, 52]. Taken as a group, the γ genes are the largest group of viral proteins, and encode many tegument, glycoprotein, and capsid proteins that make up the bulk of the structural proteins in the viral particle.

In cell culture models of HSV infections, such as in Vero cells (an African green-monkey kidney cell line), we can measure the differences in these kinetic classes of genes experimentally by inhibiting viral transcription, translation, or DNA replication at key points and measuring subsequent viral RNA or protein expression. We also can determine that in general, α gene expression peaks at 2-4 hours post infection (hpi), β gene expression peaks around 4-8 hpi, and γ genes vary more widely, with peak expression times at 8-12 hpi (depending on multiplicity of infection).

Peak expression of viral late gene products correlates with the completion viral DNA replication and subsequent packaging into completed viral capsids within infected cell nuclei. The now completed capsids containing viral DNA pass through the perinuclear space, where they briefly are enveloped by the inner nuclear membrane, before de-envelopment upon fusion with the outer nuclear membrane and trafficking into the cytoplasm[19, 53]. Here, the viral capsids undergo secondary envelopment (with lipid membranes containing viral glycoproteins) and are transported to the cellular surface via exocytotic vesicles, and the infectious particles are subsequently released[53]. In general, cellular permissiveness for lytic viral infection results in the host cellular lysis and death.

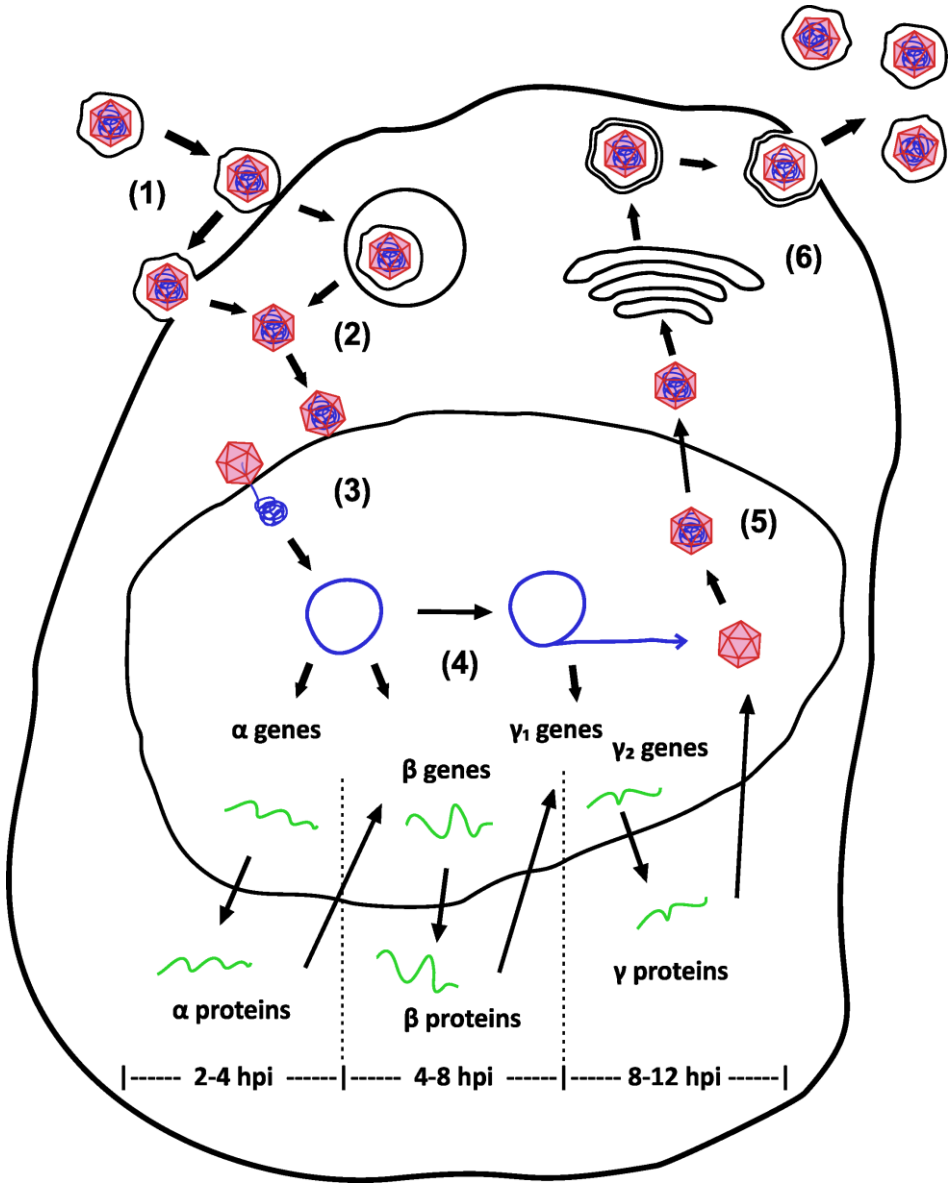

Figure 2. HSV-1 lytic replication and gene expression

(1) Initial attachment and entry mediated by viral glycoproteins, including gB, gD, and gH/gL. (2) Viral envelope fusion can occur at either the surface, or by endosomal escape within the cytosol. In both scenarios the viral capsid and tegument proteins are released into the host cytoplasm. (3) The viral nucleocapsid traffics inwards via microtubules, docks at the nuclear pore complex and viral DNA is released into the nucleus, whereupon it circularizes. (4) The tegument protein VP16 traffics into the nucleus with host transcription factors and turns on α gene expression, including the major viral transcription factor ICP4. Peak α gene expression occurs 2-4 hpi. ICP4-mediated expression of β genes peaks by 4-8 hours post infection, with low levels of γ1 genes also turned on at this time. After viral DNA replication commences, γ1 genes are maximally expressed and γ2 genes begin expressing, with these late genes peaking around 8-12 hpi. (5) Viral DNA is packaged into capsids within the nucleus. Egress from the nucleus involves a temporary envelopment as the capsid traverses the nuclear membrane. (6) In the Golgi the virus obtains its tegument and becomes doubly enveloped. Fusion of the outer envelope at the cellular membrane releases an enveloped and fully infectious virion from the cell, ready to begin the infectious cycle again. Image created in CorelDRAW x7.

1.4.3 Latency

The previous section described the lytic cycle of HSV-1, which is generally carried out at the surface cells of the host, and mainly includes mucosal epithelial cells and the surrounding tissues. Sensory neurons innervate these primary infection sites in large numbers to provide fine sensation to the host's lips, eyes, and other mucosal areas. During the primary infection, the virus ultimately gains access to the axonal termini of these neurons, and is carried along microtubules to the nucleus, where a "decision" of sorts is made. Once the viral DNA is within the nucleus of sensory neurons, either a) the nuclear environment will be permissive to viral transcription mediated by VP16-initiation of α genes, and lytic viral replication will commence or b) the viral DNA in the nucleus is not accompanied by a functional VP16 complex (which may not have transported down the axon with the viral capsid) and becomes packaged into heterochromatin, with silencing of most viral transcription[54, 55]. This latter outcome is defined as viral latency. As the course of acute viral infection at the surface is controlled by a combination of innate and adaptive immune responses, most viral genomes in the sensory ganglia have entered a latent state. Accompanying viral latency is transcription of one large region on the viral DNA, referred to as the latency associated transcript (LAT), which is surrounded by chromatin insulating elements and ultimately results in large detectable amounts of a stable intron. This RNA encodes no protein, yet many putative functions have been ascribed to it, including protection of neurons from apoptotic cell death, regulation of heterochromatin and latency, and silencing viral genes to promote the latent state [56-60]. LAT accumulates in many latently infected sensory neurons both in humans and in animal models of latency.

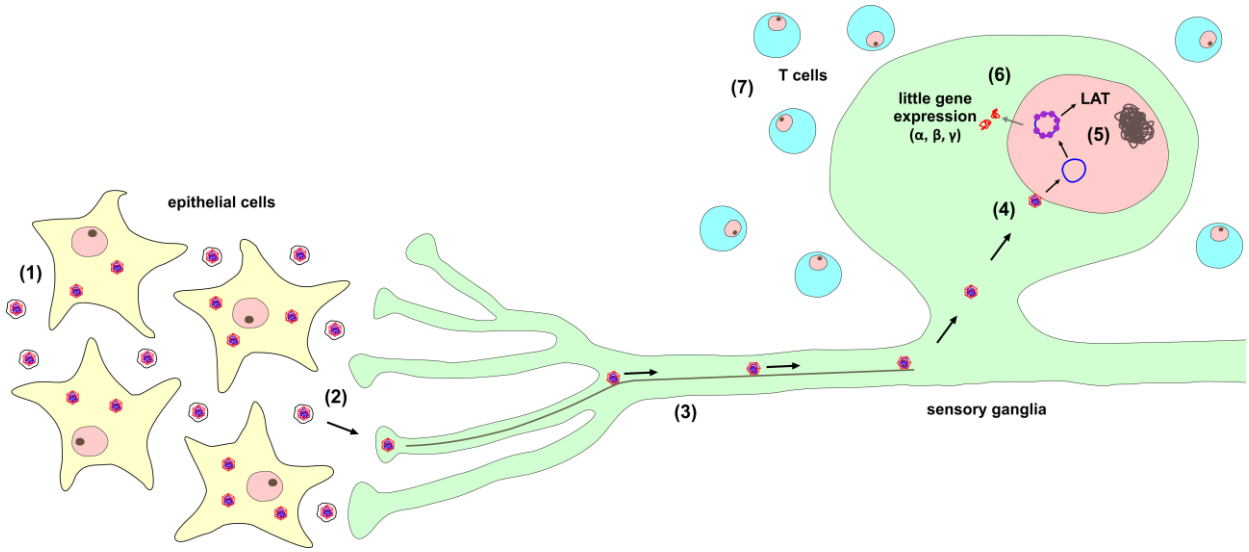

Figure 3. HSV-1 latency

(1) HSV-1 infects mucosal epithelial cells and undergoes lytic viral replication and spread. (2) The virus gains access to the axonal termini from sensory neurons, whereupon the virus binds, and releases a capsid into the axon. Of note, most viral tegument proteins become separated from the capsid at this point, including VP16, the viral α gene transactivator. (3) The viral capsid traffics in a retrograde fashion along microtubules via the motor protein dynein, which delivers the capsid to the neuronal cell body. (4) once within the cell body, viral DNA is released into the nucleus. (5) In the absence of tegument proteins to provide an environment conducive to viral gene transcription, the genome quickly becomes packaged within heterochromatin and begins the latent phase of infection. Viral LAT RNAs are the only transcripts abundantly produced during this time. (6) There is an extremely low and sporadic amount of leaky viral gene expression during latency, which is unregulated and includes α, β, and γ viral genes. This gene expression is not easily detectable by traditional methods, and during latency does not result in detectable infectious virus. (7) Accompanying viral latency is an HSV-specific T cell infiltrate into infected ganglia, which are capable of monitoring and possibly preventing potential reactivation events. Image created in CorelDRAW x7.

1.4.4 Reactivation

Latent viral genomes are maintained in this state for the life of the host, except for brief bouts of lytic viral replication cycles defined as ‘reactivation’. The events preceding viral reactivation are multifactorial and complex, but have begun to come to light in recent years. While latency has in the past been defined by the absence of viral protein expression, it has begun to be widely accepted that there is a sporadic “leaking” of viral proteins arising from

latently infected ganglia, which is termed “phase 1” or “animation”[61]. The evidence for this is multifactorial and quite convincing when taken as a whole: 1) several *in vitro* latency models show low levels of uncoordinated RNA transcription preceding true reactivation events[62-65]. 2) Single cell PCR of latently infected dorsal root ganglia (DRG) consistently detects viral transcripts that represent many lytic viral genes[66]. 3) Floxed-reporter mice latently infected with HSV that express CRE from lytic promoters show cumulatively increasing numbers of CRE-switched neurons over long term studies, indicating low levels of ongoing viral promoter activity from lytic promoters throughout latency[67]. 4) Viral-specific $CD8^+$ T cells show consistent signs of recently encountering viral antigen within latently infected ganglia[68]. Taken together, these data suggest a low-level and ongoing amount of phase 1 viral protein detection that is not detectable by traditional methods (i.e. qPCR, western blotting). Furthermore, the transcripts that are detected do not follow the classical α-β-γ gene cascade that is observed in lytic replication cycles[62]. The model that has emerged tells us that this phase 1 expression must reach a certain threshold – enough to make VP16 in amounts capable of transactivating viral α gene expression and begin the lytic cascade. Many factors affect the host transcriptional program and the state of chromatin, and hence the amount of phase 1 viral gene expression. Reduced levels of nerve growth factor, increased stress (brought on by UV-light, physical distress, or other means), reduced immune function, or chemical targeting of histone modifying enzymes all perturb this balance and can result in increased latent gene expression[59, 69, 70]. This can eventually result in “phase 2” of reactivation, where a threshold of viral transactivator expression is reached, and lytic viral replication proceeds[61].

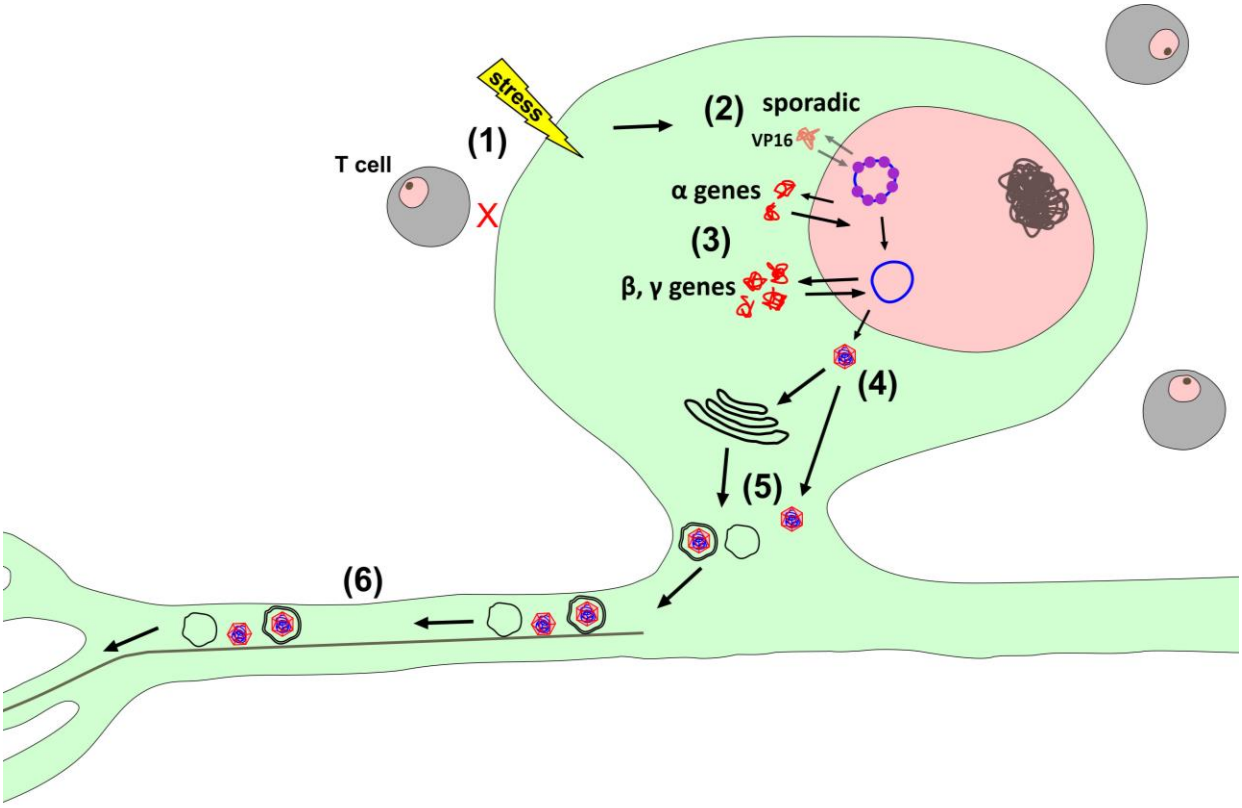

Figure 4. Reactivation from neuronal latency

(1) In the face of waning T cell functionality, and in combination with increased stress or other conditions that result in subsequent chromatin changes, viral lytic gene expression can begin to ramp up during latency. (2) Sporadic phase 1 viral gene expression leads to production of VP16, which once a certain threshold is realized, can activate viral α gene transcription in some cases. (3) The commencement of α protein synthesis begins a cascade, which releases viral genomes from heterochromatin completely, and begins a classical α-β-γ lytic cascade. (4) Lytic viral replication cycle results in production of viral capsids containing DNA. (5) It is controversial whether capsids obtain an envelope within the cell body, or whether the capsid and tegument/envelope traffic separately and form infectious particles at axonal tips. (6) There is evidence that both occur, and regardless of the anterograde transport method, infectious HSV-1 is delivered to the periphery- whereupon it obtains access to mucosal epithelial cells and causes subsequent disease. Image created in CorelDRAW x7.

1.5 MOUSE MODEL OF HSV INFECTION AND LATENCY

The natural hosts for herpes simplex virus are humans, but both HSV-1 and HSV-2 are capable of undergoing lytic replication and establishing latency in many mammalian species under experimental conditions. There are several widely-used experimental animal models of

HSV infection, including the rabbit, which reactivates frequently and is an excellent model for therapies to block viral shedding; the guinea pig, which closely mimics genital HSV-2 infection and disease; and the mouse[71-75]. Mice infected with HSV-1 are ideally suited for studying viral latency and the accompanying immune response. The latent state and immune responses to both primary and latent infections have been widely characterized in this model, and additionally there exist a myriad of immunological tools available for mouse models. In mice, latent infections are established readily, and indeed reactivation in mice is difficult for a number of reasons, which include inefficient binding of VP16 to mouse Oct-1[76]. Reactivation of mouse models is possible by 1) UV-irradiation, 2) physical stress or social discomfort, or 3) histone modifying chemicals[59]. *Ex vivo* reactivation of latently infected ganglia is also possible, which will be discussed later.

Mouse models can reproduce human diseases closely, including the blinding Herpes Stromal Keratitis (HSK) in ocular infection models, skin disease in flank infection models, and encephalitis by various infection models. In the following studies, we employ an ocular HSV infection model of C57BL/6 (B6) mice, which establishes a latent infection within the trigeminal ganglia (TG). The initial corneal infection is controlled primarily by innate immunity, followed by a subsequent adaptive response that is vital for controlling further viral progression. In particular, the latent infection is accompanied by a protective $CD8^+$ T cell response that is highly virus-specific, and is maintained in latently infected TG for the life of the animal[77, 78].

1.6 HSV-1 IMMUNOLOGY

1.6.1 Intrinsic and innate immune response to HSV-1

Primary infected cells include mainly mucosal epithelial cells at the site of initial inoculation. The virus is first sensed in infected cells, such as corneal epithelial cells and fibroblasts, by pattern recognition receptors (PRRs) that fall into several categories: Toll-like receptors (TLRs, such as TLR-2, TLR-3, TLR-7, TLR-8 and TLR-9), AIM2-like receptors, and nucleic acid sensors (such as RIG-I-like receptors, Stimulator of IFN genes (STING), IFI-16, and PKR)[79-86]. These PRRs activate intrinsic antiviral genes, like type-1 interferon (IFN) responses, which act in both autocrine and paracrine fashions to turn on interferon-inducible genes to limit viral replication and spread and to recruit inflammatory cells that can control HSV-1 replication[87]. These responses can also shut down translation in infected cells by phosphorylating eIF2α, turning on pro-apoptotic genes to induce cell death, and inducing PML protein expression to form Nuclear Dot 10 (ND10) bodies. To counter these innate responses, HSV-1 has mechanisms of its own— eIF2α phosphorylation is counteracted by ICP34.5, the viral US3 kinase counteracts host pro-apoptotic proteins by phosphorylating them, and ICP0 can degrade ND10 bodies to prevent chromatin repression [88-90]. The exact nature of the PRRs present, as well as their responses to recognizing viral patterns are very cell-type dependent, but have the net effect of limiting viral replication and spread. As mentioned previously, the viral tegument proteins and α gene products have many functions to counteract immunity, and a large portion of these are directed to counteract the host intrinsic detection and response, resulting in a push-and-pull of viral evasion vs. host defenses.

The release of type-I interferons and other cytokines, such as (IL)-1α, IL-1β, IL-6, IL-8, IFNγ, TNFα, MIP-1α, and IL-12 attract a large influx of neutrophils, macrophages, natural killers (NKs), dendritic cells (DCs), and γδ T cells to the initial site of infection in the cornea[91-99]. These cells can recognize infected cells through multiple mechanisms, and are critical for viral control. Neutrophils respond very rapidly to inflammatory signals and play a role in limiting early viral spread in the cornea at least in part by producing pro-inflammatory cytokines and reactive-oxygen species[100]. Macrophages, NKs, and γδ T cells also respond early in ganglionic infection, and limit viral replication in the TG via production of effectors, such as iNOS, TNFα, and IFNγ[101-103]. Taken together, the intrinsic and innate immune responses serve to slow down or limit the early viral replication and spread to a level that is manageable, but as RAG/SCID mouse models and depletion studies show, the subsequent adaptive B and T cell responses that develop are key to ultimate control of viral replication and disease late in infection[104].

1.6.2 Adaptive immune response to HSV-1

Upon primary infection, DCs acquire HSV-1 antigens and present them to naïve B and T cells within draining lymph nodes (DLN). The resulting HSV-specific B cells produce strong neutralizing antibodies which prevent viral particle infectivity, and by late infection help prevent viral spread[105]. To date, strong antibody responses have not been shown effective at preventing primary infections, which is one factor limiting an effective HSV-1 vaccine, however, some antibody responses are capable of reducing viral spread and disease in several models[106, 107]. HSV-1 specific $CD4^+$ and $CD8^+$ T cell responses are also generated following primary

infection, and these cells traffic to both the site of primary infection at the mucosa, and the site of latency within the ganglia[68, 108, 109]. While $CD4^+$ T cells are not suspected to play a direct role in viral latency control, they are instrumental in directing and aiding in the functionality of $CD8^+$ T cell responses, discussed in the next section[110]. Of note is the fact that $CD4^+$ T cells are also implicated in contributing to the inflammation and subsequent scarring that is seen in HSK-afflicted corneas[111, 112].

1.6.3 $CD8^+$ T cell priming and memory

$CD8^+$ T cells directed against HSV-1 antigens detect short peptides (epitopes) that are presented bound to major histocompatibility complex class I (MHC-I) at the cell surface. In our mouse model of ocular infection, HSV-1 can be detected in the TG by 2 dpi, with declining viral titers coinciding with the peak $CD8^+$ T cell infiltration into the ganglia at 8 dpi[113]. The HSV-specific T cell infiltrate that enters ganglia is detectable as early as 5 dpi, and originates from the local draining lymph nodes (DLN)[114]. In early corneal infections, local and infiltrating DCs acquire HSV antigen either by direct HSV infection, or sampling of infected epithelial/fibroblasts in the cornea. DCs then deliver viral antigens to the DLN via lymphatic vessels, where they can be directly and/or cross-presented to naïve lymphocytes. $CD8^+$ T cell priming by DCs requires proteosomal processing of cytosolic or endosomal antigens into 8-10aa peptides which are presented by MHC-I [115, 116]. However, recent investigations into the priming of $CD8^+$ T cell responses to HSV infections suggest that both infected DCs and direct presentation by migratory DCs are dispensable for efficient CD8+ T cell priming[117, 118]. Indeed, in several viral models of $CD8^+$ T cell priming there is a necessary degree of “shuffling” of viral antigen within the DLN from migratory DC subsets to DLN-resident $CD8a^+$ DC subsets

for efficient $CD8^+$ T cell priming and proliferation [119-121]. Recently primed $CD8^+$ T cells that encounter antigen more often, and in the context of stronger costimulation and longer TCR/MHC-I contacts with presenting DCs also fare a better chance of proliferating and differentiating into memory $CD8^+$ T cell populations that are key to antiviral responses[121]. There is also some evidence suggesting that in localized viral infections, naïve and developing $CD8^+$ T cells compete for these TCR/MHC-I contacts within local DLN, and that limiting costimulation is a major factor that drives immunodominant $CD8^+$ T cell responses [122].

After activation, antigen-specific $CD8^+$ T cells undergo 1) clonal expansion during which they acquire effector functionality and antiviral properties, 2) contraction of the effector population through activation induced cell death, with the survival of a small percentage of memory cells, and 3) development of the memory $CD8^+$ T cell population[123]. Generally speaking, memory $CD8^+$ T cells are long-lived, antigen specific, and rapidly respond to their cognate antigen when encountered again[124]. Memory $CD8^+$ T cells persist even in the absence of antigen, and remain at levels far higher than naïve precursor $CD8^+$ T cell populations[125]. In the case of tissue-resident $CD8^+$ T cell populations, like those found within the TG, the maturation into memory $CD8^+$ T cells presumably involves the upregulation of homing receptors that keep these cells within the tissue. Of note, there is apparently no ganglionic infiltration of circulating central memory $CD8^+$ T cells from the blood during viral latency[126].

1.6.4 $CD8^+$ T exhaustion

$CD8^+$ T cells that respond to chronic or repeated viral infections may become exhausted due to repeated antigen exposure. In LCMV, HCV, HMPV and HIV models of $CD8^+$ T cell exhaustion, the exhausted cells exhibit a reduced capacity to respond effectively when

encountering antigen[127-132]. Characteristic of exhausted $CD8^+$ T cells is the loss of ability to produce effector cytokines, such as TNFα, IFNγ, and IL-2, as well as reduced capacity to release lytic granules into target cells[127]. Concurrent with the reduced effector status, there is a reduced ability of exhausted memory $CD8^+$ T cells to proliferate, and an upregulation of suspected exhaustion markers such as PD-1, Tim3, LAG3, CD160, or 2B4[133-135]. Many factors — such as the amount and number of inhibitory receptors on exhausted cells, the amount of antigen detected over time, availability of $CD4^+$ T cell help and the chronicity of infection — all influence the severity of exhaustion[127].

1.6.5 The nature of $CD8^+$ T cell responses during latency

Evidence suggests that sporadic phase 1 viral gene expression in the latently infected ganglia is immune-recognized, particularly by a persistent resident ganglionic $CD8^+$ T cell population [66, 68, 136]. Indeed, the B6 mouse model of HSV-1 latency has been under particular scrutiny, with the initial viral occupancy of the ganglia accompanied by a large infiltration of immune cells, including both $CD4^+$ and $CD8^+$ T cells. The magnitude of this immune infiltrate peaks near the onset of latency and then rapidly contracts, leaving a persistent low-level infiltrate that is maintained for the life of the host. Persisting ganglionic immune infiltrates associated with HSV-1 latency have also been seen in other model species and in humans [78, 137-140]. The ganglionic $CD8^+$ T cells in mice show markers of an activated effector memory phenotype at early stages, which is capable of reducing HSV-1 reactivation events in *ex vivo* cultures of latently infected ganglia[68, 141].

We and others have proposed that the ganglionic $CD8^+$ T cell infiltrate surveys the ganglia for reactivation events, eventually tipping the lytic/latent balance of the virus towards the latent state[142]. If phase 1 or early phase 2 gene expression is detected in neurons at latency, and $CD8^+$ T cells respond rapidly, several effector mechanisms have been identified that can hinder viral lytic replication. This is accomplished through an IFNγ-mediated reduction of HSV-1 gene expression and a Granzyme B/perforin dependent degradation of ICP4, both of which are accomplished without inducing neuronal apoptosis, suggesting that rapid immune control following recognition of protein expression in latently infected ganglia is vital to preventing reactivation[78, 141]. Successful viral reactivation then, likely results from a failure of $CD8^+$ T cell control of viral gene expression from progressing into late phase 2, wherein viral immune evasion genes are abundant within the neuron, and capable of blocking $CD8^+$ T cell responses. Specifically, several mechanisms have been identified, including: viral ICP47, γ34.5, and US3 kinase, which are capable of preventing effective MHC-I presentation, and UL13, which can downregulate neuronal expression of the T-cell chemoattractant CXCL9[49, 50, 143-145].

1.6.6 Characteristics of gB $CD8^+$ T cell immunodominance

The C57BL/6 (B6) mouse ocular HSV infection model has been particularly useful to explore cellular $CD8^+$ T cell directed immunity, because the entire HSV-1 specific $CD8^+$ T cell target repertoire has been described [77]. In B6 mice, the $CD8^+$ T cell repertoire developed to HSV-1 is highly skewed, as a single immunodominant epitope on the essential viral glycoprotein B (gB) that accounts for approximately half of all HSV-1 specific $CD8^+$ T cells (gB-CD8s). These gB-CD8s are directed to amino acids 498-505 of gB (SSIEFARL, henceforth referred to as $gB_{498\text{-}505}$). The other HSV-1 specific $CD8^+$ T cell populations (collectively termed non-gB-

CD8s) recognize 19 additional subdominant viral epitopes on only 12 viral proteins [77]. The approximate 1:1 ratio of HSV gB-CD8s to non-gB-CD8s is maintained systemically, in the corresponding lymph nodes, the spleen, and in the TG during acute peak infiltrate and in the contracted population during latency [113, 146]. However, while gB-CD8s during HSV-1 latency show an activated and highly functional phenotype that responds to antigen stimulation, non-gB-CD8 populations show a partial loss of function, such that a significant fraction do not respond to antigen stimulation. Loss of function in the non-gB-CD8 population resembles functional exhaustion in that it is associated with increased expression of the inhibitory receptor programed death-1 (PD-1) and is regulated by IL-10 [147, 148]. Thus, the TCR repertoire of functional $CD8^+$ T cells narrows by a process akin to functional exhaustion of subdominant $CD8^+$ T cells within the latently infected TG.

2.0 SPECIFIC AIMS

HSV-1 specific $CD8^+$ T cell responses in the latently infected ganglia are of special interest due to their ability to monitor viral latency for viral gene expression and prevent reactivation events from progressing. It is of vital importance to understand $CD8^+$ T cell responses in this context, and how they interact with viral proteins expressed both during latency. We hope that this knowledge will aid in developing strategies that can manipulate the functional T cell repertoire and enhance monitoring of viral latency.

Determine the influence of an HSV-1 immunodominant $CD8^+$ T cell epitope on target hierarchy and function of subdominant $CD8^+$ T cells during viral latency

The entire subdominant $CD8^+$ T cell repertoire of HSV-1 was recently identified in B6 mice, and has been shown to be minimally functional when compared to the WT HSV-1 response. Developing a mutant that lacks this epitope allows us to investigate thoroughly the nature of a compensatory response when an immunodominant epitope is removed from the viral genome *We hypothesize that select subdominant HSV-1 responses will expand numerically and functionally to fill the TG-resident memory $CD8^+$ T compartment.*

Investigate the role that antigen expression kinetics play in generating and maintaining $CD8^+$ T cell responses during HSV-1 latency.

During HSV-1 latency, emerging evidence supports the model that viral antigen is expressed at very low levels and is monitored by a protective ganglionic-resident $CD8^+$ T cell population. *We hypothesize that altering the promoter that drives $CD8^+$ T cell epitopes during $CD8^+$ T cell priming and latency will alter the magnitude and functionality of $CD8^+$ T cell responses.*

Prime a ganglionic HSV-1 specific $CD8^+$ T cell response using AAV or PRV vectors

HSV-1 replication is controlled in part by effector $CD8^+$ T cell responses within the ganglia prior to the establishment of stable latency. Having a pre-established tissue-resident memory $CD8^+$ T cell population could reduce viral burden upon HSV-1 infection. *We hypothesize that priming a tissue-resident $CD8^+$ T cell population in the ganglia will be protective against subsequent HSV-1 infections.*

3.0 MATERIALS AND METHODS

3.1 VIRUS AND CELLS

Vero cells (ATCC, Manassas, Virginia), SV40-transformed B6 embryo fibroblast cell line B6WT3 (MHC-I compatible with C57BL/6 mice; [149]), and gB-Vero (Vero cells stably transfected with a plasmid expressing gB from the native gB promoter; obtained from Dr. William Goins, University of Pittsburgh) were grown in Dulbecco's modified Eagle's medium (DMEM) supplemented with 10% fetal bovine serum (FBS), penicillin-G (100 units/ml), streptomycin (100 mg/ml) and fungizone (250 mg/ml). All HSV-1 are based on the KOS strain originally obtained from a master stock obtained from P Schaffer. This strain was recently sequenced (GenBank JQ780693.1) [150].

Pseudorabies virus (PRV) used in this study were generated using a Becker-strain bacteria artificial chromosome (BAC) (kind gift from Lynn Enquist, Princeton University) [151] PRV expressing HSV-1 $gB_{494\text{-}509}$ in a thymidine kinase (TK) knockout virus was developed in the E. Coli strain GS1783 by placing a kanamycin-resistance cassette containing monomeric red fluorescent protein in frame with TK at site 59,595 (Genbank JF797219.1) followed by a CMV promoter driving expression of 4 repeats of HSV-1 $gB_{494\text{-}509}$. This cassette was amplified using the following primers: Forward, 5'-GCGGCAACCTGGTGGTGGCCTCGCT GGACCCGGACGAGCACATGGCCTCCTCCGAGGACGTCAT-3'; Reverse, 5’-

TCAGGTAGCGCGACGTGTTGACCAGCATGGCGTAGACGTTCCTCGCGAGGGATCGG CTAGAGTC -3’ and inserted into the PRV BAC using recombineering [152]. The kanamycin-resistance cassette was resolved using two-step red-mediated recombination, with a resultant disruption of the TK gene. PRV was propagated to high titer in PK15 (porcine kidney 15, ATCC CCL-33) epithelial cells, purified as done for HSV, and gB-peptide expression confirmed by stimulation of gB-specific T cells, as described below.

Adeno-Associated Virus (AAV) fluorescent reporter constructs were purchased from Vector Biolabs.

3.2 VIRUS PURIFICATION

All HSV-1 and PRV used in these studies were purified from infected Vero cell (for HSV-1) or PK15 (for PRV) monolayers in T175 flasks. After cytopathic effect in >90% of cells, NaCl is added to a final concentration of 0.45M in culture media, rocked for 1 hour, and centrifuged at 2000g for 10min to pellet cellular debris. Supernatants are passed through 0.8um filters, then used to overlay 1-2mL of a 50% sucrose cushion, and pelleted at 142,000g for 1h. After removing most supernatant, the virus pellet was carefully resuspended in a 500uL volume of the remaining sucrose cushion and media.

3.3 DERIVATION OF HSV-1 WITH GB$_{498\text{-}505}$ MUTATIONS

DNAs were amplified by polymerase chain reactions (PCR) using a proofreading polymerase [Expand (Roche) or Primestar (Takara)] with "Hot start" conditions and in reactions containing 4% DMSO, as detailed previously [153]. A plasmid was derived in which genomic recombination into HSV-1 would replace the approximately N terminal half of the gB coding sequence with EGFP, using a pUC19-based plasmid (gC Rescue construct, Fig 1) detailed previously [153] containing HSV-1 DNA from 54,475bp to 56,464bp (sequences given in reference to HSV-1 KOS Genbank JQ780693.1) containing the gB promoter and partial gB coding region. The construct had a unique EcoRI flanking at 54,475 and unique HindIII site flanked 56,464, and a unique AvrII site at position 58,476bp, immediately upstream of the gB ORF start and designed not to alter the coding of the upstream UL28 protein. The AvrII-EcoRI fragment of this plasmid was replaced with a PCR fragment encoding gB residues 507 to the stop codon, generated using primers 5'-GCGCCTAGGCTCGGATCCCAGTTTACGTACAAC-3' and 5'-GAGCGGAATTCATTTACAACAAACCCCCCATCA-3' (restriction sites underlined). This construct (termed pgBp-gBend) was then further modified by inserting a PCR-amplified fragment containing EGFP using the primers: 5' CCCTAGGCTACCTGACGGCGGGCACGACGG 3' and 5' CGTAGGATCCTTACTTGTACAGCTCGTC 3'. The BamHI-AvrII fragment was inserted into BamHI-AvrII digested pgBp-gBend, resulting in the flanking of EGFP by the gB promoter sequences, and sequence encoding gB residues 507- 904 (Fig 1). When this linearized plasmid was then cotransfected with infectious HSV-1 DNA on gB-Vero cells, recombinant viruses showing EGFP positivity were selected and grown on complementing gB-Vero cells. Infectious HSV-1 KOS DNA was obtained using methods outlined previously [153]. Recombinant viruses

(HSV-1 gB-null-EGFP) were then verified for correct DNA insertion by DNA sequencing of the junctions and by Southern blot analyses.

Plasmid pgBp-gBend was digested with AvrII-SnaBI to remove the EGFP cassette, and replaced with PCR amplified sequence encoding gB residues 1-509 with altered residues in the gB SSIEFARL motif (Table 1). The primers shown in table 1 were used in conjunction with the primer 5' GCCCTAGGCTACCTGACGGGGGGCACGACGGGCCCCCGTAG 3'. Each PCR was then cloned as an AvrII-SnaBI fragment and sequence verified. Linearized plasmids were then individually cotransfected with HSV-1 gB-null-EGFP infectious DNA on Vero cells, and HSV-1 recombinants replicating on Vero cells, lacking GFP expression, and containing the mutations in the $gB_{498\text{-}505}$ region were plaque-purified. HSV-1 containing gB L505A (designated HSV L8A) and gB S498L (designated HSV S1L) were derived. We also derived expression plasmids for each epitope-mutated gB protein by placing the AvrII-EcoRI fragment containing the entire altered gB protein coding region into the vector pEGFP-C3, digested with NheI and EcoRI to place gB under the control of the human cytomegalovirus Immediate early (CMV IE) promoter and SV40 polyadenylation signals.

3.4 CONSTRUCTION OF HSV-1 WITH $GB_{498\text{-}505}$ EXPRESSED FROM VARIOUS PROMOTERS

DNAs were amplified by polymerase chain reactions (PCR) using a proofreading polymerase [Primestar (Takara)] with reactions containing 4% DMSO, as detailed previously [153]. The constructs used to derive recombinant viruses were developed in a manner similar to that detailed previously in which gene cassettes were inserted into the nonessential gC locus

encoded by UL44 [153]. Briefly, the parent vector was a previously detailed plasmid that contained the gC promoter driving expression of EGFP inserted neat the ATG of UL44, followed by part of the gC ORF[154]. The EGFP gene was an NheI - XbaI fragment obtained from the plasmid EGFP N-1 that is translationally stopped before the gC ORF. To develop a $gB_{498\text{-}505}$ epitope fusion, two complementary oligonucleotides were purchased from IDT Inc. the sense oligo - 5' – GAT CCC ACC **ATG** GCG CAT AAG ACC ACC TCC TCC ATC GAG TTC GCC AGG CTG CAG TTT ACG TAC AAC CAC AA-3' - and the antisense oligo - 5' GATC TTGTGGTTGTACGTAAACTGCAGCCTGGCGAACTCGATGGAGGAGGTGGTCTTATGC GCCATGGTGG-3' were hybridized together at 70oC for 5min, slow cooled, phosphorylated using T4 polynucleotide kinase, and ligated together overnight with T4 DNA ligase at room temperature. Reaction was then doubled in volume, heat inactivated and digested with BamHI and BglII to remove head-to-head and tail-to-tail concatemers. Following electrophoresis on 6% PAGE gels, fragments corresponding to different copies of the repeats were extracted by electroelution, purified and then ligated into the unique BamHI site immediately upstream of EGFP in the plasmid pgC-EGFP. A clone (gCp-pep4-EGFP) containing one or four copies was selected for further use that contained the peptide corresponding to $gB_{495\text{-}511,}$ expressed in frame with EGFP and with an initiating start codon (Fig 1) (-T**M**A*HKTTSSIEFARLQFTYNH*KDP-)^4-GFP. The different promoters used in this work, with the exception of LAT, were generated by PCR methods to contain a minimum of 500 bp of sequence immediately upstream of the respective ORF ATG using primers (Table 1) with a 5' additional sequence encoding flanking unique HindIII site distally and a unique BamHI site at the proximal end of the promoter. These were cloned into the vector gCp-pep4-EGFP cut with BamHI and HindIII. Finally, DNA containing monomeric fluorescent protein mRFP with its bovine growth hormone

polyadenylation A sequence was generated from the plasmid pgC-RFP/pgB-EGFP detailed previously (Ramachandran et al. 2008) and cloned into the unique NheI-and HindIII sites to place the red fluorescent protein gene downstream of the gC promoter. For the HSV-1 LAT promoter, a SacI – BamHI DNA fragment of the vector pBS-KS:LAP1 (a kind gift of David Bloom, University of Florida) representing bp 117,396 to 119,289 of HSV strain 17+, including the LAT promoter and LAT 5' exon region) was cloned into the gCp-pep4-EGFP cut with BamHI and SacI, and then subjected to cloning of the mRFP protein as just detailed for other constructs. In all constructs, sequences corresponding to the promoter of gC drives the expression of the mRFP protein followed by poly A signal. This is followed by the selected promoter sequence driving a 4mer repeat of a peptide that contains the gB494-511 in frame with the EGFP protein. This is followed by a portion of the gC open reading frame, and the flanking gC promoter and gC ORF portion permit recombination into the gC locus.

Recombinant viruses were derived by cotransfection of plasmids just outlined after linearization with SspI or EcoRI with HSV-1 KOS S1L infectious DNA in a manner similar to that detailed previously[153, 155]. Virus plaques were then selected based on gain of red fluorescence and plaque purified to homogeneity as determined by fluorescence. We did not use EGFP to select, as the n terminal fusion of the peptide reduced fluorescence to low levels that were difficult to visualize.

3.5 ANIMAL INFECTION

Six to eight week old female C57BL/6 mice (Purchased from Jackson Labs) or gB-T1 mice [156] were used in these studies. All animal experiments were conducted in accordance

with protocols approved by the University of Pittsburgh Institutional Animal Care and Use Committee. Corneas of anesthetized mice were scarified using a 30g prior to HSV-1 corneal infections, as detailed previously [153]. HSV-1 (1 x 10^5 PFU of purified HSV-1 in 2-3 µl RPMI media) was then applied to each eye. When infections were performed in the mouse flank, a small (5mm x 5mm) region of skin was denuded of hair, and the same amount of virus was applied to abraded skin. For AAV, corneas were abraded as in HSV-1 infections, with 1*10^10 genome copies/eye applied.

3.6 TISSUE PREPARATION

Tissues for subsequent flow cytometry analyses were obtained from anesthetized mice injected first i.p. with 0.3 ml of 1000 U/ml heparin (Sigma-Aldrich, St. Louis, MO) and then euthanized by exsanguination. Lymph nodes, TG were removed and subsequently digested in RPMI containing 10% fetal bovine serum and 400 U/ml collagenase type I (Sigma-Aldrich) for 45-60 minutes at 37^{o}C. Tissues were mechanically dissociated and triturated into single-cell suspensions and then filtered through a 40 µm nylon cell strainer (BD Biosciences, Bedford, MA). Spleens were treated with red blood cell lysis buffer (BD Pharm Lyse) for three minutes prior to analyses. Corneas were excised, processed under a dissecting microscope to separate the cornea and conjunctival tissue, and mounted onto microscope slides.

3.7 *EX VIVO* REACTIVATION STUDIES

For *ex vivo* reactivation, TG samples were first rendered into single cell suspensions as just detailed, but without filtering. In cases where endogenous $CD8^+$ T cells were depleted, we used antibody/complement mediated lysis using Low-Tox M rabbit complement (Cedarlane) and anti CD8, as previously described[78]. The efficiency of depletion was assessed by flow cytometry and was considered effective if >95% of the $CD8^+$ T cells were depleted. Mock depleted suspensions used an IgG isotype control under the same conditions. Single-cell TG suspensions were then plated at one-fifth TG equivalents per well in 48-well culture plates in 400 μl of DMEM containing 10% FBS, 10 mM HEPES buffer, 10 U/ml recombinant murine IL-2 (R&D Systems), and 50 μM 2-mercaptoethanol. Where indicated, cultures were supplemented with exogenous expanded gB-CD8s made as described previously at 2×10^4 $CD8^+$ T cells/well [141]. TG cultures were monitored for reactivation by testing 50uL culture supernatant fluid for live virus by standard viral plaque assays as previously described [78]. The 50uL was replaced each time with fresh media. Supernatants were tested every two days for a total of ten days in culture. Data are represented as the percent of wells that were positive for viral reactivation.

3.8 $CD8^+$ T CELL EXPANSION AND STIMULATION

$CD8^+$ T cells specific for $gB_{498\text{-}505}$ were expanded from TG preparations taken 8 days post infection (dpi) from mice infected with HSV-1, as detailed previously [141], or with collagen-dissociated suspensions of TGs. Cultures were maintained for up to 10 days, followed by MACS

bead purification of the $CD8^+$ T cells. Resulting populations were >95% $CD3^+$, $CD8^+$, and positive for $gB_{498\text{-}505}$/H-$2K^B$ tetramer. For preparing target B6WT3 fibroblasts, the (WT) and mutant gB proteins were expressed in B6WT3 (1×10^5 cells) transfections with 5 μg of plasmids expressing each gB protein or the epitope mutant protein under the CMV IE promoter. At 24 hours post-transfection, co-cultures for stimulations were established, with 5×10^4 expanded gB-$CD8^+$ or $CD8^+$ T cells obtained from the TG of HSV-1 infected gB-T1 mice added per 1×10^5 target B6WT3 cells. Co-cultures were maintained for 6 h in the presence of Brefeldin A, and then subsequently stained for surface CD45, CD8 and intracellular IFNγ and/or TNFα as markers of activation.

T cell phenotypic characterization by flow cytometry was performed essentially as detailed previously [77]. Single cell suspensions of TGs and spleens were stained with antibodies to CD45, CD3, and CD8α, and with tetramers for 1 hr at room temperature prior to fixing for 20 minutes with Cytofix/Cytoperm (BD Biosciences, Bedford, MA). Washed cells were then analyzed by flow cytometry. $CD8^+$ T cell recognition of HSV-1 target antigens was determined by pulsing cultured B6WT3 fibroblasts with the respective peptide [77] at a concentration of 1 μg/ml for 30 min at 37°C/5% CO_2. Alternatively, B6WT3 fibroblasts were infected for 6-12 hours at an MOI of 5 with recombinant HSV-1 or PRV, and then virus was UV-inactivated prior to stimulation. The dispersed TG or spleen cells were added to peptide-pulsed or infected fibroblasts in the presence of Brefeldin A and anti-CD107a (BD clone 1D4B) for 6 hr at 37°C/5% CO_2. After stimulation, cells were stained for surface expression of anti-CD45 and CD8α, permeabilized and fixed using Cytofix/Cytoperm and then subjected to intracellular stain for IFNγ and TNFα. The peptides used in this work were detailed previously

[77]. For each peptide, both TGs from a minimal total of five mice per peptide were separately analyzed for reactivity.

3.9 ANTIBODY REAGENTS AND FLOW CYTOMETRY

Phycoerythrin (PE)-conjugated or BV421-conjugated H-2K^b tetramers complexed with the $gB_{498-505}$, $RR1_{982-989}$, or $RR1_{822-829}$ peptide were provided by the National Institute of Allergy and Infectious Diseases Tetramer Core Facility (Emory University Vaccine Center, Atlanta, GA). Efluor-450 conjugated anti-CD3 (clone 17A2) was purchased from eBioscience. Pacific-Blue-conjugated anti-CD8α (clone 53-6.7), APC-conjugated anti- IFNγ (clone XMG1.2), PerCP-conjugated anti-CD45 (clone 30-F11), PE-Cy7-conjugated anti-TNFα (clone MP6-XT22), APC-conjugated anti-granzyme B (clone GB11), and BD Cytofix/Cytoperm Fixation/Permeabilization Solution Kit were purchased from BD Pharmingen (San Diego, CA). The appropriate isotype control antibodies were purchased from the same company used for the reactive antibody and used as controls for intracellular staining. All flow cytometry samples were collected on BD FACSAria cytometer and analyzed by FACSDiva and/or FlowJo software.

3.10 BRDU PROLIFERATION ASSAY

Latently infected mice (28-34 dpi) were pulsed for two days prior to harvest with 1mg/mouse of BrdU in 0.1ml PBS via i.p. injection. The TGs were harvested at 48hr later and cells were prepared for flow cytometric analysis. An FITC BrdU Flow Kit (BD Pharmingen, San

Diego, CA) was used as per manufacturer instructions, briefly: TG cells were washed twice with FACS buffer (1% FBS, 0.1% sodium azide in PBS) prior to surface antibody staining in the presence of Fc block. Following surface staining, cells were permeabilized with Cytofix/Cytoperm solution for 20 min on ice and then Cytofix/Cytoperm Plus for 10 minutes on ice. After being washed, cells were treated with 30 µg of DNAse for 1hr at 37°C, washed with 1X BD Perm/Wash solution, and cells were then incubated for 30 minutes in BrdU antibody diluted in 1X BD Perm/Wash. After labeling, suspensions were washed with 1X Perm/Wash and resuspended in FACS buffer for analysis by flow cytometry.

3.11 MURINE OCULAR DISEASE SCORING

Corneal reflex was tested and recorded as positive (1) or negative (0) by loosely holding the mouse and touching all areas of the cornea with a surgical spear, being careful to avoid touching the eyelashes and whiskers. A loss of BR indicated a complete loss of corneal sensation such that the mouse failed to blink when any area of the cornea was touched. A positive reflex indicated retention of some degree of sensation such that the mouse blinked when at least one area of the cornea was touched.

Corneal disease was monitored by at least two investigators in using slit-lamp examination after PRV or HSV-1 corneal infection. HSK, characterized by corneal opacity and neovascularization, was monitored by slit-lamp examination and scored based on opacity: 0.5, any imperfection of the cornea; 1, mild corneal haze; 2, moderate opacity; 2.5, moderate opacity with regional dense opacity; 3, severe, dense opacity obscuring the iris; 3.5, severe, dense opacity with corneal ulcer; and 4, corneal perforation.

Neovascularization was determined visually by dividing the cornea into 4 quadrants, and each quadrant was scored as 0 (no vessels visible), 1 (vessels extending into one quadrant of the cornea), 2 (vessels extending into 2 quadrants of the cornea), 3 (vessels extending into 3 quadrants of the cornea) or 4 (severe vascularization in all quadrants or extending significantly into the central cornea). Discrepancies between observers were averaged.

3.12 QUANTITATIVE REAL-TIME PCR

HSV-1 or PRV genome copy number in infected TG was determined by quantitative real-time PCR as previously described using primers that recognize the sequences of the gH gene [157].

3.13 STATISTICAL ANALYSIS

All statistical analyses were performed using GraphPad Prism software package. The specific statistical applications are shown in the legends to each figure.

3.14 ETHICS STATEMENT

All animal experiments were conducted in accordance with protocol # 15076444, approved by the University of Pittsburgh Institutional Animal Care and Use Committee. This

protocol meets the standards for humane animal care and use as set by the Animal Welfare Act and the NIH Guide for the Care and Use of Laboratory Animals.

4.0 INFLUENCE OF AN IMMUNODOMINANT HSV-1 CD8$^+$ T CELL EPITOPE ON THE TARGET HIERARCHY AND FUNCTION OF SUBDOMINANT CD8$^+$ T CELLS

The CD8$^+$ T cell dominance hierarchy seen in the B6 mouse model and the strong dominance of the HSV-1 gB$_{498\text{-}505}$ epitope is remarkable. It is not clear why the gB$_{498\text{-}505}$ epitope is so immunodominant, as the position of an epitope within the dominance hierarchy can be influenced by many factors [158]. However, while during HSV-1 latency gB-CD8s show an activated and highly functional phenotype that responds to antigen stimulation and is capable of reducing HSV-1 reactivation events in *ex vivo* cultures, non-gB-CD8 populations show a major loss of function, such that a significant fraction cannot respond to antigen stimulation, [77, 141]. These observations suggest a role of gB-CD8s in regulating the HSV-1 latent/lytic decisions *in vivo*. The combination of a strongly immunodominant epitope and a completely defined TCR repertoire make HSV-1 an excellent model to investigate the effect of removing an immunodominant epitope on the resulting non-gB-CD8 repertoire and changes in functionality associated with the latent state. To understand how dominance hierarchies relate to CD8$^+$ T cell function during latency, we characterized the TG-associated CD8$^+$ T cells following corneal infection with a recombinant HSV-1 lacking the immunodominant gB$_{498\text{-}505}$ epitope (S1L). Gaining insights into how CD8$^+$ T cell-peptide recognition dynamics during the establishment and maintenance of latency alter functionality may lead to strategies that improve ganglionic

immune infiltrates and increase protection from HSV-1 reactivation and subsequent disease [159].

4.1 MUTATIONS IN HSV-1 $GB_{498-505}$ PREVENT ANTIGEN RECOGNITION BY GB-CD8S

A series of gB mutants in the 498-505 amino acid region was generated and evaluated for recognition by gB-CD8s. The eight gB mutations (Table 1) included: mutations of the predicted MHC-I anchoring residues in the peptide (L8A, S1L, S1G, L8A/S1G, and L8A/R7K); mutations in the predicted T cell receptor binding region (F5L and S1G/I3A): and a mutation that changed the HSV-1 $gB_{498-505}$ region to that of VZV, S1G/l3N/F5L/E4S (SIFE). The L8A mutation was previously reported (referred to as L505A) to abrogate gB-CD8 development upon flank skin infection of B6 mice [160]. We found that most of the eight mutant gB genes expressed a protein from plasmids that were detected by gB-specific antibodies of the size expected for gB (Fig 5). When each mutant gB protein was expressed in transfected B6WT3 fibroblasts, only wild-type (WT) gB could stimulate the production of intracellular IFNγ in an expanded population of gB-CD8s (Fig 5). While only a modest fraction of gB-CD8s showed activation, it was clear that all eight mutations of the $gB_{498-505}$ region mostly or completely abrogated gB-CD8 recognition.

Table 1. Primer sequences to generate mutations in the gB epitope

Name	Mutation	Reverse primers used*
WT	SSIEFARL (none)	5’ GTT G**TA CGT A**AA CTG CAG CCT GGC GAA CTC GAT GGA GGA GGT GGT CTT GAT GCG CTC CA 3’
L8A	SSIEFARA	5 ‘ GTT G**TA CGT A**AA CTG agc CCT GGC GAA CTC GAT GGA GGA GGT GGT CTT GAT GCG CTC CA 3’
F5L	SSIELARL	5’ GTT G**TA CGT A**AA CTG CAG CCT GGC cAA CTC GAT GGA GGT GGT CTT GAT GCG CTC CA 3’
S1G	GSIEFARL	5’ GTT G**TA CGT A**AA CTG CAG CCT GGC GAA CTC GAT GGA ccc GGT CTT GAT GCG CTC CA 3’
S1L	LSIEFARL	5’ GTT G**TA CGT A**AA CTG CAG CCT GGC GAA CTC GAT GGA caa GGT GGT CTT GAT GCG CTC CA 3’
S1G/L8A	GSIEFARA	5’ GTT G**TA CGT A**AA CGT agc CCT GGC GAA CTC GAT GGA ccc GGT GGT CTT GAT GCG CTC CA 3’
S1G/I3A	GSAEFARL	5’ GTT G**TA CGT A**AA CTG CAG CCT GGC GAA CTC Ggc GGA ccc GGT GGT CTT GAT GCG CTC CA 3’
L8A/R7K	SSIEFAKA	5’ GTT G**TA CGT A**AA CGT agc CtT GGC GAA CTC GAT GGA GGA GGT GGT CTT GAT GCG CTC CA 3’
S1G/I3N/F5L/E4S (SIFE)	GSNSLARL	5’ GTT G**TA CGT A**AA Ctg CAG CCT GGC cAA gct GtT GGA ccc GGT GGT CTT GAT GCG CTC CA 3’

*The restriction site of SnaBI used in cloning is shown in bold. Changes from the wild type sequence are shown in lower case letters.

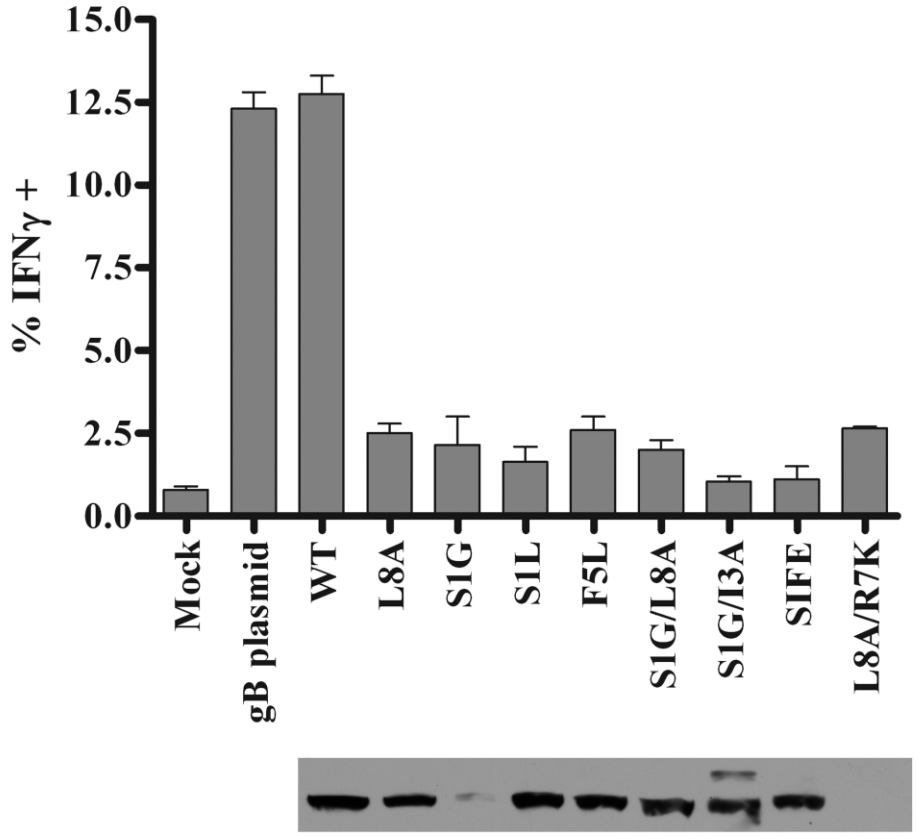

Figure 5. Mutant gB proteins and recognition by gB-CD8s

Untreated B6WT3 cells (mock) or cells transfected with plasmids to express WT gB or $gB_{498\text{-}505}$ epitope mutants were incubated for eighteen hours. The labeling of the mutations is as depicted in Table 1; WT is a plasmid which went through the mutagenesis procedure without changes. Cells were harvested for expression analysis by immunoblotting using a monoclonal gB-specific antibody (lower panel) or, in parallel, transfected cells were combined with $5x10^4$ gB-CD8s from an endogenously expanded clone and stimulated for 5 h in the presence of Brefeldin A. gB-CD8s were surface stained for CD45 and CD8, permeabilized, and stained for intracellular IFNγ. The graph depicts one of two representative experiments, with the mean percent of $IFN\gamma^+$ cells (n = 2/group) and standard error of the mean (SEM) for each stimulation. Studies completed by Sarah Bidula.

HSV-1 recombinants containing each mutation were developed (Fig 6) by rescue of the growth of a gB-null-EGFP virus on gB-complementing Vero cells, and all yielded virus that could form plaques on non-complementing cells. Recombinant HSV-1 with the following mutations in gB formed small plaques, indicating they were growth-impaired: S1G, F5L, S1G/I3A, S1G/L8A, and S1G/I3N/F5L/E4S (Table 1). This was confirmed following ocular

infection of B6 mice, where low viral replication was detected at 4 dpi within the TG of mice (Fig 7A). These impaired viruses were not studied further. However, the S1L and L8A viruses could replicate to levels not significantly different from WT HSV-1 at 4 dpi in the TG (Fig 7A). They also establish equivalent latent genomic loads in the TG at 8 dpi (Fig 7B), and replicate to the levels of parental WT virus in both multi-step (infected at MOI of 0.01) and single step (infected at MOI of 10) growth curves in cultured Vero cells (Fig 7C). Since viral load and fitness in mice might influence $CD8^+$ T cell hierarchy [161], we initially focused on these two HSV-1 mutants and then conducted detailed studies on HSV-1 S1L.

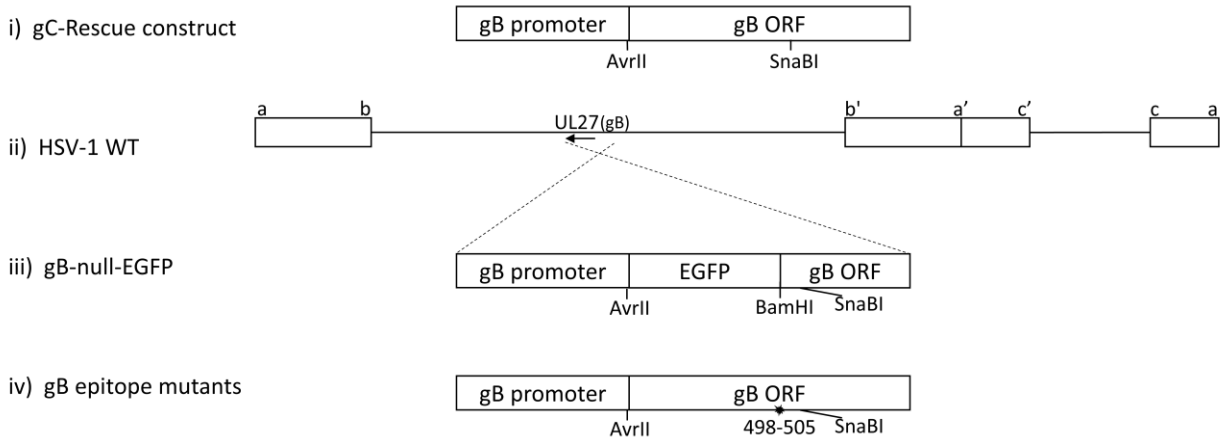

Figure 6. Construction of gB null virus and of HSV-1 with $gB_{498\text{-}505}$ mutations

Line i represents the parental plasmid used for derivation of the constructs in this study, detailed previously [47]. Line iii represents the replacement of the gB ORF with EGFP followed by the remaining part of the gB ORF from residue 509 to the end (gB ORF Back) that was developed to obtain a gB null EGFP virus. Line ii represents the HSV genome and the approximate coding position and direction of the gene for gB. Line iv represents the replacement gB genes and the site of the epitope mutations with respect to the SnaBI site used for derivation, as detailed in the text. AvrII and SnaBI are restriction sites used to clone the replacing region of gB.

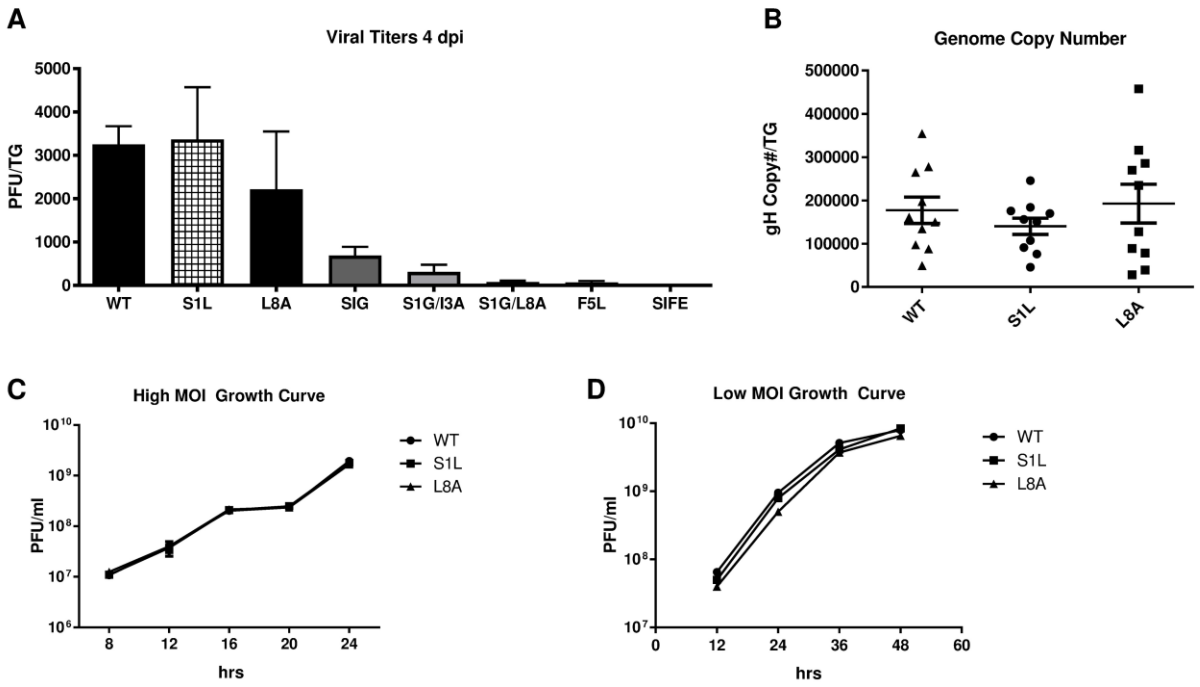

Figure 7. Growth of HSV gB mutants *in vitro* and *in vivo*

(A) Virus growth in the TG of B6 mice was determined at 4 days post ocular infection with $1x10^5$ PFU of either HSV-1 WT or HSV-1 containing the $gB_{498-505}$ epitope mutants detailed in table 1. TG were harvested and subjected to three freeze thaw cycles and infectious virus released into the supernatant was titrated on Vero cells. The graph represents the mean virus titer for each virus ± SEM of the mean (n = 5 mice). This is a representative of two separate studies with similar results. **(B)** Genome copy number determined by qPCR in the TG of mice infected with HSV-1 WT, S1L, or L8A following harvest at day 8 post ocular infection (n=10). Values are representative of the total copies per TG. **(C)** Monolayer cultures of Vero cells were infected at a multiplicity of infection (MOI) of 10 PFU/cell (high MOI Growth Curve) or 0.01 PFU/cell (Low MOI Growth Curve) respectively with HSV-1 WT, S1L, or L8A. At the indicated hours post-infection, cells and supernatants were pooled, subjected to three freeze–thaw cycles and the viral titers were determined by plaque assay. The mean PFU/culture ± standard error of the means (SEM) is shown at each time. Studies completed by Sarah Bidula and Srividya R. Ramachandran.

4.2 HSV-1 LACKING THE $GB_{498-505}$ EPITOPE INDUCES AN EQUIVALENT TG $CD8^+$ T CELL RESPONSE THAT IS NOT DIRECTED TO $GB_{498-505}$

Following ocular infection of B6 mice, the peak $CD8^+$ T cell infiltration in the TG occurs at 8 dpi and subsequently contracts to a low but persistent level that remains for the life of the host. The total $CD8^+$ T cell infiltrates into TG of mice that received corneal infections with

HSV-1 S1L and L8A were not statistically different from those induced by WT HSV-1 infection (Fig 8A). However, while approximately half of the $CD8^+$ T cells infiltrating TG infected with WT HSV-1 [114] stained positively with $gB_{498\text{-}505}$ H2-K^B tetramers, $CD8^+$ T cells infiltrating TG infected with HSV-1 S1L and L8A showed extremely low $gB_{498\text{-}505}$ tetramer staining (Fig 8B). The $gB_{498\text{-}505}$ tetramer positive cells were also virtually undetectable in spleens and the local draining lymph nodes (DLN) of S1L infected mice (Fig 8C and 8D). This suggests that there is an HSV-specific $CD8^+$ T cell response in the TG that compensates for the loss of the immunodominant gB-CD8 population, as seen previously[160].

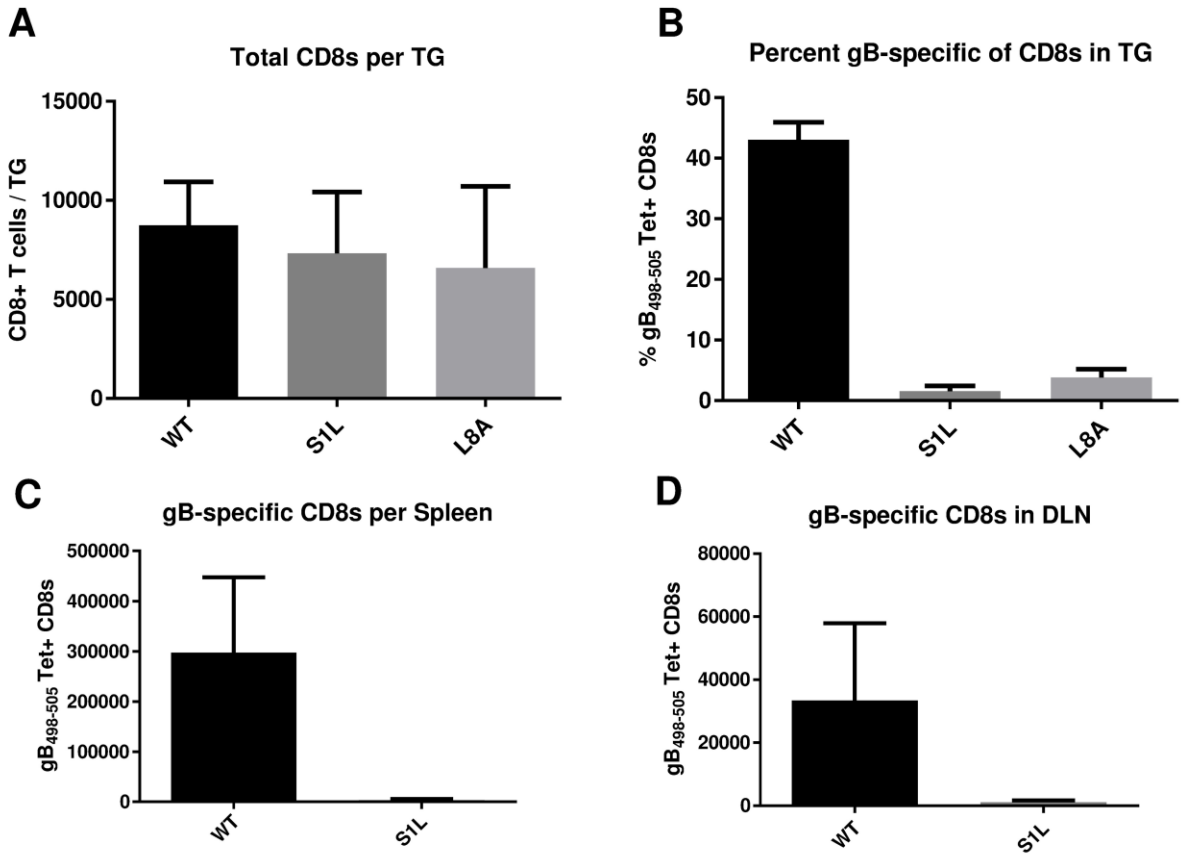

Figure 8. Acute $CD8^+$ T cell infiltrates in the ganglia of mice after corneal infection with WT HSV-1 or recombinant HSV-1 containing $gB_{498\text{-}505}$ mutations.

Corneas of mice were infected with $1x10^5$ PFU/eye of HSV-1 WT, S1L, or L8A. At 8 dpi (peak $CD8^+$ T cell infiltrate), the TG, spleen, or DLN were dissociated into single cell suspensions and surface stained with antibodies to CD45, CD3, CD8 and with MHC-I $gB_{498-505}$ tetramer as detailed in Methods. Cells were analyzed by flow cytometry, and the data are presented as the mean +/- SEM (n=5 mice, 10 TGs) of **(A)** absolute number of $CD3^+CD8^+$ T cells per TG, **(B)** the percent of $gB_{498-505}$ tetramer positive $CD8^+$ T cells in each TG, or **(C, D)** the total number of $gB_{498-505}$ tetramer specific cells per spleen and local DLN. The experiment shown is representative of three additional experiments, all producing similar results. The absolute numbers of $CD8^+$ T cells induced in the TG with each virus were not statistically different as shown by a one-way ANOVA followed by Tukey's posttest (p=0.58).

Failure of gB-CD8s to recognize the S1L mutation was further assessed by testing the ability of exogenous gB-CD8s to block HSV-1 S1L reactivation in *ex vivo* ganglionic explant cultures. TG of B6 mice harboring equivalent WT HSV-1 or S1L virus were excised at latency (34 dpi), dispersed with collagenase, depleted of endogenous $CD8^+$ T cells and then plated in 1/5 TG cell equivalents per culture well, either alone or with $2x10^4$ gB-CD8s from a previously described clone, all under conditions that maintain T cell viability [141]. In the absence of $CD8^+$ T cells, approximately 50-60% of TG cultures showed HSV-1 reactivation and virus release into the media, with reactivation frequency that was not statistically different in TG infected with WT and S1L virus (Fig. 9A). These data establish that HSV-1 S1L possesses robust ability to establish latency and reactivate in *ex vivo* cultures. However, in the presence of gB-CD8s, the reactivation of WT HSV was nearly abrogated, as expected from similar previous studies [68, 78]. In contrast, reactivation of S1L was not affected by addition of gB-CD8s, as a similar proportion of cultures reactivated with or without gB-CD8s (Fig 9A). However, the endogenous $CD8^+$ T cells in TG that were latently infected with S1L HSV-1 were still able to inhibit S1L reactivation from latency as effectively as endogenous $CD8^+$ T cells in TG latently infected with WT HSV-1 (Fig. 9B). Taken together, these results indicate that S1L reactivation events do not appear to be recognized by gB-CD8s, but the endogenous S1L-induced $CD8^+$ T cell response is equally effective as that of WT at reducing reactivation events.

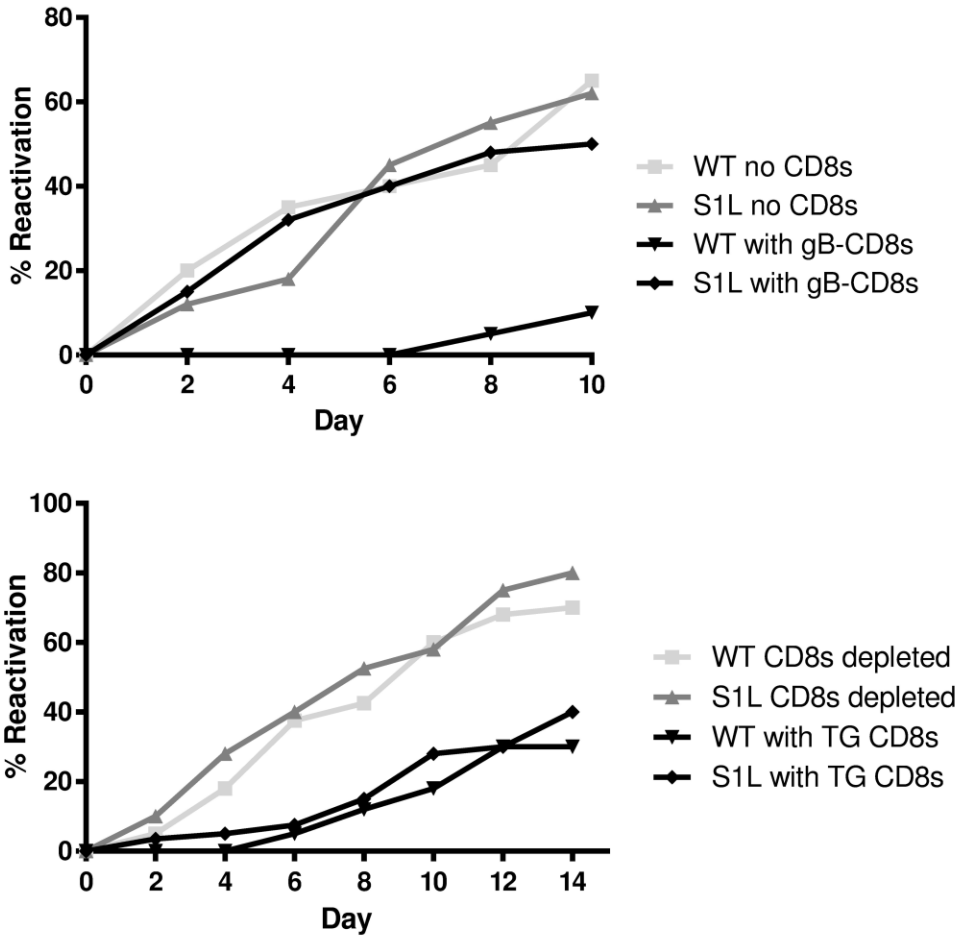

Figure 9. ***Ex vivo*** **ganglionic reactivation of WT and S1L HSV-1**

Corneas of B6 mice were infected with $1x10^5$ PFU of WT or S1L HSV-1. At 34 dpi latently infected TGs were dispersed with collagenase. **(A)** The TG cells were depleted at >95% of endogenous $CD8^+$ T cells and distributed to wells of a 48-well tissue culture plate (0.2 TG equivalent/well) and cultured in culture medium containing IL-2 alone, or with 2 x 10^4 gB-CD8s added per well**.** Culture fluid samples were removed and replaced with fresh media every two days. The presence of infectious virus in culture fluid (indicating HSV-1 reactivation) was then determined by plaque assay. **(B)** TG cells were mock depleted or depleted of 95% of endogenous $CD8^+$ T cells by treatment with anti-CD8α antibody and complement, then distributed to wells of a tissue culture plate and cultured as described in **A** above. (A & B) Data plotted as total percentage of wells that reactivated (showing infectious virus in culture supernatant) at the indicated time of culture. n=10 TG per condition. Data for each experiment are representative of one of two repeats, but experiment-to-experiment variability in reactivation rates are routinely observed. Studies completed by Sarah Bidula.

Our previous work demonstrated that the vast majority of $CD8^+$ T cells in WT HSV-1 acutely infected TG at 8 dpi are HSV-1 specific [77]. We considered several possible explanations for the compensated $CD8^+$ T cell TG infiltrate observed here (Fig 8) in the absence of gB-CD8s. We assessed if a $CD8^+$ T cell response developed to the mutated forms of the $gB_{498-505}$ epitope. B6WT3 fibroblasts were pulsed with the S1L, L8A, or WT $gB_{498-505}$ peptides and co-cultured with $CD8^+$ T cells from TGs of S1L, L8A, or WT infected B6 mice. The ability of $CD8^+$ T cells to recognize these peptides was determined by staining $CD8^+$ T cells for intracellular IFNγ production (Fig 10). Ganglionic $CD8^+$ T cells induced by a WT HSV-1 infection responded robustly to stimulation with WT peptide-pulsed fibroblasts, but failed to respond to B6WT3 cells pulsed with S1L and L8A peptides. This suggested there is little or no cross-recognition of the mutant peptides by gB-CD8s. Furthermore, the compensatory ganglionic $CD8^+$ T cell populations induced by HSV-1 S1L or L8A infection failed to produce IFNγ when stimulated with fibroblasts pulsed with any of the 3 peptides (Fig 10). This strongly suggested that the compensation of the ganglionic $CD8^+$ T cell response was not due to the development of $CD8^+$ T cells directed to the mutated gB peptides.

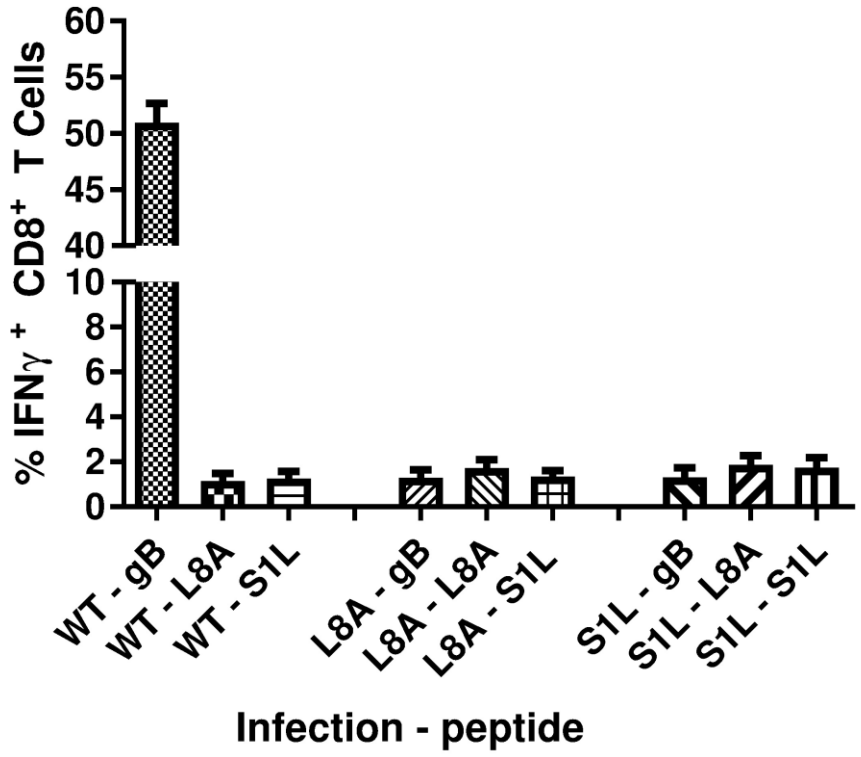

Figure 10. Stimulation of acute TG-resident CD8$^+$ T cell populations with WT, SIL, or L8A gB peptides

B6 mice received corneal infections with HSV-1 expressing WT, S1L, or L8A gB. TG were obtained at 8 dpi, dispersed into single cell suspensions, and the endogenous CD8$^+$ T cells were stimulated for 6 hours with B6WT3 fibroblasts pulsed individually with WT, S1L, or L8A $gB_{498-505}$ peptides, in the presence of brefeldin A. Cells were surface stained for CD45 and CD8, followed by an intracellular stain for IFNγ. The data are represented as the mean percentage of CD8$^+$ T cells that produced IFNγ +/- SEM (n=5 mice per group). * represents significance of $p<0.0001$ for each group compared to gB peptide stimulation of wild-type infected control (first column) using one-way ANOVA with Dunnett's multiple comparisons posttest.

4.3 A COMPENSATORY RESPONSE TO HSV-1 SUBDOMINANT EPITOPES IN S1L-INFECTED TG

We next addressed the possibility that the compensatory CD8$^+$ T cell responses to S1L contained an expansion of CD8s directed to other HSV-1 epitopes. CD8$^+$ T cells obtained from TG of mice infected with either WT or S1L HSV-1 were assessed both for total ganglionic CD8$^+$

T cell infiltrates (Fig 11A) and for their ability to be stimulated by infected fibroblasts at different times post-infection (Fig 11B and 11C). The total ganglionic $CD8^+$ T cell infiltrate for both WT and S1L showed a similar characteristic peak at 8 dpi and a subsequent contraction by 30 dpi (Fig 11A). However, at 16 dpi S1L infected TGs had a significantly smaller $CD8^+$ T cell infiltrate, suggesting a more rapid $CD8^+$ T cell contraction occurred.

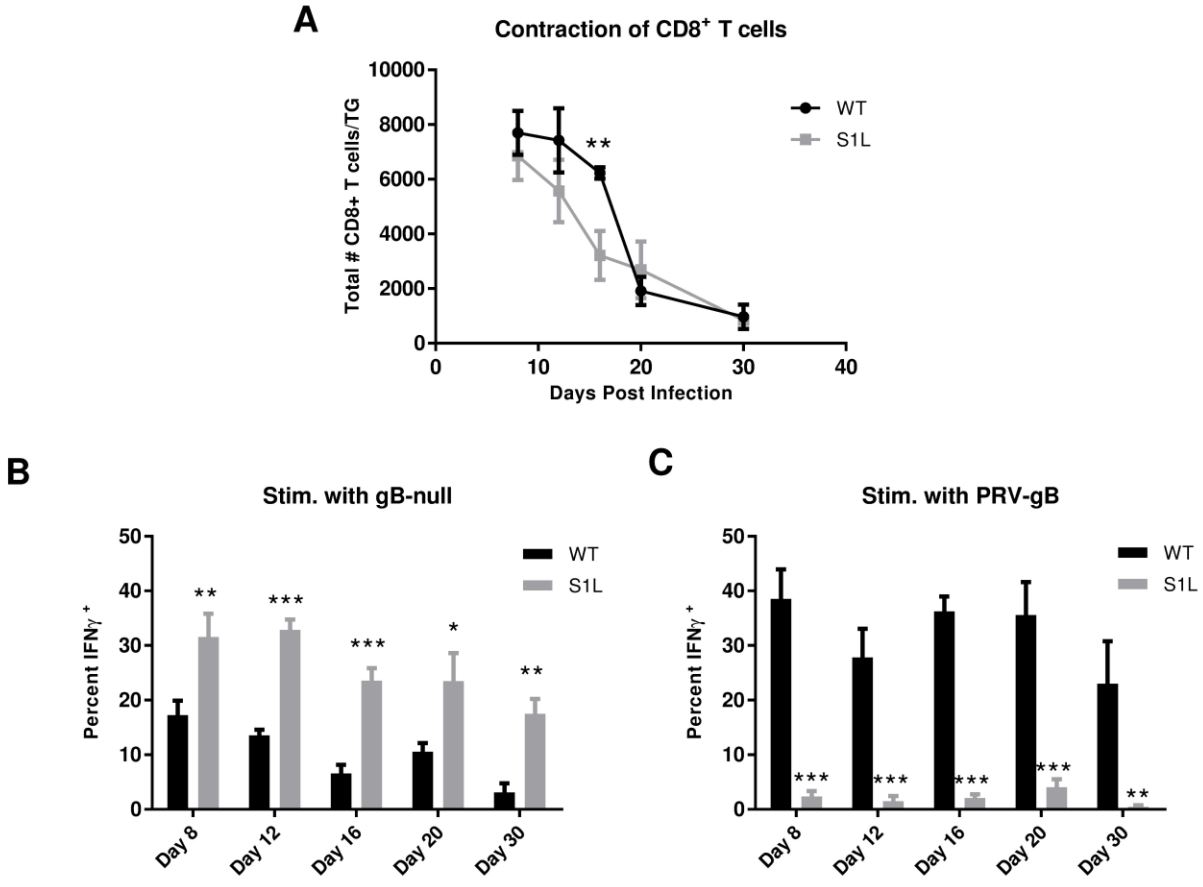

Figure 11. The $CD8^+$ T cell population in S1L infected TG contract more rapidly and contain a higher frequency of active non-gB-CD8s

B6 mice received corneal infections with either WT or the S1L mutant at $1x10^5$ PFU/cornea. TGs were harvested at 8, 12, 16, 20, or 30 dpi and: **(A)** stained for CD45, CD3, and CD8, analyzed by flow cytometry, and data recorded as the mean number of $CD8^+$ T cells/TG; or stimulated for 6 hrs with **(B)** HSV-1 gB-null(EGFP) infected or **(C)** PRV-gB infected B6WT3 fibroblasts in the presence of Brefeldin A. The cells were then stained for surface CD45, CD3, and CD8 and for intracellular IFNγ. Data in B and C are presented as the mean ± SEM frequency of $IFN\gamma^+$ $CD8^+$ T cells in each TG as a fraction of total $CD8^+$ T cells. * $p<0.05$, ** $p<0.01$, ***$p<0.001$ based on a t-test comparison at each time.

To assess the response to non-$gB_{498-505}$ HSV-1 epitopes, TG from WT or S1L infected mice during latency were dispersed, stimulated for 6 hrs with B6WT3 fibroblasts infected with HSV-1 gB-null-EGFP virus, and intracellular IFNγ in $CD3^+CD8^+$ T cell populations was measured by flow cytometry (Fig 11B). We found a significantly higher frequency of $IFN\gamma^+$ $CD8^+$ T cells in S1L-infected TG compared to WT infected TG following stimulation with UV-irradiated B6WT3 cells infected with HSV-1 lacking gB. At the acute stage (8 dpi), the frequency of S1L stimulated CD8s was approximately twice that of the WT-stimulated $CD8^+$ T cells. Intriguingly, in a WT infection, the fraction of ganglionic non-gB-CD8s responding to antigen drops over time. These data are consistent with our observation that in WT infected TG, $CD8^+$ T cells specific for subdominant HSV-1 epitopes become functionally compromised by 30 dpi (14). However, we found that while non-$gB_{498-505}$ $CD8^+$ T cells in an S1L infection also dropped as latency was established, over 4x more non-gB-CD8s responded to infected target cells by producing IFNγ in this assay. This is more than can be explained by a simple doubling of stimulated cells to fill the gB-CD8 compartment. Rather, this observation suggests that the non-gB-CD8s still target HSV-1 epitopes and are more functional in TG infected with HSV-1 S1L.

To separately assess $CD8^+$ T cell responses to the gB immunodominant epitope in a similar assay, we stimulated $CD8^+$ T cells obtained from S1L and WT latently infected TG for 6 hrs with B6WT3 cells infected with a recombinant pseudorabies virus (PRV) that expresses the HSV gB residues 494-509 containing the HSV immunodominant peptide (SSIEFARL) under control of the CMV promoter (PRV-gB) and measured intracellular IFNγ (Fig. 11C). $CD8^+$ T cells in S1L infected TG responded minimally to stimulation with the PRV-$gB_{494-509}$ virus infected cells whereas $CD8^+$ T cells in WT HSV-1 infected TG showed a robust response that

was maintained throughout the establishment of latency. These data agree with our previous finding that $CD8^+$ T cells specific for the immunodominant $gB_{498-505}$ epitope remain highly functional in TG latently infected with WT HSV-1 (14). They also demonstrate that $CD8^+$ T cells in S1L-infected TG do not cross react to any presented PRV MHC-I epitopes in this assay. These results indicate that the compensatory response to S1L in the ganglia appears to reflect an increased number of $CD8^+$ T cells directed to HSV epitopes other than $gB_{498-505}$, and that these $CD8^+$ T appear more functional in S1L infected TG compared to those in TG infected with WT HSV-1.

4.4 EFFICIENT TG-RETENTION OF $GB_{498-505}$ SPECIFIC $CD8^+$ T CELLS REQUIRES ANTIGEN

It was previously shown that activated, exogenously introduced, non-HSV-specific OT-I $CD8^+$ T cells could enter the TG during acute infection, but were not retained in the TG over time, presumably due to lack of cognate antigen recognition within the tissue [114]. The availability of an HSV-1 variant lacking the immunodominant peptide allowed us to assess the necessity of HSV-1 antigen presence in retaining ganglionic $CD8^+$ T cell populations *in vivo.* We performed simultaneous corneal infections with the S1L virus lacking the immunodominant $gB_{498-505}$ epitope in conjunction with ocular or flank infections with WT virus (Fig 12A). These infection models were designed to induce a systemic $CD8^+$ T cell response to the $gB_{498-505}$ epitope and assess the retention of that response under conditions where the epitope was or was not expressed in the TG. As expected, mice receiving corneal infection of either WT or S1L virus developed acute systemic and TG $CD8^+$ T cell responses that contained or lacked the gB_{498-}

$_{505}$ specific $CD8^+$ T cell populations, respectively (Fig 12B and 12C). When a $gB_{498\text{-}505}$ specific $CD8^+$ T cell response was primed in S1L ocular infected mice by coinfection with WT HSV-1, either in the other eye or by flank infection, we noted that the infiltrate of the S1L infected TG contained a $CD8^+$ T cell response to $gB_{498\text{-}505}$. Indeed, the $CD8^+$ T cell infiltration of the S1L- and WT-infected TG were quite similar at 8 dpi, with equivalent levels of both gB-CD8s and non-gB-CD8s. These data fit with the previously reported observation that acute ganglionic infection draws most or all activated $CD8^+$ T cells into the ganglia [114]. However, a different pattern emerged by 30 dpi at HSV latency. In WT latently infected TG, irrespective of whether or not they received simultaneous corneal infection with S1L virus, an approximate 50:50 proportion of gB-CD8 to non-gB-CD8 T cells was retained during latency (Fig 12D). However, in S1L latently infected mice that were co-infected with WT virus ocularly or by flank infection, the gB-CD8 populations were greatly reduced by 30 dpi in the S1L infected ganglia. These results strongly support the conclusion that while most activated $CD8^+$ T cell populations can infiltrate the ganglia at acute stages of infection, the maintenance of ganglia-resident HSV-specific $CD8^+$ T cell populations requires antigen expression within the TG.

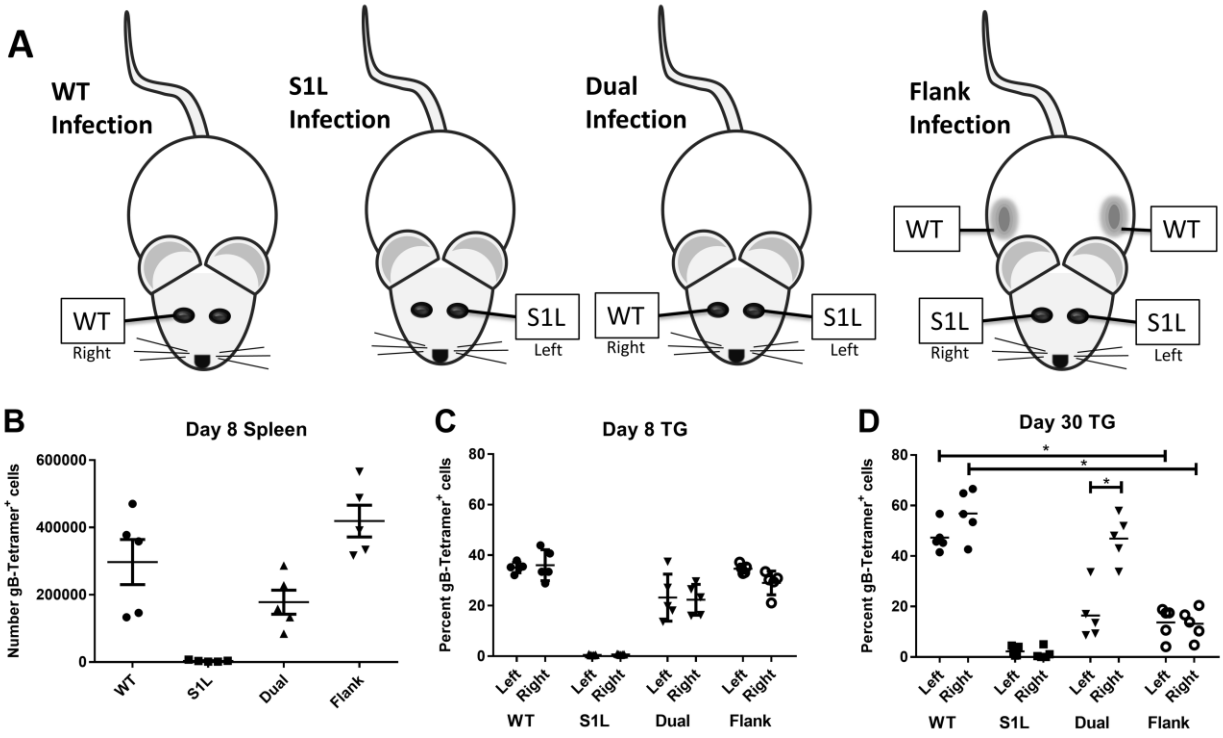

Figure 12. gB-CD8$^+$ T cell retention in the HSV-1 latently infected ganglia is dependent on antigen expression

(A) Representation of infection models in which mice received unilateral corneal infections with WT (WT only) or S1L (S1L only) HSV-1, bilateral infections with WT on one cornea and S1L on the other cornea (dual infection); or bilateral corneal infection with S1L and flank infection with WT HSV-1. All corneal infections were with $1x10^5$ PFU/scarified cornea, and flank infections were with $1x10^6$ PFU on a scarified flank. At 8 or 30 dpi, TG and spleen suspensions were analyzed by flow cytometry for CD45, CD3, CD8, and gB-tetramer. **(B)** Total number of gB-tetramer$^+$ cells/spleen. **(C and D)** Frequency of CD3$^+$CD8$^+$ T cells in the TG that are gB-tetramer$^+$. * Statistical significance by one-way ANOVA with $p<0.01$.

4.5 DEFINING THE ANTIGENIC REPERTOIRE OF THE CD8$^+$ T CELL RESPONSE TO HSV S1L

Virtually the entire CD8 antigenic repertoire to WT HSV-1 in B6 mice was recently defined [77]. This gave us the opportunity to examine the specific nature of the compensation to HSV-1 subdominant epitopes. We utilized the known HSV-1 subdominant epitope library to determine the size of each subdominant-epitope population that responds to peptide within the

TG. HSV-1 induced $CD8^+$ T cells infiltrating the ganglia at 8 dpi were evaluated for their ability to produce cytokines following stimulation with B6WT3 cells pulsed with each known epitope. For WT HSV-1, just over half of the $CD8^+$ T cells in the TG of infected mice at 8 dpi responded to the immunodominant $gB_{498\text{-}505}$ epitope, while the remaining $CD8^+$ T cells responded at much lower levels to the 19 subdominant epitopes reported previously, with the addition of one minor epitope that is discussed below [77]. In contrast, $CD8^+$ T cells infiltrating S1L infected TG showed no reactivity to the $gB_{498\text{-}505}$ epitope, but showed a statistically significant increase in responses to most of the tested subdominant epitopes (Fig 13A). The response to a few subdominant epitopes remained statistically unaffected in the HSV S1L induced $CD8^+$ T cell population, though an overall trend of increased levels was evident. Epitopes that featured prominently in the altered dominance hierarchy induced by HSV-1 S1L included RR1 (ribonucleotide reductase large subunit 1, UL39), with T cell epitope frequencies being the most abundant ($RR1_{982\text{-}989}$) and fourth most abundant ($RR1_{822\text{-}829}$) in the altered hierarchy. Interestingly, $gB_{560\text{-}567}$ rose to position two in the hierarchy. Addition of the fractions responding to each peptide indicated that most of the $CD8^+$ T cells were accounted for, with the fraction responding to each epitope adding to a total of 125.6 $^+$/-33.8 percent (Fig 13B). This strongly suggests that the compensation was not a result of the development of significant $CD8^+$ T cell populations to new epitopes, although we cannot exclude the possibility that minor populations directed to previously unreported epitopes were present in HSV-1 S1L infected mice. We also evaluated a subgroup of five of the specific epitopes for recognition by the HSV-1 L8A-induced ganglionic $CD8^+$ T cell response, and the results suggested this virus induced a similar compensatory response to that of S1L (Fig 13C). Finally, it was reported by Stock, et al. (2007) that the systemic response to the only known epitope at that time ($RR1_{822\text{-}829}$) did not expand

systemically; In contrast, we found that $RR1_{982-989}$-specific $CD8^+$ T cells, defined by tetramer, were expanded at both acute and late times (Fig 13D). These results indicate that the compensatory $CD8^+$ T cell response to HSV-1 lacking the immunodominant gB epitope at 8 dpi is due to increased $CD8^+$ T cell populations directed to the other tested subdominant epitopes.

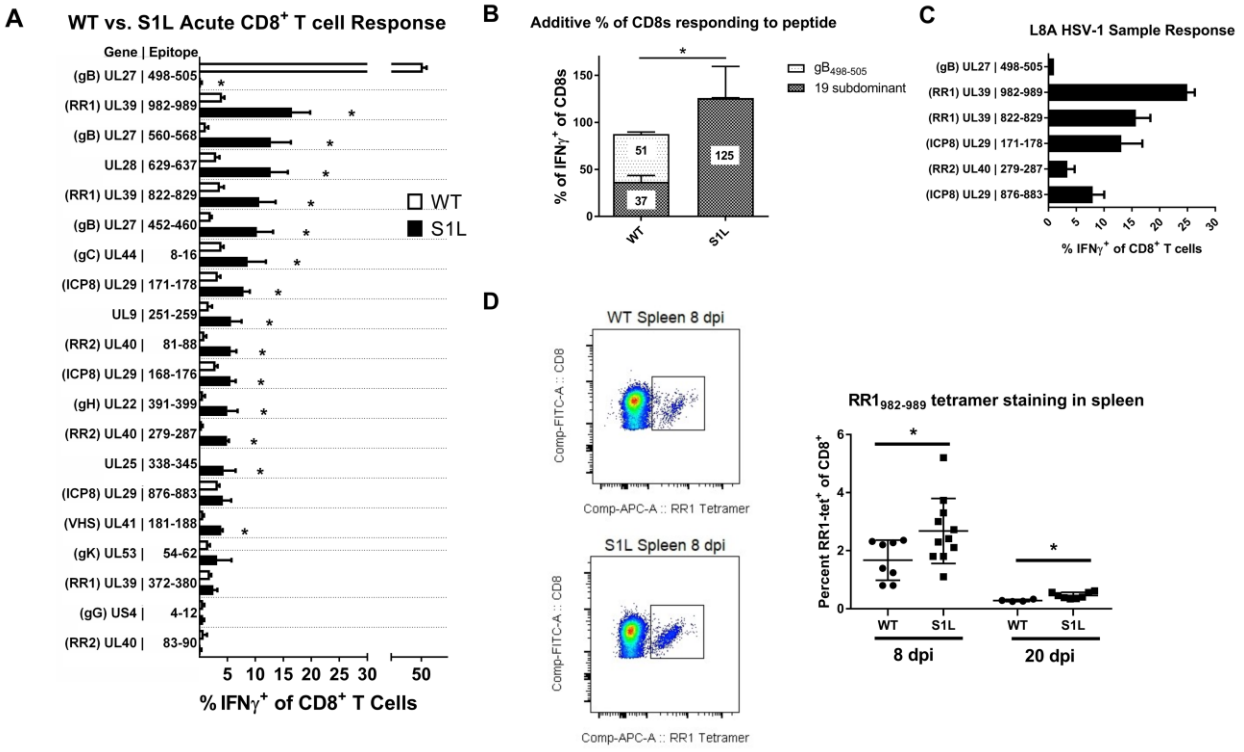

Figure 13. Subdominant HSV-1 epitopes expand to accommodate the loss of the immunodominant $gB_{498-505}$ epitope during acute infiltration into the TG

B6 mice received corneal infections with **(A, B, D)** HSV-1 WT, S1L, or **(C)** L8A. TG were excised at 8 dpi, dispersed into single cell suspensions, stimulated for 6 hrs in the presence of Brefeldin A with B6WT3 cells pulsed with peptides corresponding to known HSV-specific $CD8^+$ T cell epitopes, stained for surface CD45 CD8, and intracellular IFNγ. **(A)** The graph shows the percent of the total $CD8^+$ T cell population staining for intracellular IFNγ by flow cytometry. The bars represent the mean ± SEM frequency of $CD8^+$ T cells producing IFNγ in response to each epitope. **(B)** Total fraction of $gB_{498-505}$ or non-gB-CD8s responding to peptide stimulations as seen in (A). N = 3-8 TG equivalents per peptide. **(C)** A fraction of the peptide library was analyzed as in (A), but for the HSV-1 L8A. **(D)** Spleens were also excised at 8 and 20 dpi and examined for $RR1_{982-989}$ tetramer positive cells. Shown is example of tetramer staining, and a graph depicting the total fraction of splenic CD8+ T cells that stained positive for tetramer. A t-test was performed for each matched pair of responding $CD8^+$ T cells, and * denotes $p<0.05$. Some studies completed with help from Sarah Bidula.

Intriguingly, a quite different pattern emerged at 30 dpi, when HSV-1 is considered to be latent. The total average numbers of non-gB $CD8^+$ T cells per latently infected ganglion that produce $IFN\gamma^+$ in response to peptide presentation (Fig 14A). In a WT infection, the ganglionic $CD8^+$ T cells to $gB_{498\text{-}505}$ still responded to stimulation with peptide pulsed cells, and accounted for nearly half of the total $CD8^+$ T cells detected in the ganglia (Fig 14B). However, the combined non-gB-CD8 populations in WT HSV-1 infected TG showed a much poorer response, with a total of only 27.3% of the subdominant CD8s producing IFNγ when stimulated with each of the subdominant peptides on B6WT3 cells. These data fit well with earlier reports indicating that a significant fraction of the non-gB-CD8s in the WT latently infected ganglia are not able to respond efficiently to antigen[147]. In contrast, the landscape of epitopes to which S1L induced $CD8^+$ T cells can respond was changed dramatically, with 3-4 epitopes rising to prominence or co-dominance (Fig 14A). The most prominent responses were to $UL28_{629\text{-}637}$(DNA packaging terminase), $ICP8_{168\text{-}176}$, and the two large subunit ribonucleotide reductase epitopes; $RR1_{982\text{-}989}$ and $RR1_{822\text{-}829}$. This contrasts to the sub-dominant response hierarchy against WT HSV-1, which changed little over time. Secondly, when the $CD8^+$ T cells from S1L latently infected ganglia that responded to peptide were totaled, 89.3 ± 16.5% of the $CD8^+$ T cells were functionally able to produce IFNγ upon stimulation (Fig 14B). This does not simply reflect enrichment due to the lack of a $gB_{498\text{-}505}$ response since the proportion of functional non-$gB_{498\text{-}505}$ cells in this assay were significantly higher (Fig 14C). This is also in line with the data presented in figure 11B showing that loss of the immunodominant epitope results in a functional increase in non-gB-CD8s at latency.

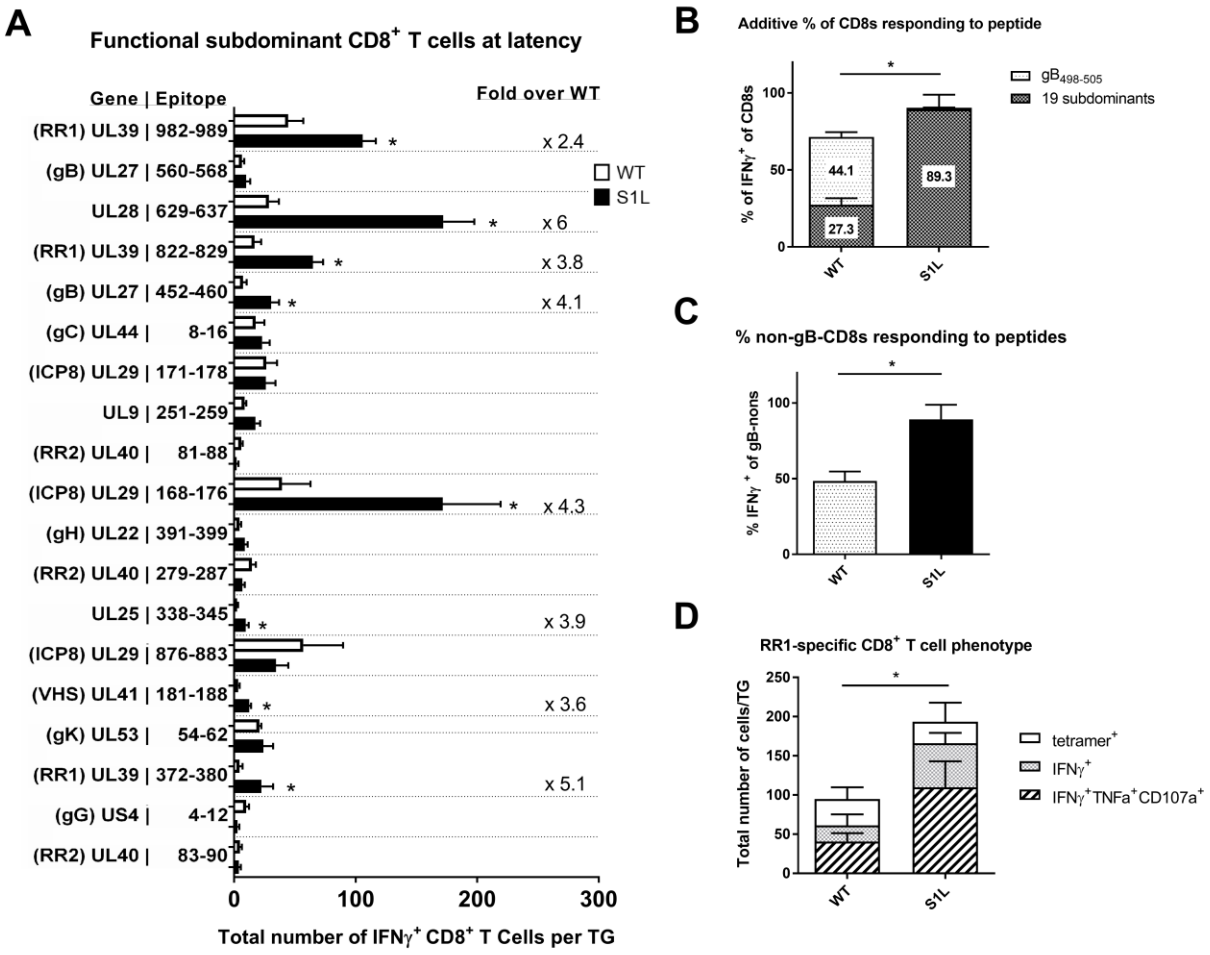

Figure 14. Certain subdominant HSV-1 epitopes become more functional and arise to codominance in TG during HSV-1 S1L latency

Studies were as detailed in Figure 13, except that TGs were harvested from infected mice at 30-33 dpi. **(A)** The order of epitopes is identical to those shown in Figure 13. For clarity, only the non-$gB_{498-505}$ responses are shown in A, but the total percentages are displayed in (B). The bars represent the total number of $CD8^+$ T cells producing $IFN\gamma^+$ in response to peptide stimulation, and error bars represent SEM. For significantly different populations, the average fold change increase in population over wild-type is shown. **(B)** Total fraction of $gB_{498-505}$ or non-gB-CD8s depicted in figure (A) that are responding to peptide stimulations. **(C)** Total fraction of the non-$gB_{498-505}$ specific CD8+ T cells depicted in figure (A) that make IFNγ after peptide stimulation. **(D)** 30 dpi TGs suspensions were stained with tetramers specific to RR1-specific subdominant CD8+ T cell populations (tetramers for RR1 982-989 and 822-829). Shown are the total number of each RR1-specific CD8+ T cell population per TG. The total number of single functional ($IFN\gamma^+$) or multifunctional ($IFN\gamma^+TNF\alpha^+CD107a^+$) $CD8^+$ T cells after stimulation with a combination RR1 982-989 and 822-829 peptides is also shown. N = 3-7 TG equivalents per group. A t-test was performed for each matched pair of responding $CD8^+$ T cells, and a * denotes $p<0.05$. Some studies completed with help from Sarah Bidula.

Comparing the total fraction of a $CD8^+$ T cell population present by tetramer, to that identified by IFNγ production after peptide stimulation should tell us what percentage of that specific population is functional. We could not obtain working tetramers for most CD8 populations described here, but we were able to further characterize the functionality of $RR1_{982-989}$ and $RR1_{822-829}$ $CD8^+$ T cell populations. This was done both by tetramer staining, and by determining multifunctionality (ability to produce multiple cytokines) following a peptide stimulation (Fig 14D). In a wild-type infected TG at latency, about 95 $CD8^+$ T cells stained positive for these tetramers, with about 64% of these cells producing IFNγ, and 43% exhibiting multifunctionality ($IFN\gamma^+$, $TNF\alpha^+$, and $CD107a^+$) after stimulation. In contrast, an average of about 204 $CD8^+$ T cells were tetramer positive in an S1L infected TG, with 84% capable of producing IFNγ, and 54% being multifunctional. This increase in functionality was statistically significant. Taken together, these results suggest that the presence of a strongly immunodominant $CD8^+$ T cell population in latently infected ganglia adversely affects the functionality of those T cells reactive to subdominant epitopes.

4.6 DISCUSSION

Given the general propensity of $CD8^+$ T cells to recognize only a limited and highly restricted array of the potential epitope repertoire of a pathogen and develop a hierarchical response to them, it is important to understand how the presence or absence of one epitope, particularly an immunodominant epitope, influences the functionality and hierarchy of the $CD8^+$ T cell response to others for a specific pathogen. Recent studies have revealed that HSV-1 specific $CD8^+$ T cell responses to prior HSV infections in humans are highly limited, with only

select proteins arising to dominance or co-dominance[162]. The unusually strong immunodominance to $gB_{498-505}$ in the B6 mouse model of HSV-1 infection and its known $CD8^+$ T cell hierarchy makes it a highly suitable and manipulatable model to address the issue of how loss of one epitope affects the remaining response. Previously, the nature of CD8 compensation for loss of immunodominance could not be more precisely defined for HSV, because the HSV-specific $CD8^+$ T cell repertoire in B6 has only recently been described [77]. That study demonstrated that the entire HSV-1 $CD8^+$ T cell repertoire generated in the spleen was represented and not significantly modified in the TG, and that the vast majority of $CD8^+$ T cells in the acutely infected TG at 8 dpi were HSV-specific [114].

Prior to this work, only one study had addressed the question of immunodominance loss in HSV-1, wherein B6 mouse skin infection with the HSV-1 L8A point mutation in the $gB_{498-505}$ epitope was shown to induce a normal-sized expansion of HSV-specific $CD8^+$ T cells in the spleen that lacked any specificity for the immunodominant $gB_{498-505}$ epitope [160]. However, the authors concluded that the compensation reflected an additional response to previously unrecognized cryptic epitopes, based largely on the observation that $CD8^+$ T cells to the one known subdominant HSV-1 epitope defined at that time, $RR1_{822-829}$, were not increased in frequency of recognition by the compensated response. This finding is similar to a study by Holtappels et. al with murine cytomegalovirus (MCMV), wherein they demonstrated that deleting two MCMV immunodominant $CD8^+$ T cell epitopes resulted in an altered immune response that was still protective, but contained small changes to known subdominant $CD8^+$ T cells to known epitopes, with one specific epitope identified as rising in the absence of these deletions [163]. Similarly, Kotturi et. al deleted several immunodominant epitopes within Lymphocytic Choriomeningitis virus (LCMV), and show the altered immune response contained

only limited increases in the subdominant $CD8^+$ T cell hierarchy [164]. In our current study, we have found a somewhat different result in HSV-1 latently infected ganglia. Here we define the complete nature of the compensatory response in the TG and show a broad increase in the numbers and function of subdominant CD8 populations. Furthermore, assessment of the splenic response for one epitope indicates that at least part of the subdominant compensation occurs systemically in our model (Fig 9).

Of the several recombinant viruses developed to lack the $gB_{498\text{-}505}$ epitope, two retained WT levels of pathogenicity in the mouse model. We chose S1L for most of the detailed studies, since L8A trended toward a marginally reduced ganglionic infiltrate in the TG (Fig 4) although differences were not significant [160]. Reduced virus replication in the eye or TG may affect the level of antigen available for $CD8^+$ T cell priming, recruitment and/or retention, as has been observed in the LCMV model [165]. S1L not only established latency with the same genomic loads as WT HSV-1, but also reactivated to the same efficiency in the absence of T cells. Both S1L and L8A viruses induced total ganglionic $CD8^+$ T cell responses numerically identical to WT, despite the fact that the ~50% $gB_{498\text{-}505}$ specific response was absent. Importantly, we show that neither S1L nor L8A virus induced a $CD8^+$ T cell response to the native or mutated $gB_{498\text{-}505}$ epitope, as demonstrated by priming and peptide stimulation assays (Fig 6). The lack of response to the S1L modified $gB_{498\text{-}505}$ epitope was also established by demonstrating that (i) $CD8^+$ T cells from mice infected with WT HSV failed to respond to the S1L modified gB protein: (ii) $CD8^+$ T cells in TG harboring the S1L virus showed negligible binding to tetramers containing the native $gB_{498\text{-}505}$ epitope; and (iii) $gB_{498\text{-}505}$-specific $CD8^+$ T cells that effectively prevented reactivation of the parental wild-type HSV-1 strain had no effect in reducing reactivation of S1L from latently infected TG in *ex vivo* cultures. The epitope-specific nature of

the reactivation blockade by gB-CD8s (Fig. 5) also provides strong evidence that MHC-I presentation and cognate $CD8^+$ T cell recognition are absolutely required to stop viral exit from latency in this model. This is consistent with our previous finding that HSV-1 specific $CD8^+$ T cells from C57BL/6 mice can block HSV-1 reactivation in latently infected TG of C57BL/6, but not BALB/c mice [68], and contrary to a recent study suggesting that $CD8^+$ T cells do not control HSV-1 reactivation events[166].

The nature of the compensatory $CD8^+$ T cell response in the acute infected TG to an immunodominant epitope-mutated HSV-1 reported here appears to be predominantly or entirely due to CD8s specific to other HSV-1 epitopes (Fig 7B). The compensatory increase of subdominant $CD8^+$ T cell responses to epitope deleted viruses has been seen in other viruses, for example, following infection with an influenza virus that lacked an immunodominant epitope [167]. However, $CD8^+$ T cell compensation was not observed following infection with epitope deleted LCMV, where the $CD8^+$ T cell response was both numerically reduced and delayed [168, 169]. As noted by Stock et al [160] it is not clear if this difference in the ability to compensate for the loss of an immunodominant epitope reflects the difference between a local infection, like influenza and HSV-1, and a systemic infection like LCMV. Our studies using B6WT3 cells pulsed with each of the 19 known subdominant $CD8^+$ T cell epitopes to stimulate IFNγ expression in $CD8^+$ T cells indicate that most subdominant CD8 populations increased in size to compensate for the loss of an immunodominant epitope. The added total $CD8^+$ T cell response accounts for all (125.6% ± 33.8%) $CD8^+$ T cells in S1L acutely infected TG, not only confirming that they are still HSV-1 specific, but suggesting negligible induction of $CD8^+$ T cells specific for new cryptic HSV-1 epitopes. One possible exception to this is $UL25_{338\text{-}345}$, which was a low frequency epitope identified, but not reported, in our previous study[77]. This $CD8^+$ T cell

population was identified as a small response (~0.2% of the total) in WT HSV-1 infections in our initial screen, but not in the subsequent repeat, suggesting a possible low frequency response in WT HSV-1. In an S1L infection, however, this epitope represented ~4% of the total acute TG infiltrate. We interpret this finding as an expansion of an existing low-frequency epitope-specific $CD8^+$ T cell response. While we cannot exclude the possibility that S1L induced additional $CD8^+$ T cell populations arising to new or cryptic epitopes, these would necessarily be small populations that would be difficult to identify via peptide library screening.

The change in the acute dominance hierarchy in the absence of the immunodominant $gB_{498\text{-}505}$ epitope was not predictable. Compared to WT, the frequency of acute $CD8^+$ T cells in the TG reactive to some epitopes such as $UL39_{982\text{-}989}$ increased 4-fold, while the response to others such as $UL29_{876\text{-}883}$ were only modestly increased. The response to others such as $US4_{4\text{-}12}$ showed little change compared to WT. However, 14 of the 19 subdominant $CD8^+$ T cell populations in the S1L infected ganglia showed a significant increase (Fig 9). The reason for this differential rise of epitope-specific $CD8^+$ T cell responses in the absence of the immunodominant epitope is not clear. Priming of the initial $CD8^+$ T cell hierarchy as well as expansion of memory subsets are very dependent on the context of naïve T-cell-APC interactions, and T cells directly compete for antigen on APCs very early in this process[170-172]. $CD8^+$ T cell population hierarchies also depend on naïve precursor frequency as well as peptide processing and MHC binding strength[164]. Selection in our model is not completely attributable to MHC binding capacity, since epitopes that changed little in the dominance hierarchy such as $UL29_{876\text{-}883}$ and $UL40_{83\text{-}90}$ were previously reported [77] to have higher MHC-binding capacity (IC_{50} = 6.2 nM and 5.4 nM, respectively). Epitopes such as gB_{560} that rose substantially in the S1L dominance hierarchy had a much lower MHC binding capacity (IC_{50} =

9206 nM). The naïve precursor frequencies for the full HSV-specific response in our model have not yet been fully explored, but are outside the scope of this study. The kinetics of viral protein production are also likely to influence $CD8^+$ T cell hierarchy, since a majority (~80%) of the epitopes recognized by $CD8^+$ T cells in B6 mice are encoded by viral early (β) and leaky late (γ1) genes. This would be consistent with our previous finding that expressing gB as a true late (γ2) gene greatly reduced $gB_{498\text{-}505}$ immunodominance [153]. Other studies using MCMV, Vaccinia, and Epstein-Barr epitopes also suggest that the context and kinetics of viral antigen expression contribute heavily to CD8 immunodominance, with the trend of stronger and earlier expression and presentation being important for the development of immunodominant CD8 populations[173-176]. However, we note differential rise to dominance of epitopes on the same viral protein in TG infected with S1L, suggesting that the level of expression of a particular viral gene product cannot by itself explain changes in immunodominance.

In the LCMV model it has been observed that when the virus is cleared acutely, the lasting memory $CD8^+$ T cell hierarchy is maintained at similar proportions, but when a chronic strain is used, the hierarchy changes over time[177]. It is thus intriguing that the hierarchy at latency in the S1L-infected TG is quite different from the hierarchy at acute infection. With our dual eye infection or flank infection models, we show that gB-CD8s are not retained in TG latently infected with the S1L virus that lacks this epitope (Fig 8), agreeing with previously published data demonstrating that antigen is necessary to effectively maintain exogenously added memory $CD8^+$ T cells in nonlymphoid tissues[136, 178]. Thus, differential expression of viral proteins or peptides during contraction/latency appears to be one among a complex set of mechanisms that define the $CD8^+$ TCR repertoire in latently infected TG. This indicates a requirement for ongoing antigen detection to maintain memory $CD8^+$ T cells in TG during

latency, and also implied ongoing recognition by non-gB-CD8s in the TG of latently S1L-infected mice during latency. Various levels of antigen recognition during the contraction phase may also explain the faster $CD8^+$ T cell contraction observed in the S1L infected TG at 16 dpi (Fig 7A). Although the pool of possible ganglionic memory $CD8^+$ T cells is shaped early in the lymphoid tissue, it is likely that competition for antigen recognition is a major factor responsible for determining which $CD8^+$ T cell populations are retained efficiently and which subsequently arise to prominence in latently infected TG.

We present several lines of evidence to suggest that the subdominant $CD8^+$ T cells in the S1L latently infected TG are more functional than those in the WT HSV-1 latently infected TGs. Specifically, in stimulations with gB-null HSV-1 infected cells, the fraction of responding CD8s in TG latently infected with S1L was four-fold higher than the fraction of responding cells in TG infected with WT virus (Fig 7B). This was considerably more than that expected from a simple doubling of numbers due to the compensatory response for loss of the gB-CD8s. In addition, the total number of all $CD8^+$ T cells responding to peptide stimulation in S1L latently infected TG was approximately twice that of the fraction of subdominant CD8s responding in a WT latent infection (Fig 10B). Indeed, the response seemed to account for most of the $CD8^+$ T cells in those S1L latently infected TG. Finally, measuring of two major subdominant populations directed to RR1 by parallel tetramer staining and analysis in response to peptide stimulation indicated that proportionally more of these RR1-specific cells show multifunctionality than do those same T cells from a WT latent infection (Fig 10C). Taken together, these data suggest that eliminating the strongly immunodominant $gB_{498\text{-}505}$ epitope increases the function of remaining $CD8^+$ T cells specific for some non-$gB_{498\text{-}505}$ HSV-1 epitopes.

We previously demonstrated that i) subdominant $CD8^+$ T cells have a higher frequency and express higher levels of PD-1 and show less apoptosis when PD-1 ligation is blocked within latently infected TG [148]; and ii) in vivo IL-10R blockade significantly increased the number, but not the frequency of subdominant $CD8^+$ T cells in TG latently infected with WT HSV-1, and increased their ability to block HSV-1 reactivation from latency in *ex vivo* TG cultures[147]. These characteristics are consistent with an exhausted phenotype. Here and in previous studies [147, 148] we show that TG that are latently infected with WT virus contain functionally exhausted subdominant CD8s, but near fully functional immunodominant gB-CD8s. Thus, in TG latently infected with WT HSV-1 the frequency of cytokine producing cells following peptide stimulation was similar to the frequency of the corresponding tetramer positive cells in the immunodominant population, but significantly lower in subdominant populations. Using the same analysis, we now show significantly reduced functional exhaustion of the subdominant $CD8^+$ T cells in TG that lack the $gB_{498\text{-}505}$ immunodominance. We further demonstrate a significantly increased number of multifunctional subdominant $CD8^+$ T cells in TG latently infected with HSV-1 lacking the immunodominant epitope when compared to those infected with WT HSV-1.

It is unclear why i) subdominant $CD8^+$ T cells become partially exhausted in latently infected TG while immunodominant $gB_{498\text{-}505}$-specific $CD8^+$ T cells retain nearly full functionality; and ii) subdominant $CD8^+$ T cells show less functional exhaustion in latently infected TG that lack the immunodominant population. Given the recent evidence demonstrating the unregulated nature of antigen expression in periods of phase 1 “animation” during latency[66], effective $CD8^+$ T cell surveillance of a variety of viral targets may provide better monitoring of neurons in the early stages of reactivation. There is likely an interplay between the

amount of leaky viral antigen presentation during latency and the number of specific $CD8^+$ T cells that can possibly "see" that antigen. However, this interplay may also explain the phenomena observed here- wherein there exist an apparently very low frequency of latently infected neurons that express viral proteins[67]. The absence of the $gB_{498\text{-}505}$-specific responses by immunodominant T cells may itself influence sporadic antigen expression during latency in the TG, which may change how other T cells see such expression in general. This may in turn affect the function of the subdominant T cells. Furthermore, in TG infected with WT HSV-1, the frequency of $gB_{498\text{-}505}$-specific $CD8^+$ T cells is high, reducing the likelihood of any one cell receiving the multiple exposures to cognate antigen required for functional exhaustion over time. In contrast, the frequency of subdominant $CD8^+$ T cell populations is low, increasing the likelihood of such repeat encounters with cognate antigen. In TG harboring latent S1L virus, the subdominant populations are greatly expanded, which should alter the dynamics and reduce the likelihood of repeat antigenic exposure. As such, the mechanisms underlying the functional differences may be very complex and multifactorial.

In summary, we have precisely defined the nature of a compensatory subdominant T cell response infiltrating the TG, a site of HSV-1 latency in our model, and show that it is due to expansion of the non-gB-CD8 populations. However, during latency, this population adopts a state where there are multiple $CD8^+$ T cell populations that rise to co-dominance, in part due to ongoing antigen expression within the TG during contraction. Furthermore, at latency these CD8s demonstrate an increased functionality compared to their WT-induced counterparts. This results in a broader repertoire of functional HSV-specific $CD8^+$ T cells, which should increase the set of antigenic targets that can be used by $CD8^+$ T cells to prevent HSV-1 reactivation from latency.

5.0 ALTERING PROMOTERS THAT DRIVE AN IMMUNODOMINANT HSV-1 EPITOPE INFLUENCES CD8$^+$ T CELL PRIMING, DEVELOPMENT, AND GANGLIONIC RETENTION AT LATENCY

Multiple factors influence the antigen hierarchy, function and breath of the CD8$^+$ T cell response to a specific pathogen. These include precursor frequency of T cells to a specific antigen, the level and chronicity of protein expression and the presentation of antigens to the developing T cells in the lymphoid organs in the priming process[164, 170-172]. For HSV, it is remarkable that the $gB_{498-505}$ epitope is so powerfully immunodominant and the important factors governing this are not clear. To investigate such factors, we recently detailed a study of the CD8$^+$ T cell response to a recombinant virus in which expression kinetics of gB were altered to $\gamma 2$ kinetics [153]. Indeed, this virus primed an effective immunodominant gB-CD8 response, but there were considerably less $gB_{498-505}$ specific CD8$^+$ T cells retained in the ganglia throughout latency, compared to the response directed to a wild-type HSV[153]. The data suggested that delaying the expression of gB results in reduced antigenic exposure during latency and less ganglionic retention of gB-CD8s. However, interpretation of these results was complicated by a growth impairment of the virus, most likely as a result of the elimination of some roles of gB early in infection. We therefore decided that a thorough analysis of the contribution of viral promoters and different kinetics of expression on CD8$^+$ T cell populations was further warranted.

Here, we evaluate the contributions of different viral promoters by exploiting a recently described recombinant HSV-1 in which the native $gB_{498-505}$ epitope is not present, but gB is expressed normally and appears to maintain its functions[155]. This was used to derive recombinant viruses in which the missing epitope was expressed at an ectopic site under the control of several different promoters. Thus, the immunodominant $gB_{498-505}$ epitope expression profile could be altered independently of the essential and important gB protein. It allowed us to address two questions: (1) can the immunodominance of the $CD8^+$ T cell population to $gB_{498-505}$ be increased by increasing expression of this epitope, or by expressing it from more active or earlier expressed viral promoters? and (2) does epitope expression from candidate late promoters alter the development of the $CD8^+$ T cell response and ganglionic retention? Establishing the requirements for efficiently eliciting and maintaining an effective $CD8^+$ T cell population throughout latency is vital for maintaining HSV-1 in its latent state. Here, we show that changing epitope expression does not appear to increase the immunodominant fraction of $CD8^+$ T cells beyond the WT levels of ~50%, but expression from different late promoters can influence overall $CD8^+$ T cell priming, ganglionic infiltration and retention of $CD8^+$ T cell populations associated with HSV -1 latency.

5.1 ECTOPIC EXPRESSION OF THE $GB_{498-505}$ PEPTIDE RESTORES A STRONG GB-CD8 T CELL RESPONSE

The goal of these studies was to determine how the activity of different constitutive, early, late and latency-active promoters influence the numerical and functional gB-CD8 response

in the HSV latently infected ganglia. We aimed to determine if the fraction of immunodominant gB-CD8s in the ganglionic $CD8^+$ T cell population could be increased by using promoters that mediate greater long-term expression. We were also interested in further evaluating how true-late γ2 promoters affect the hierarchy, since our previous data had suggested that γ2 promoter activity was poor at retaining gB-CD8 populations within the ganglia[153]. Finally, we aimed to determine if the promoter of LAT could be used to enhance the infiltrate. Given that HSV gB (containing the immunodominant $gB_{498\text{-}505}$ epitope) has multiple essential roles at several stages of HSV infection, we considered it unwise to adopt the same strategy, where expression of the complete gB was altered. Indeed, we found that altering the kinetics of gB expression to a true late gene had a fitness cost to the virus[153]. We therefore aimed to separate the peptide from the gB protein using a recently detailed recombinant HSV-1 that contains a single point mutation (S1L) in the $gB_{498\text{-}505}$ epitope that eliminates the priming and development of $gB_{498\text{-}505}$ specific $CD8^+$ T cells in B6 mice, but does not appear to alter virus fitness[155]. The S1L virus appears to be as pathogenically fit as wild type, generates an equivalent sized $CD8^+$ T cell response in the ganglia as seen with wild type virus, but gB-CD8s are not primed. Rather $CD8^+$ T cells to subdominant HSV-1 epitopes expand to fill the absent gB-CD8 T cell compartment[155]. In this background, we derived a recombinant HSV-1 that expressed a 4-mer of the $gB_{494\text{-}509}$ peptide as a GFP fusion protein, all under sequences containing the gB promoter (gBp), and placed at the gC locus (Fig 15A). Recombinant HSV-1 with insertions disrupting the expression of gC are not pathogenically impaired, compared to wild type HSV-1 KOS, in the corneal scarification B6 model[179]. When mice were infected by the ocular route with recombinant virus expressing the epitope ectopically (HSV gBp), we found an efficient generation of HSV-1 specific $CD8^+$ T cell responses in the TG-infiltrating population that contained $gB_{498\text{-}505}$ specific CD8s, detected using

$gB_{498-505}$ $H2K^b$ MHC-I tetramers, at 46.7%, a level not significantly different from that seen for WT HSV infected mice (Fig 15B). Thus, we can effectively separate expression of the SSIEFARL epitope from gB protein. This allows us to manipulate this epitope's expression without affecting essential protein gB, with both the kinetics of expression and its function in infection unaffected in our subsequent recombinant viruses.

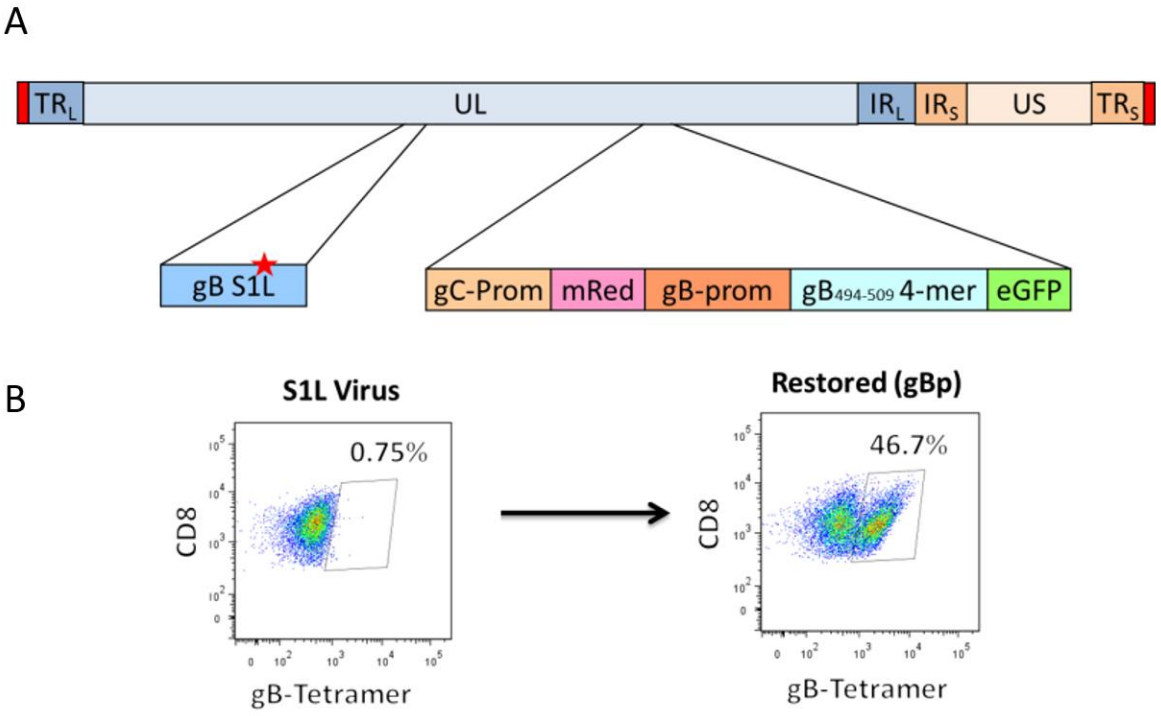

Figure 15. Ectopic restoration of $gB_{498-505}$ specific $CD8^+$ T cell response in S1L parental strain under gB promoter

A) Depiction of ectopically restored gB peptide expressing virus. In a gB-S1L point mutation parental strain, the native gC promoter drives a monomeric red fluorescent protein (mRed, mRFP), followed by an inserted gB promoter and $gB_{494-509}$ 4x repeat linked to EGFP. **B)** B6 mice infected at $1x10^5$ PFU/eye with either S1L parental strain or the ectopically restored gBp virus. At 8 days post infection, TGs were removed and single cell suspensions obtained as described in materials and methods. Resulting cell suspensions were stained with αCD45, CD3, CD8, and $gB_{498-505}$ tetramer. Depiction is representative of one of five similar results for each group, with flow cytometric analysis of $gB_{498-505}$ tetramer staining of the total ganglionic $CD45^+CD3^+CD8^+$ T cells shown.

5.2 EXPRESSION KINETICS OF THE $GB_{498-505}$ EPITOPE FROM DIFFERENT PROMOTERS IN RECOMBINANT HSV-1

Since we can restore the gB response with ectopic peptide expression, we used the same strategy to develop recombinant HSV-1 with different promoters driving expression of the $gB_{498-505}$ epitope. One goal was to determine if constitutive or potentially more active promoters might be capable of driving an even higher skewing of the $CD8^+$ T cell response to the gB epitope, over that made by the gB promoter in the wild-type virus. The constitutive CMV immediate early promoter (CMVp) and ICP0 immediate early promoter (ICP0p) were evaluated because they are known to be efficiently expressed during a viral lytic infection and the CMV IE promoter may be active during latency. We also evaluated the VP16 promoter (VP16p), which is expressed in a lytic infection with leaky-late or γ1 kinetics, like the gB protein. Intriguingly, recent work suggests that VP16 is controlled in ganglia as a "phase 1" gene, expressed before α genes in the context of murine HSV reactivation from latency [180]. We also evaluated three true late γ2 promoters to build on our previous studies[153], but without the complication of a considerably less fit virus background (from the gC, UL38, and UL41 genes; HSV-gCp, UL38p, and UL41p respectively). UL41 has been suggested to be expressed especially late in the infectious cycle, based on transcription analyses, with little to no transcript detectable 2 hours post infection[181]. Finally, we examined virus in which gB epitope was expressed from the full latency active promoter (LAP) which is responsible for abundant expression of LAT transcripts in neurons during latency[182-184].

Table 2. Promoters chosen for ectopic $gB_{498-505}$ peptide expression

Promoter	Description	Forward Primer 5'-3'	Reverse Primer 5'-3'
gBp	HSV-1 γ1 late promoter for glycoprotein B	GGATCCGGATCCGC ACGACGGGCCCCCG TAG	AAGCTTAAGCTTTA ATACAGCGCGGTGT TGG
CMVp	CMV α promoter, constitutive expression	GGATCCGGATCCCT GAGTCCGGTAGCGC TAGCGGATCTGACG GTTCACTAAA	AAGCTTAAGCTTTAG TTATTAATAGTAATC AATT
ICP0p	HSV-1 α promoter for ICP0	GGATCCGGATCCGG GTCGTATGCGGCTG GAG	AAGCTTAAGCTTACTT GCAAGAGGCTTTGTTC
VP16p	HSV-1 γ1 late promoter for the VP16 transactivator	GGATCCGGATCCGG TTGATACGGGAAAG ACGATATC	AAGCTTAAGCTTCACG GCGACTCGAGGGCGT TC
gCp	HSV-1 γ2 late promoter for glycoprotein C	Native promoter region	Detailed in methods
UL38p	HSV-1 γ2 late promoter for UL38 capsid protein	GGATCCGGATCCTG GTCTTCATTGCGAC CAC	AAGCTTAAGCTTTGCC GTCTCGGCCGTGGG
UL41p	HSV-1 γ2 late promoter for UL41, Virion host shutoff gene	GGATCCGGATCCGA TGTCAGGTCAATTG TAA	AAGCTTAAGCTTCGG CGCCCTGCAGGACCAC
LAP	Full 2kb HSV-1 LAP1/2 promoter for LAT	Fragment generated by restriction digestion	Detailed in methods

All recombinant HSV-1 in this study contained the epitope expression cassette at the gC locus and were derived using classical homologous recombination. Expression of red fluorescent proteins from the gC locus was used to plaque purify virus to homogenous recombinant stocks. Infectious virus was gradient purified for all subsequent studies. A fitness study of each recombinant virus using a single-step growth curve in Vero cells showed no significant differences in growth, compared to both the KOS parental strain (Fig 16) and the HSV-1 S1L parental virus.

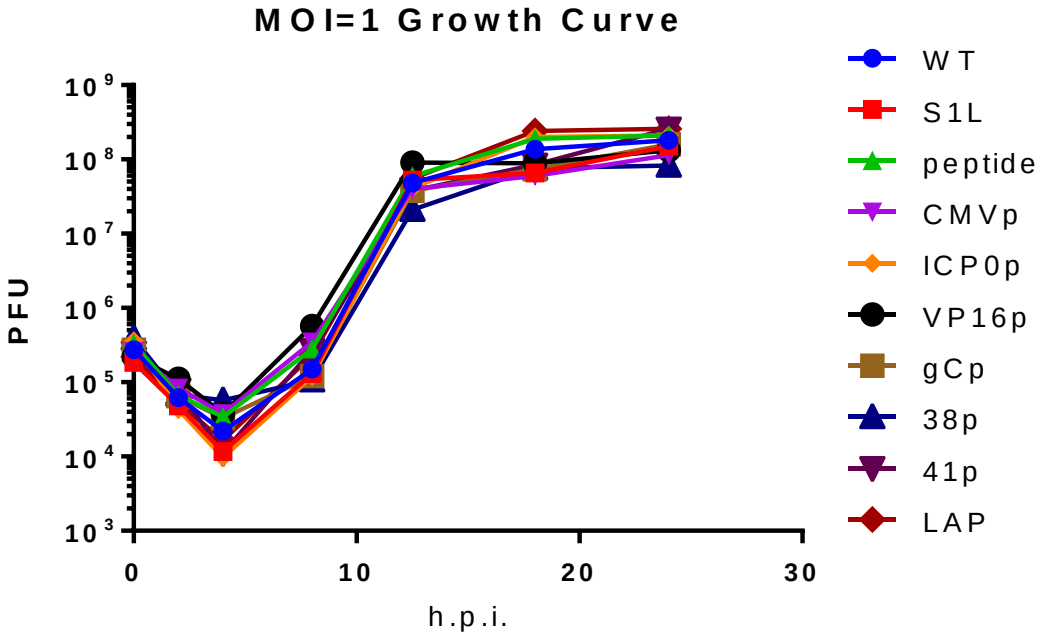

Figure 16. Growth curve of recombinant viruses

5*10^5 Vero cells were infected at an MOI of 1. An initial 0 hour timepoint is the inoculum, with 2, 4, 8, 12, 18, and 24 hour timepoints taken, freeze-thawed 3x, and virus concentration determined by plaque assay on Vero monolayers.

We next sought to establish if the gB-epitope peptide was expressed from these viruses as expected. While the strategy was designed yield viruses that express the gB peptides as GFP fusions, we did not see GFP signals in the appropriate channels by fluorescence microscopy, and immunoblot analyses for GFP protein in recombinant virus-infected cell extracts showed little protein of the expected size (data not shown). We suspected that the peptide-GFP protein was unstable, but reasoned that increased proteosomal degradation may permit rapid surface MHC-I presentation of peptide to $CD8^+$ T cells. Peptide expression was thus evaluated using a modified gB-CD8 T cell stimulation assay, previously used to show the very early (<2 hrs) expression of gB in a lytic HSV infection[185]. Monolayers of the MHC-I compatible B6 mouse-derived fibroblast cell line, B6WT3, were infected with each virus and infections halted at 4, 8 and 24

hpi by a pre-calibrated exposure to 254nm UV light under sterile conditions. Cells were then cocultured with 1 x 10^5 splenic gB-$CD8^+$ T cells/culture derived from the spleen of 8 dpi HSV-infected gB-T mice (Fig 17A). The gB-T1 mice are transgenic for a $gB_{498-505}$ specific T cell receptor, so that the vast majority of activated $CD8^+$ T cells recognize the $gB_{498-505}$ epitope [156]. Coculture in the presence of Brefeldin A allowed intracellular cytokine accumulation of TNFα and IFNγ for immunodetection and flow cytometry quantification in cells gated for CD45, CD3 and CD8 (Fig 17B).

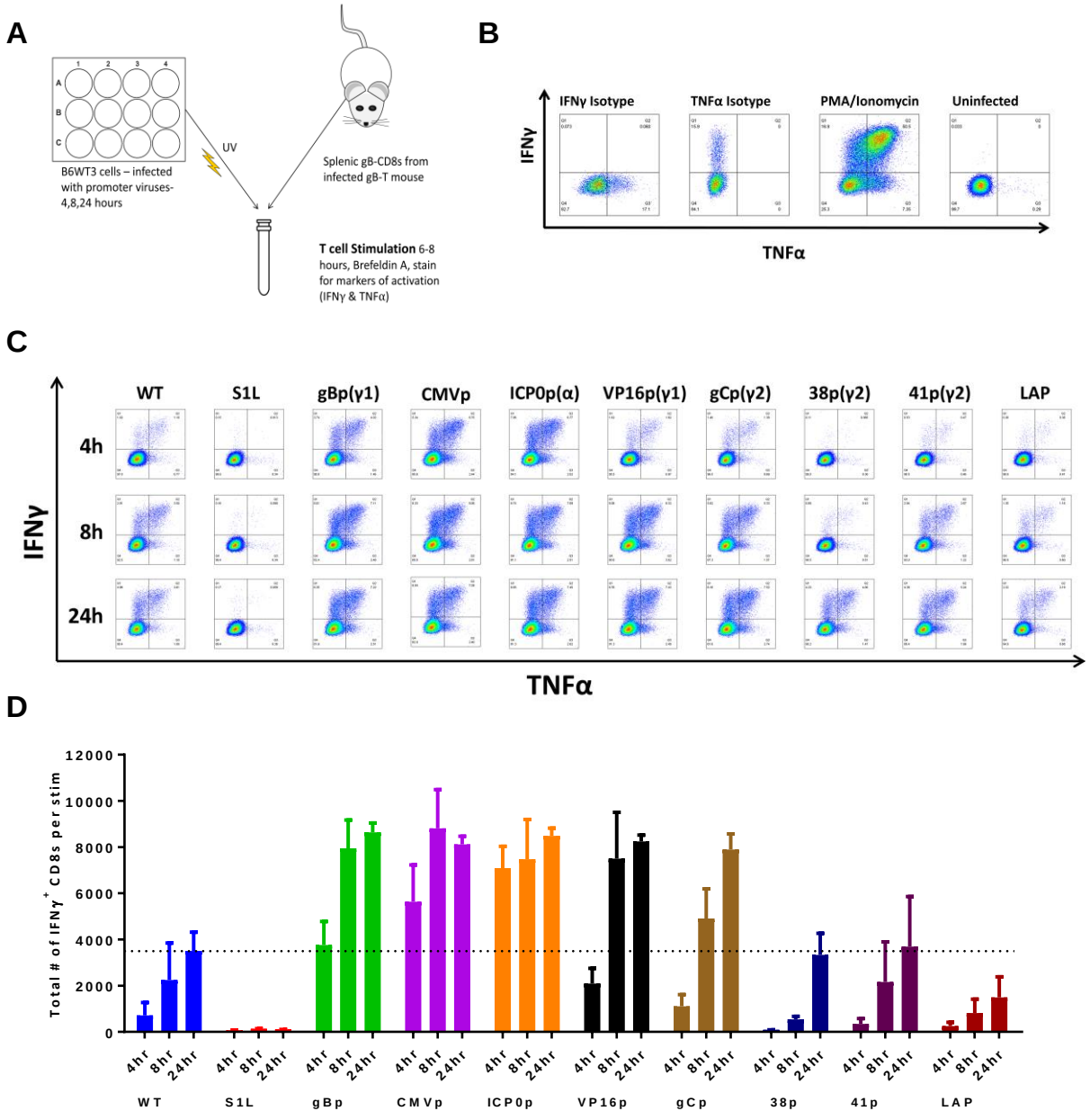

Figure 17. Viral expression of $gB_{498-505}$ from selected promoters is detected by $gB_{495-505}$ specific $CD8^+$ T cells

(A) Depiction of experimental setup. Confluent 12-wells of B6WT3 cells were infected with approximately $1x10^6$ PFU at an MOI of 1 with WT HSV-1, S1L, or each promoter virus. At 4, 8, or 24 hours each plate was UV-inactivated (with less than 10 PFU remaining per well), and combined into coculture with $1x10^5$ splenic cells derived from an 8 dpi infected gB-T mouse for 6-8 hours in the presence of Brefeldin A. Cocultures were then stained for CD45, CD8, IFNγ and TNFα. **(B)** Flow cytometry controls including isotype antibodies for IFNγ and TNFα, a PMA/Ionomycin positive control, and an uninfected B6WT3 fibroblast negative control. **(C)** Representative flow cytometric analysis from each group of intracellular staining for IFNγ and TNFα**. D)** Quantitation of data representative of five experiments, with the total number of $IFN\gamma^+$ $CD8^+$ T cells per coculture stimulation shown.

In summary, each promoter-recombinant HSV-1 stimulated $gB_{498-505}$-specific $CD8^+$ T cell responded in a manner consistent with the promoter chosen. A small number of gB-CD8s recognized wild-type HSV -1 KOS infected B6WT3 fibroblasts at 4 hpi, with numbers increasing to 24 hours, consistent with the leaky-late expression kinetics expected for gBp. In contrast, cells infected with HSV S1L, the parental virus lacking the $gB_{498-505}$ epitope, did not elicit any detectable cytokine production in $gB_{498-505}$-specific $CD8^+$ T cells, establishing the specificity of the assay and showing that cytokine-positive $CD8^+$ T cells were a specific response to MHC-I presented $gB_{498-505}$ peptide. Similar timing and kinetics of gB-CD8 activation were seen with cells infected by HSV-gBp, compared to wild-type HSV KOS, although they were consistently higher in number at every timepoint analyzed. This was not unexpected, because the peptide cassette expressed in these studies was a 4-mer repeat of $gB_{494-509}$ linked to GFP. Recombinant HSV with peptide driven by the constitutive CMV IE promoter and the ICP0 promoter activated gB-CD8s considerably more efficiently at 4 hrs, and to much higher levels than seen from the gB promoter at 4 and 8 hpi, as might be expected from immediate early expression programs following initiation of infection. The gB-CD8s also responded at high levels to cells infected with HSV expressing the epitope under the VP16p, with relative levels similar to that expressed from the gB promoter at each time point. Again, many more activated gB-CD8s developed intracellular cytokine expression than that seen in parallel wild-type HSV infected cells at each timepoint. In contrast, expression from the true late promoters gCp, 38p, and 41p resulted in only low levels of recognition at 4 hrs, but by 24 hr post-infection, the levels of activated $CD8^+$ T cells were similar (38p) or higher (gCp) than those of wild-type HSV-1 KOS at the same time point. This was consistent with expected true-late gene expression kinetics. Only the LAP showed a weaker activation of T cells than wild type infections by 24

hpi. (Fig 17C). This would be consistent with previously published data indicating LAP activity in lytic infections expresses with true-late gene kinetics, but only at low levels [182, 186].

5.3 $CD8^+$ T CELL RESPONSES IN MICE INFECTED WITH HSV EXPRESSING $GB_{498-505}$ FROM DIFFERENT PROMOTERS

The panel of recombinant HSV-1 promoter-peptide viruses were next evaluated for *in vivo* fitness by measuring their ability to both reach the murine TG after ocular infection and to induce a ganglionic $CD8^+$ T cell response at the onset of latency. Parental S1L virus was previously shown to induce a ganglionic viral load at day 8 at levels similar to that for mice infected with HSV-1 KOS, and to also induce an equivalent sized ganglionic $CD8^+$ T cell infiltrate[155]. Corneas of B6 mice were infected with $1x10^5$ PFU of HSV-1, the S1L mutant, or each promoter virus. Ganglionic loads were determined using qPCR real time methods at 8 dpi using a well characterized primer set recognizing sequences in gH [153]. As expected, S1L and KOS viral DNA loads in the ganglia at day 8 were similar. All the new recombinant HSV generated from S1L yielded a ganglionic DNA load at least as robust as wild type HSV S1L, indicating that they were sufficiently robust to establish latent genome loads at least as efficiently as the parent S1L and wild type HSV (Fig 18). When T cells were assessed, the total number of $CD8^+$ T cells infiltrating the ganglia at the peak infiltrate time of 8 dpi (Fig 19A) and the contracted infiltrates at latency (day 30-35) were similar to those induced by wild type HSV-1 (Fig 19B). We previously observed that significantly attenuated viruses do not induce large $CD8^+$ T cell infiltrates (unpublished data). We take these data to indicate that recombinant viruses used in this study were not significantly attenuated in either establishing latency, or

generating the peak ganglionic $CD8^+$ T cell infiltrate that are retained after contraction and throughout latency.

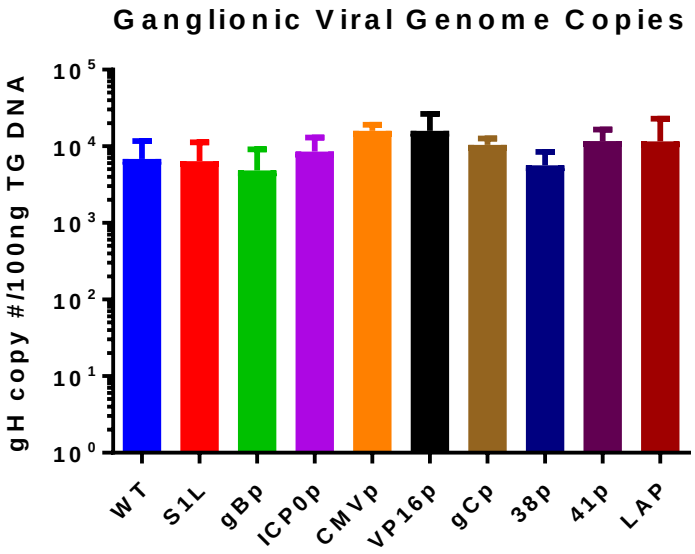

Figure 18. Ganglionic viral genome copy number in C57Bl/6 mice

Genome copy number determined by qPCR in the TG of mice ocularly infected with 1x10^5 PFU of HSV-1 WT, S1L, or $gB_{498\text{-}505}$ promoter-viruses following harvest at day 8 post infection (n=4-10 per group). Values are representative of the total copies per 100ng of TG DNA recovered. No significant differences from WT. HSV-1 BAC standards used as a positive control for detection, as well as calculations for viral copy number.

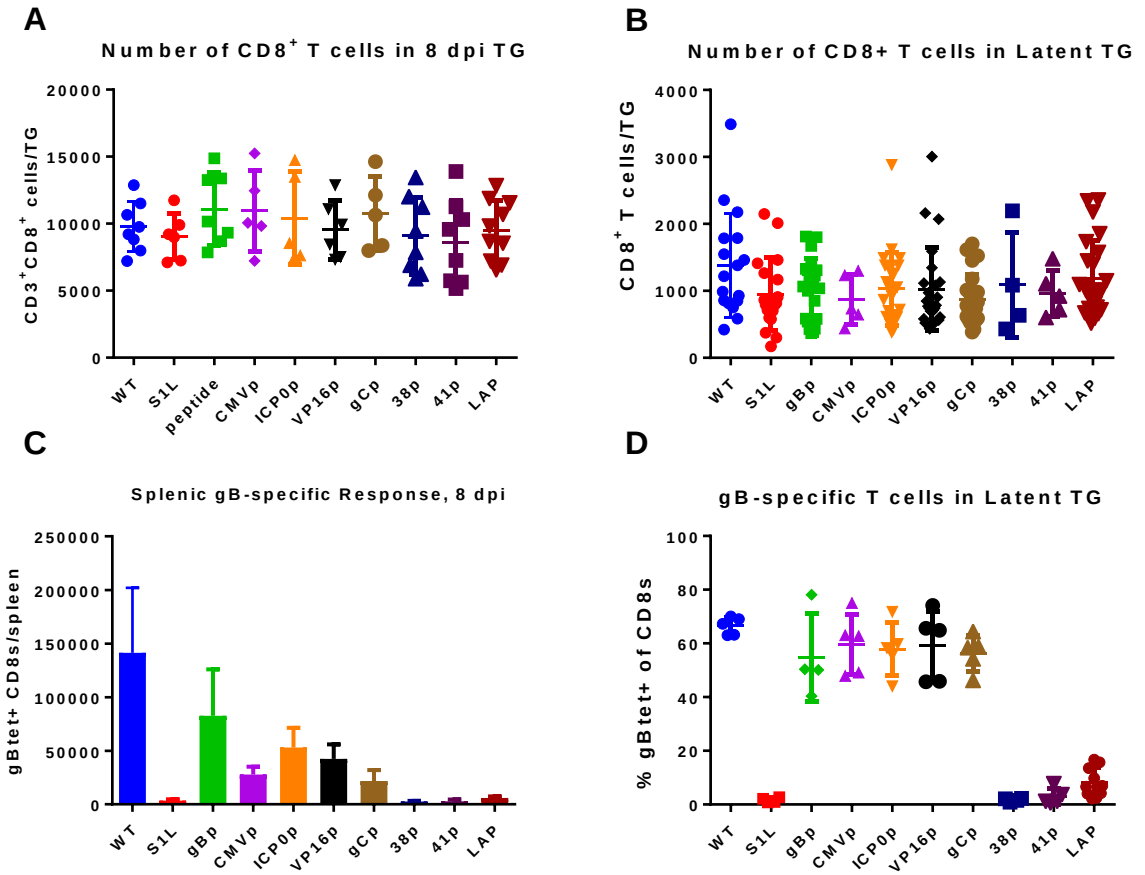

Figure 19. $gB_{498\text{-}505}$ specific $CD8^+$ T cell responses to selected $gB_{498\text{-}505}$ promoter viruses

Corneas of mice were infected with $1x10^5$ PFU/eye of HSV-1 WT, S1L, or a recombinant HSV-1 expressing $gB_{498\text{-}505}$ from the indicated promoter. At 8 dpi (peak $CD8^+$ T cell infiltrate) or 30 dpi (latency), TG and spleen were dissociated into single cell suspensions and surface stained with antibodies to CD45, CD3, CD8, and with MHC-I $gB_{498\text{-}505}$ tetramer as detailed in Methods. Cells were subsequently analyzed by flow cytometry and show total $CD8^+$ T cells per TG at **(A)** 8 dpi. or **(B)** 30 dpi. **(C)** The total number of $gB_{498\text{-}505}$ tetramer positive $CD8^+$ T cells in each spleen at 8 dpi. are also shown. **(D)** The fraction of $gB_{498\text{-}505}$ tetramer positive cells among the total $CD8^+$ T cells in the TG at day 30 is shown.

One aspect of these that viruses differed was their induction of the gB-CD8 compartment, which was quantified using $gB_{498\text{-}505}$ specific tetramers to identify gB-CD8s (Fig 19C, D). Quantifying the priming by splenic gB-CD8 T cell levels revealed that five of the viruses (CMVp, gBp, ICP0p, VP16p and gCp) primed strong gB-specific responses, although levels in the spleen differed somewhat from virus to virus. Surprisingly, three viruses induced very few

splenic gB specific CD8 T cells by day 8, suggesting a lack of gB-CD8 T cell priming. In the infected TG at 8 days, when HSV begins to enter latency, viruses that primed gB splenic $CD8^+$ T cell responses showed remarkably similar fractions of the ganglionic infiltrate to be $gB_{498\text{-}505}$ specific- in all cases representing more than 40% of the CD8s in the ganglia. This is within the range of that induced by wild type HSV-1 infections. One exception was HSV-1 gCp, where few gB-CD8s were seen at day 8, despite an apparent systemic priming. Not surprisingly, gB-CD8s were not detectable in ganglia latently infected with viruses that failed to prime an early gB-specific CD8 response.

Examination of the contracted and retained $CD8^+$ T cell infiltrate at latency indicated that the above viruses could be divided into one of two groups: those that developed an immunodominant gB-CD8 response, and those that did not (Fig 19D). Viruses that effectively primed a $gB_{498\text{-}505}$ specific $CD8^+$ T cell response, including HSV-gCp, developed a ganglionic infiltrate that was typically dominated by gB-CD8s at levels seen in mice infected with wild type HSV-1. Given that these ectopic peptide-promoter viruses expressed higher numbers of $gB_{498\text{-}505}$ epitopes than wild type as measured by T cell activation (Fig 17), this strongly suggests that neither higher epitope expression levels nor earlier expression in the context of a lytic HSV infection results in a higher proportional gB-CD8 response in the ganglia. This result suggests that the differential expression from stronger promoters is unlikely to increase the gB-CD8 T cell fraction in the ganglionic population at latency. The second group of viruses (38p, 41p, LAP), which primed few to no ganglionic gB-CD8s, showed comparatively very little to no gB-CD8 infiltration in the latently infected ganglia. However, these are further analyzed in studies described below.

We next addressed functionality of the gB-CD8 and non-gB-CD8s in the TG at latency for the five viruses in which a gB-CD8 response was primed. Previous work indicated that a wild-type HSV infection results in development of ganglionic gB-specific CD8s of high functionality from onset through HSV-1 latency, even up to 90 days post infection[68, 147]. However, non-gB-CD8 populations develop signs of functional exhaustion and express less granzyme B and significantly more of the exhaustion marker PD-1 on their cell surface. We hypothesized that the different expression kinetics from the various promoters may result in changed levels of functional phenotype markers for the gB-CD8 and non-gB-CD8 populations. One factor influencing $CD8^+$ T cell functionality is the chronicity of antigen expression during viral persistence [187]. We therefore examined long-term latent infections of each virus for the phenotype of ganglionic $CD8^+$ T cells, using surface expression of the exhaustion marker PD-1 and intracellular staining for the functional marker granzyme B. By 90 days post-ocular infection, all viruses maintained an immunodominant gB-CD8 infiltrate, accounting for 50% CD8+ T cells (Fig 20A). Wild type HSV-1 gB-CD8s showed only very low levels of surface PD-1, while non-gB-CD8s showed considerably more with surface PD-1 expression, reaching average levels more than 21% (Fig 20B). A reverse correlation was seen for granzyme B, in that most gB-CD8s stained positive for granzyme B, while less than 20% of the non-gB-CD8s were granzyme B positive (Fig 20C). When examining the infiltrates to the different promoter-epitope viruses, there was overall a similar phenotype to that seen for wild-type, in that gB-CD8s showed high functionality and low PD-1, while non-gB-CD8s were consistently higher in PD-1 levels compared to gB-CD8s. Subtle differences were apparent; the fraction of granzyme B positive gB-CD8s were highest for wild type and the HSV-1 gBp viruses and trended lower in ganglionic gB-CD8s for all other promoter viruses. Again, all viruses induced higher levels of PD-1 on

non-gB-CD8s than the gB-CD8s. We take these results to indicate that the different promoters do not greatly affect the proportion of gB-CD8 vs. non-gB-CD8 T cells that are functional, and for all viruses, $CD8^+$ T cells that recognize the gB epitope retain a more functional phenotype than the non-gB-CD8s.

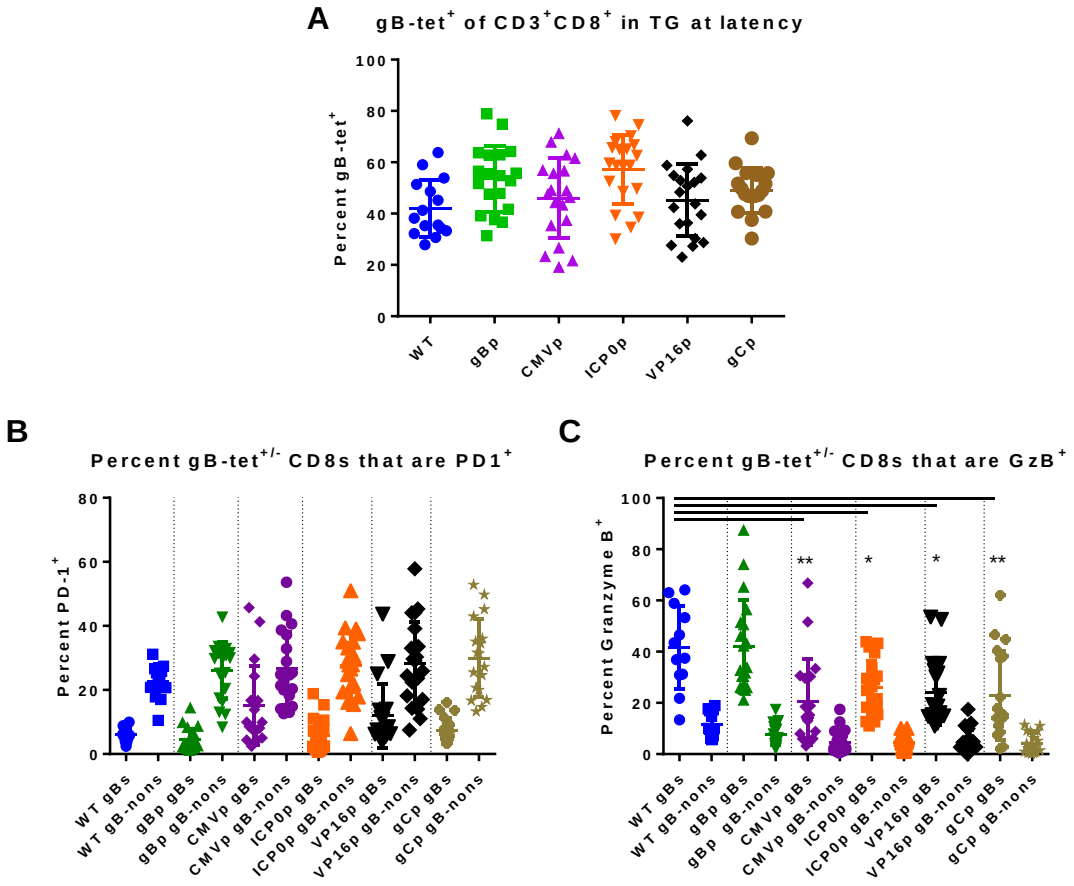

Figure 20. gB-specific $CD8^+$ T cells remain more activated during long-term latency than subdominant ones

Corneas of mice were infected with $1x10^5$ PFU/eye of HSV-1 WT KOS, gBp, CMVp, ICP0p, VP16p, or gCp. At long-term latency timepoint, 90 dpi. TG were dissociated into single cell suspensions and surface stained with antibodies to CD45, CD3, CD8, PD-1, and MHC-I $gB_{498-505}$ tetramer, and stained intracellularly for GzB, as detailed in Methods. Cells were analyzed by flow cytometry, and the data are presented as the mean +/- SEM (n=5-10 mice per group [10-20 TGs per group]) of **(A)** percentage gB-tetramer$^+$ of total $CD8^+$ T cells per TG. The percent of $gB_{498-505}$ tetramer positive (gBs) or negative (gB-nons) $CD8^+$ T cells in each TG that are **(B)** PD-1 or **(C)** GzB positive are also shown. The data shown is representative of two separate experiments. * denotes $p<0.05$, ** denotes $p<.01$, by one-way ANOVA with multiple comparisons.

5.4 EPITOPE EXPRESSION FROM CANDIDATE TRUE LATE PROMOTERS RESULTS IN POOR GB-CD8 PRIMING

Additional studies were undertaken with HSV expressing epitope from gCp. Infection with this virus clearly primed a systemic gB-CD8 response, but few gB-CD8s infiltrated the ganglia at day 8, while a typical half fraction of total CD8s at day 30 latency were $gB_{498\text{-}505}$ specific (Fig 21A). When the ganglionic infiltrate began to contract from day 10 onwards, the fraction of CD8s specific for gB increased, and by day 12, it reached the level of immunodominance seen for wild type HSV-1 (Fig 21B). These data indicates that expression from the gCp results in a preferential retention of this minor infiltrating population, that becomes a delayed gB immunodominance by latency. As our previous data have shown that antigen expression in part drives a preferential retention of $CD8^+$ T cell populations [155], the gC promoter is likely expressing at a low level throughout the establishment of latency.

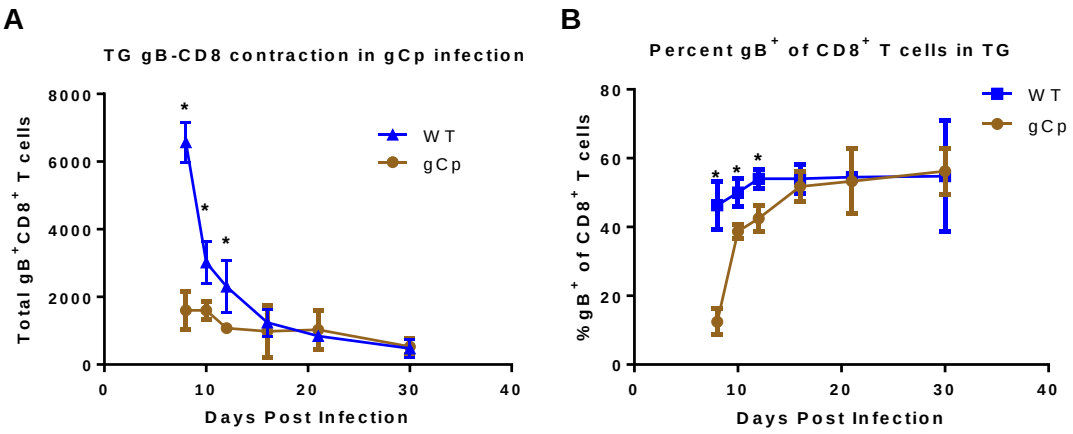

Figure 21. $gB_{498\text{-}505}$ expressed from gCp results in a delayed gB-$CD8^+$ T cell immunodominance in ganglia

Corneas of mice were infected as previously, with $1x10^5$ PFU/eye of HSV-1 WT or recombinant HSV-1 expressing $gB_{498\text{-}505}$ from the gC promoter. At 8, 10, 12, 16, 21, and 30 dpi TG were dissociated and stained with antibodies to CD45, CD3, CD8, and with MHC-I $gB_{498\text{-}505}$ tetramer as detailed in Methods. **(A)** The total number of TG-infiltrating gB-specific CD8s is shown over time in a gCp infection. **(B)** The fraction of $gB_{498\text{-}505}$ tetramer positive cells among the total $CD8^+$ T cells in the TG is shown over time in each infection. * denotes $p<0.01$ by one-way ANOVA.

Viruses expressing the peptide from the UL38, UL41, and LAT promoters showed an even larger defect in priming of the gB-CD8 response, despite presenting gB peptide at levels similar to that from wild type infections *in vitro* by 24 hpi (Fig 17). The reason for lack of priming is not clear, but reduced or absent priming from protein antigens expressed late in the growth cycle has been reported in other viruses[188, 189]. We note that while true-late genes form the majority of the HSV-encoded proteome, they are vastly underrepresented in the antigens recognized by an HSV-1 specific T cell response in B6 mice[77]. We then asked if these viral promoters were sufficiently active during latency to retain a gB-CD8 T cell response if such T cells were efficiently primed at the onset of infection. We exploited the observation that at the time of the peak infiltrate into the ganglia at day 8, any activated systemic CD8 T cells will enter the acutely infected ganglia, independent of antigen presentation[155].

5.5 EPITOPE EXPRESSION FROM THE LAT PROMOTER RESULTS IN DELAYED LOW LEVEL GB-CD8 RESPONSES

HSV expressing the gB epitope-GFP gene from the LAP did not induce a robust gB specific immune response like the viruses expressing the epitope from constitutive or γ1 promoters. Nevertheless, a small but significant fraction of gB-CD8 T cells was detected in the systemic response (Fig 19C) and also in the latently infected ganglia at later times post infection over that seen for S1L (Fig 19D). We therefore conducted additional studies on this virus to track the ganglionic gB-CD8 response. While the LAP is weakly expressed in a lytic infection with γ2 kinetics, it was expected to be more active during latency.

Quantification of the total gB-CD8s by tetramer staining over time revealed that while no gB-CD8s were seen at the peak of the infiltrate at day 8 post-infection, a small-but-significant fraction of ganglionic gB-CD8s developed by 20 dpi, which represented approximately 11% of the total contracted CD8 populations in the ganglia during latency (Fig 22A and B). This low level was maintained out to 60 dpi. To determine if this low late developing population was due to an expansion of a very low small population infiltrating the ganglia at the onset of latency, we performed BrdU pulse labelling for 2 days to identify dividing $CD8^+$ T cells in the ganglia at day 20 and 60 post-infection. For wild type HSV-1, few cells were labelled at day 20 and day 60, indicating that the majority of the $CD8^+$ T cells were not recently dividing. However, the LAP virus did contain significantly more replicating $CD8^+$ T cells at 20 dpi, and analyses with tetramer revealed the gB populations were expanding at 20 dpi (Fig 22C). These cells were still undergoing a marginal expansion at day 60, significantly more than for wild type virus at both short- and long-term latency (Fig 22D).

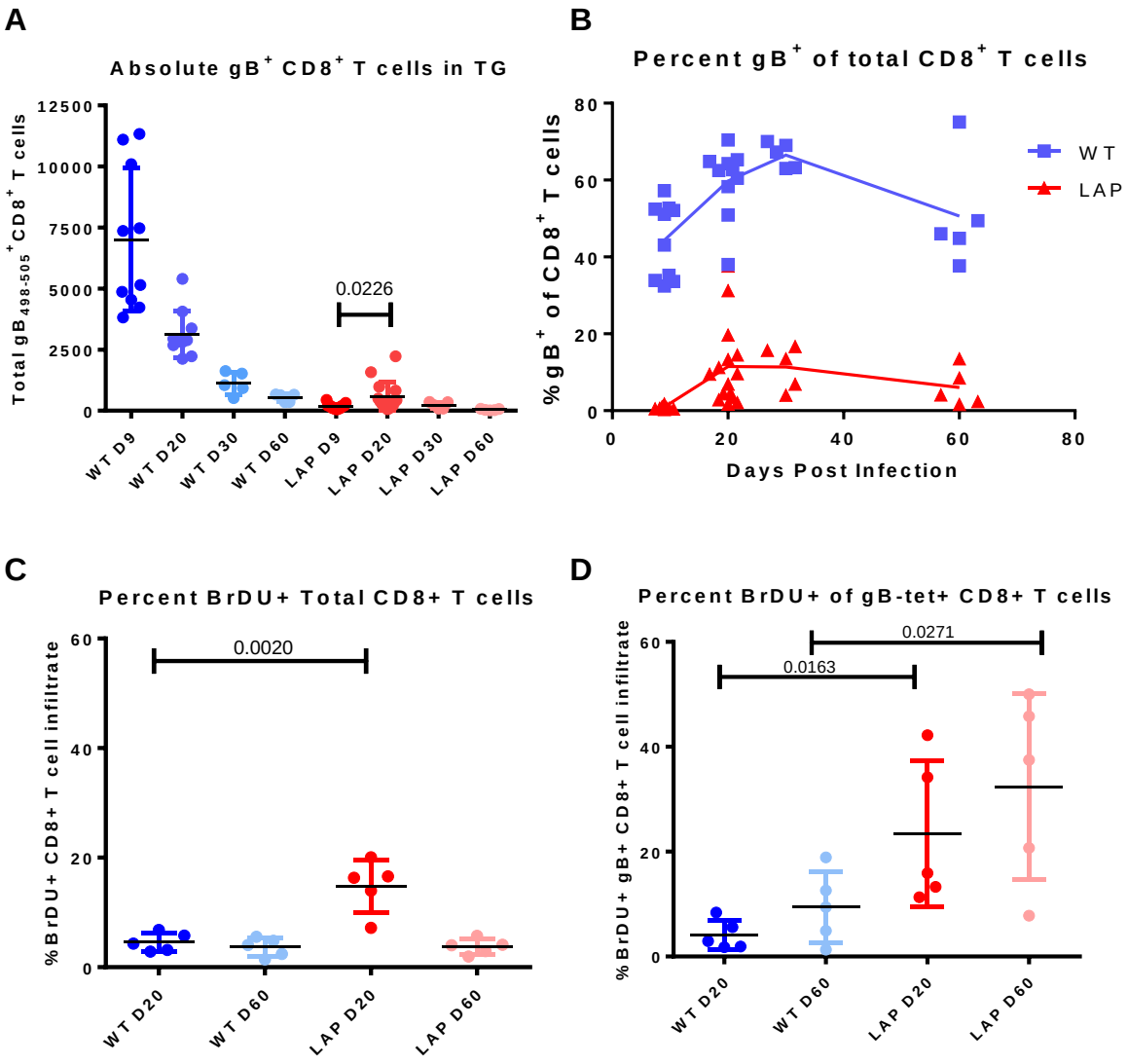

Figure 22. Latent expression of $gB_{498-505}$ results in reduced and delayed gB-specific $CD8^+$ T cell infiltrate

Corneas of mice were infected as previously, with $1x10^5$ PFU/eye of HSV-1 WT or recombinant HSV-1 expressing $gB_{498-505}$ from the LAT promoter. 2 days prior to harvest at 20 and 60 dpi, mice were pulsed with 1mg/mouse BrdU. At 9, 20, 30, and 60 dpi TG were dissociated and stained with antibodies to CD45, CD3, CD8, BrdU, and MHC-I $gB_{498-505}$ tetramer as detailed in Methods. **(A)** The total number of TG-infiltrating gB-specific CD8s is shown over time. **(B)** The fraction of $gB_{498-505}$ tetramer positive cells among the total $CD8^+$ T cells in the TG is shown over time in each infection. BrdU staining of **(C)** total CD8s and **(D)** $gB_{498-505}$ specific CD8s is shown at 20 and 60 dpi. P-values shown represent significance by t-test.

5.6 TRUE LATE AND LAP PROMOTER ACTIVITY IS SUFFICIENT TO RETAIN GB-CD8$^+$ T CELL INFILTRATES PRIMED BY WT-HSV INFECTIONS

LAP-driven antigen primed a negligible gB-CD8 response that was only detectable at late times post-infection within the latently infected tissue, and γ2 late promoters failed to prime gB-CD8 responses at all. Therefore, we next asked whether these promoters can activate and retain WT-primed gB-CD8 responses within latently infected tissue. We employed a dual infection strategy in which the ocular route was used for infection by the late promoter viruses, but a simultaneous flank infection with WT HSV-1 was used to systemically prime a gB-CD8 T cell response (Fig 23A). At day 8, all ganglia infected with the non-priming HSV-1 were shown to contain gB-CD8s, consistent with the notion that recently activated CD8$^+$ T cells will traffic to sites of infection (Fig 23B). As the CD8 population contracts at the onset of viral latency, only ganglia that harbor the cognate $gB_{498\text{-}505}$ antigen can retain a sizable gB-CD8 infiltrate. At latency, greatly reduced levels of the gB-CD8s were seen in ganglia latently infected with S1L at latency, which does not express a recognizable gB epitope at any time. For both viruses expressing the gB epitope under control of promoters that fail to prime a large initial response (UL38p, UL41p, and LAP), the level of gB-CD8s retained in the ganglia were at a level significantly higher than the gB-CD8s retained in the ganglia for S1L (Fig 23C). The level was much lower for these two γ2 promoters than that seen for viruses expressing peptide under control of LAP, the latency active promoter. We conclude that expression of the peptide from these true late promoters is not sufficient to prime a significant gB-CD8 T cell response. However when such a response is effectively primed from the flank, the low level of γ2 late gene expression within the ganglia is sufficient to activate and retain a small number of CD8$^+$ T cells within the latently infected ganglia. In contrast, the LAP can efficiently retain a much larger gB-

CD8 response, consistent with the idea that this promoter expresses during $CD8^+$ T cell contraction and latency. Taken together with the data from Figure 22, this indicates that the kinetics of LAP in a lytic infection are not sufficient to induce antigen levels sufficient for priming a large $CD8^+$ T response. However, during latency LAP-driven antigens are sufficient to mediate efficient ganglionic retention driven by ongoing antigen expression, and in these cases poor priming and generation of tissue-resident memory gB-CD8s can be bypassed by priming the responses at another location on the animal.

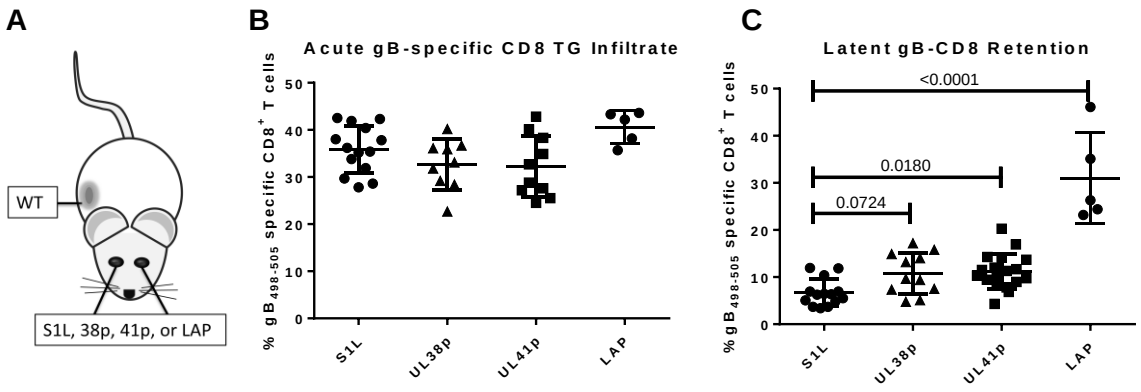

Figure 23. True late or latent promoters deficient in priming gB-CD8s are capable of maintaining more gB-CD8s at latency

(A) Representation of infection model in which mice received bilateral corneal infections with S1L, UL38p or UL41p HSV-1 and flank infection with WT HSV-1. All corneal infections were with $1x10^5$ PFU/scarified cornea, and flank infections were with $1x10^6$ PFU on a scarified flank. **(B and C)** At 8 (acute) or 30 (latent) dpi, TG suspensions were analyzed by flow cytometry for CD45, CD3, CD8, and $gB_{498-505}$-tetramer. Frequency of $CD3^+CD8^+$ T cells in the TG that are gB-$tetramer^+$. 5-10 mice analyzed per group. Statistical significance by one-way ANOVA displayed above each group at latency.

5.7 HSV-1 EXPRESSING AN MCHERRY-GB-PEPTIDE FUSION PROTEIN FROM THE UL41 GENE

Further considerations need to be taken into account when addressing the lack of $CD8^+$ T cell priming by $gB_{498\text{-}505}$ peptide expressed as a γ2 gene, as seen with both the UL38 or UL41 promoters. In all the promoter-peptide constructs that were presented within this chapter, the $gB_{498\text{-}505}$ peptide was expressed as a 4mer-$gB_{494\text{-}509}$ peptide fused with EGFP, which proved to be rather unstable and not easily detectable by fluorescence or western blotting (data not shown). This is actually advantageous for efficient antigen presentation, as unstable proteins are rapidly degraded and peptides become available for MHC-I presentation. However, this construct may differ greatly in peptide-protein stability and subcellular localization when compared to HSV-1 epitopes derived from native viral proteins. In a WT HSV-1 infection, the $gB_{498\text{-}505}$ peptide is located within the gB protein, which is located both on the membranes of infected cells, and as part of the array of viral glycoproteins displayed on the viral envelope (Fig 1).

To address this discrepancy with antigenic stability, we tested several fluorescent-protein-$gB_{494\text{-}509}$ fusion constructs. Among these, we created an mCherry protein either N- or C-terminally tagged with a single copy of $gB_{494\text{-}509}$ expressed from the UL41 locus. These recombinant viruses express $gB_{494\text{-}509}$-mCherry as a bicistronic message linked to UL41 expression by utilizing a T2A linking sequence, and this construct was generated in the S1L background (Fig 24A). These viruses all have very bright mCherry fluorescence, and detectable mCherry protein by western blot, indicating greatly increased stability compare to the EGFP-linked peptide used in earlier studies (data not shown). When these viruses were tested for ability to present peptides in gB-CD8 T cell cocultures with infected fibroblasts as detailed for Fig 17, maximal presentation was detected by 24 hpi, consistent with γ2 late gene kinetics (Fig 24B).

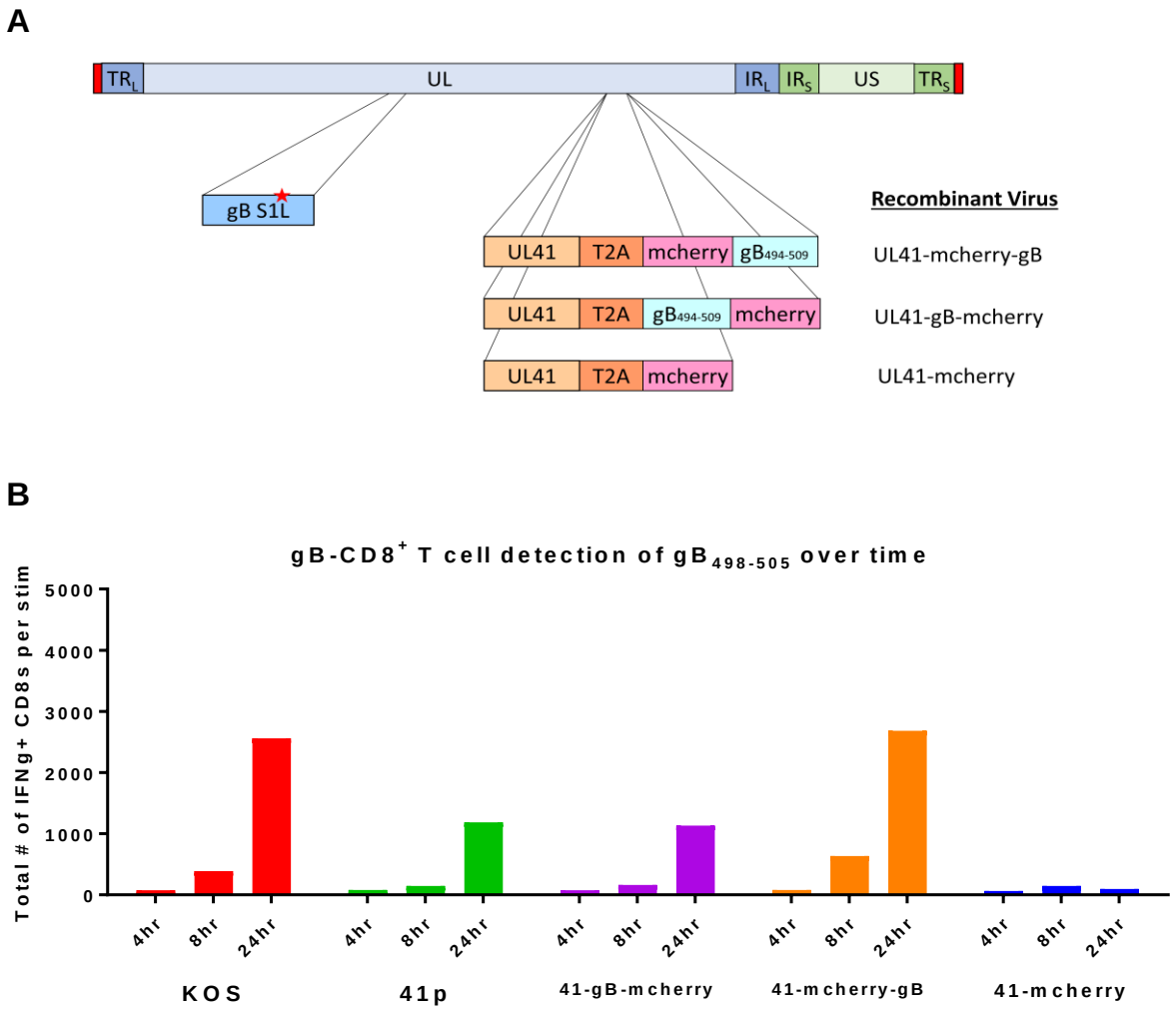

Figure 24. UL41-T2A-mCherry linked gB-peptide viruses present $gB_{498-505}$ peptide with kinetics similar to UL41p virus

Confluent B6WT3 cells were infected with approximately $1x10^6$ PFU at an MOI of 1 with WT HSV-1, S1L, 41p, 41-gB-mCherry or 41-mcherry-gB. At 4, 8, or 24 hours each plate was UV-inactivated (with less than 10 PFU remaining per well), and combined into coculture with $1x10^5$ splenic cells derived from an 8 dpi infected gB-T mouse for 6-8 hours in the presence of Brefeldin A. Cocultures were then stained for CD45, CD8, IFNγ and TNFα. Quantitation of representative of the total number of $IFN\gamma^+$ $CD8^+$ T cells per coculture stimulation shown.

Mice ocularly infected with these gB-peptide recombinant viruses containing gB-mCherry (N-terminal fusion) or mCherry-gB (C-terminal fusion) show a varying ganglionic $gB_{498-505}$ specific CD8 response (Fig 25). Unexpectedly, the N-terminal mCherry peptide fusion

elicited an intermediate amount of gB-CD8 infiltrate (~18% of total CD8s), while the C-terminal version was not significantly different from the control mCherry virus that does not contain the gB-peptide. This trend was also seen systemically, in the spleen, and suggests that the C-terminal fusion does not prime gB-CD8s, while the N-terminal version does (data not shown). These results do not reflect the amount of gB-epitope detected in the *in vitro* presentation assay in figure 24B, and further studies need to be done to explain this phenomenon.

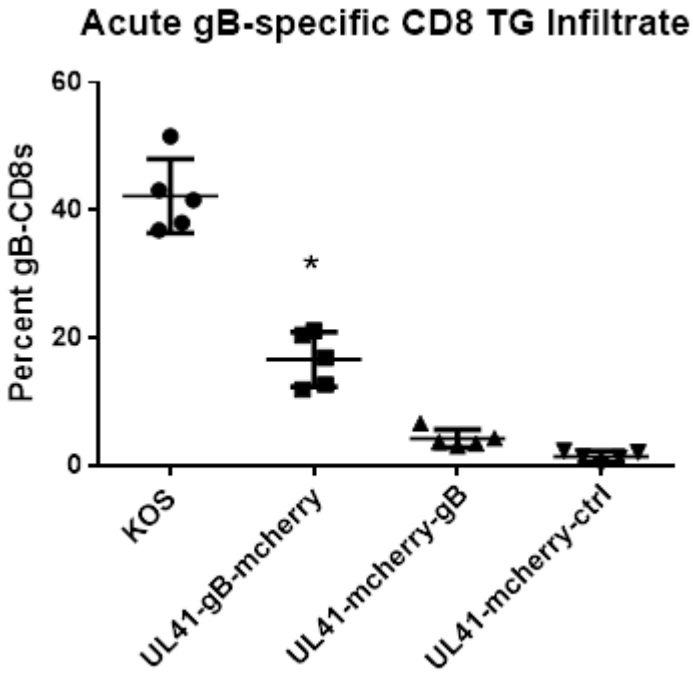

Figure 25. UL41-T2A-mCherry linked gB-peptide viruses elicit differing CD8+ T cell responses

Corneas of mice were infected with $1x10^5$ PFU/eye of HSV-1 WT UL41-gB-mcherry, UL41-mcherry-gB, or UL41-mCherry-ctrl. At 9 dpi (peak $CD8^+$ T cell infiltrate) TG were dissociated into single cell suspensions and surface stained with antibodies to CD45, CD3, CD8, and with MHC-I $gB_{498-505}$ tetramer as detailed in Methods. Cells were subsequently analyzed by flow cytometry and show total $CD8^+$ T cells per TG.

5.8 DISCUSSION

Factors that determine which antigens of a pathogen are targeted by the developing cellular immune response, and the hierarchal order of the antigens targeted, are complex and multifactorial[158]. The B6 mouse model is unique in that the dominance hierarchy is so heavily skewed to one epitope, for reasons that are not entirely clear. One aspect that may contribute to the immunodominance pattern is the activity of the promoter— it may be that the gB promoter is ideally suited to generate a highly skewed response in the B6 mouse. Secondly, it has become apparent that an additional level of complexity governs the hierarchy of the $CD8^+$ T cell immune response associated with the HSV ganglionic latent state, since it is not only influenced by the antigenic repertoire of $CD8^+$ T cells primed, but also by the viral gene expression events that sporadically occur during HSV-1 latency[66, 67, 162]. Several lines of evidence strongly indicate that a majority of CD8 T cell ganglionic retention during the HSV-1 latent state requires antigen expression[146, 155]. These observations were the driving factors in the hypotheses behind the current study: do different promoters driving the expression from the HSV genome of a strong immunodominant HSV-1 $CD8^+$ T cell epitope in B6 mice ($gB_{498\text{-}505}$ [SSIEFARL]) influence the proportion of gB-CD8 T cells in the ganglionic population at latency? We were particularly focused on determining if the proportion of gB-CD8s in the latently ganglia could be numerically increased by use of predicted strong promoters, given the fact that gB-CD8s are more active and able to better prevent reactivation events in WT infections[155].

We concluded that the promoter selected to express the epitope in the context of HSV genomes can influence both the priming efficiency of the $CD8^+$ T cell response and the long-term retention in the latently infected murine ganglia. While several of the promoters evaluated expressed HSV-1 epitopes to levels that efficiently primed a $CD8^+$ T cell response, we saw quite

different responses and priming with the epitope expressed from three true late and the Latency associated gene promoters. Recombinant viruses developed here to express $gB_{498\text{-}505}$ epitope from the various promoters (Table 1) used a recently described single amino acid mutation (S1L) mutated in the $gB_{498—505}$ epitope that ablates gB $CD8^+$ T cell priming and recognition[155]. This strategy separated the epitope from the gB protein, and allowed us to examine the $CD8^+$ T cell response in viruses that were comparatively pathogenically fit in the murine model. This strategy was necessary because a previous similar study aimed at addressing the contribution of promoters to immunodominance used a virus in which the expression of the whole gB was altered to a true late gene. This resulted in a considerable cost in viral fitness and a resulting altered development and ganglionic infiltration of the HSV-specific CD8 T cell response [153]. All recombinant viruses used here induced ganglionic latent loads at least as efficiently as wild-type virus and a total peak of the immune infiltrate in the ganglia similar to WT-equivalent total $CD8^+$ T cells. Some viruses were slightly more efficient than wild-type at establishing a latent load. The basis for this was not clear, since in comparing these viruses, all promoters were at the same ectopic locus, in the gC gene. While this had the caveat that the strategy might not completely reflect the full range of expression from the native loci or the promoter, it also reduced any influence of genomic location or the behavior of the $CD8^+$ T cell response across multiple viruses. Disruption of the gC open reading frame had no observable effect in our mouse model of scarified corneal infection, seen here or in previous studies [23, 179]. Thus, all differences seen in the $CD8^+$ T cell responses are the result of contribution of the different viral promoter activities.

A second conclusion is that the gB promoter is not necessarily a “goldilocks” promoter, and other promoters can easily generate a strongly primed gB immunodominant phenotype. Most

intriguingly, all promoters in the subset of viruses that primed a significant gB-CD8 T cell response resulted in a near identical fraction of gB-CD8s at latency— even in the case of the gC promoter, where there was a small fraction of gB-CD8s primed that were selectively retained to become immunodominant by late times (Fig 21). Thus, it does appear that increased lytic expression of an epitope does not necessarily lead to increased level of $CD8^+$ T cell immunodominance in the ganglia as we hypothesized. In a WT HSV-1 infection, glycoprotein B is expressed as an γ1 leaky-late gene that is, nevertheless, capable of being detected within two hours post-infection [185]. Here, HSV with constitutively active regulated CMVp and α regulated ICP0p driven expression of the epitope showed only marginal differences in the priming of the splenic gB-CD8 T cell response, despite the observation that these viruses could activate over five times as many $CD8^+$ T cells by four hours post infection in *in vitro* activation assays over that by wild type HSV-1. There is a caveat that we cannot establish that these promoters are more active than the gB promoter in the latently infected murine ganglia, but the CMV promoter has been found to be active from the HSV genome for up to 30 days in the murine TG, and the ICP0 protein is needed for reactivation [190] . However, we also increased the amount of epitope expressed from the gB promoter during latency, using a multimeric peptide strategy. This approach did not increase immunodominance levels in the latently infected ganglia, even though it clearly increased levels of the epitope made in a lytic infection from the respective gB promoter on the surface of infected cells (Fig 17). The VP16 promoter was as active as gB promoter and did not result in a higher immunodominant response. We examined VP16p since it has been reported to be a possible pre-α gene that precedes immediate-early genes in sporadic reactivation events from ganglia[62, 180]. We conclude that for this subset of the viruses, the minimal ganglionic expression level required to retain robust gB-CD8 infiltrates

during the onset of latency was reached for each virus. This implies that expression above this minimal level neither primes a more immunodominant $CD8^+$ T cell response nor maintains a higher level of immunodominance during latency than that seen for WT virus. What defines this limit is not yet clear. It is possible that any promoter will only drive a limited level of gene expression during latency that is defined not by the activity of the promoter in lytic context, but how its repression is influenced by chromatin changes that defines the TG immunodominant population and the sporadic reactivations that act to retain them.

An additional minor (if negative) conclusion was the observation that, in the entire $CD8^+$ T cell repertoire to HSV in B6 mice, there are no representative CD8 populations targeting epitopes on α proteins. We considered the possibility that α expressed proteins might have unique properties that act to prevent their ability to prime the $CD8^+$ T cell response. However, this does not seem to be the case, since α promoter driven expression of the epitope stimulates a robust and strong immune response. Taken together, while one of the goals of this project was to create a virus that rapidly expressed a large amount of $gB_{498\text{-}505}$ epitope, as this immunodominant epitope elicits a $CD8^+$ T cell response that remains particularly active and capable of effector functions throughout latency in C57Bl/6 mice, it seems that this is not easily achieved by altering epitope expression alone. There seems to be an unidentified mechanism preventing tissue-specific $CD8^+$ T cell responses from becoming skewed completely to one epitope. This mechanism is likely to involve cytokine competition within the TG, competition for antigen, viral immune evasion strategies, and other factors [158, 188]. One possibility is that as viral $gB_{498\text{-}505}$ antigen is detected and shut down by gB-CD8s, there is less antigen available for other gB-CD8s to detect, leading to an inability to rise above a certain threshold of gB-CD8s. From a host evolutionary perspective, it also makes sense to not focus all attention on one epitope, which

would provide opportunities for viral escape mutants, and therefore there may be interactions among specific CD8 populations preventing full immunodominance within the tissue.

In contrast to the early and strong lytic promoters, γ2 late promoter driven epitopes from UL38p or UL41p demonstrated a greatly reduced ability in both priming gB-CD8 responses and in retaining CD8s in the ganglia when the $gB_{498\text{-}505}$ response is exogenously primed by a wild-type infection. These two promoters were clearly active during lytic infections, since *in vitro* by 24 hpi, both viruses could elicit gB-$CD8^+$ T cell activation levels that equaled or exceeded the WT virus response (Fig 17). However, they were less active than the strong/immediate early promoters, and neither virus was able to activate a significant fraction of the gB CD8s at 4h post infection, consistent with the delayed expression expected for a true late promoter. The non-gB-CD8 T cells that make up the rest of the response have been thoroughly characterized for S1L [77], and we have previously shown that expansion of the subdominant responses occur when gB responses fail to prime[155], and we assume that a similar compensation occurs for these viruses. Why these promoters did not efficiently prime a response is not clear. However, it has come to light that generating effector-memory $CD8^+$ T cells requires several naïve T cell interactions with DCs in the draining lymph nodes[191, 192], with epitope being presented on specific dendritic cell subsets, and cross-presented by other DC subsets being vital steps in generating memory $CD8^+$ T cell responses. Altering both the expression kinetics of the peptide as well as the location within the protein— resulting in a terminal peptide multimer instead of a residue within the gB gene—may very well change the amount of epitope that these DC populations have access to via either direct or cross-presentation. Finally, we note that both γ2 promoters could retain an exogenously primed gB-CD8 T cell response, but at levels nowhere near that seen for the active viruses detailed above. This suggests that these promoters might be less

active during latency than others, but does indicate there is a low-level of late gene expression within the ganglia. This would fit with our previous observation that the subdominant population hierarchy retained in the S1L latently infected TG is quite different from the systemic response, suggesting that some promoters are more active during latency than others, and thus their cognate $CD8^+$ T cell populations are selectively retained. Different rates of firing of sporadic reactivation for different promoters were also seen by the Tscharke group[67]. This conflicts with the general de-repression model put forward by Wilson and colleagues [62], and suggests that there are genomic regions that are preferentially active in sporadic reactivation events.

Intriguingly, we found that the gC and LAP promoters show different patterns of priming and retention. In lytic infections, gC is a γ2 late gene that strictly requires new viral DNA synthesis for expression, but it appears to express at levels higher than the UL38 and UL41 promoters by 24 hpi in gB-CD8 T cell activation assays (Fig 17). In mice, the primed splenic responses were considerably reduced in comparison to the WT, gBp, CMVp and ICP0p (Fig 4C). More strikingly, TG infiltration of gB-CD8s were delayed compared to WT, with only about 10% of the ganglionic CD8s being gB-specific at day 8 (Fig 21), as compared to 50% for a wild type infection. Our data suggests gB $CD8^+$ T cells are retained very efficiently for this virus and become a typical immunodominant population seen during latency. This suggests that the gC promoter is sufficiently active to drive priming of the gB-CD8 population, but the activity of the promoter during latency is above the minimal level that is required for 50% immunodominance just discussed. This fits well with data from studies in which both gC RNA and protein were both found to be expressed during latency [67, 193, 194].

Finally, the LAP promoter shows a unique pattern in priming and ganglionic retention. In lytic infections, the full 2kb LAT promoter driving expression of $gB_{498\text{-}505}$ from an ectopic locus induced some expression by 24 hpi, and activated a small number of *in vitro* gB-CD8s compared to wild-type virus (Fig 17). While HSV LAT is known to be active during latency, it has previously been reported to be expressed during lytic infection, with kinetics of a late regulated gene[195]. The LAT promoter virus showed very little priming within the time of the initial infection of B6 mice, with such a small splenic response that it was not significantly different from the epitope knockout (S1L, Fig 17). However, mice infected with this virus over time develop a significant expansion of gB-CD8s into the murine TG (Fig 22A). This expansion correlates with an increase in BrdU uptake by these gB-CD8s clearly demonstrating that they are likely seeing expressed antigen (Fig 22C-D). This gB-CD8 expansion is maintained as a significant percentage (~10%) of the CD8 response throughout latency, despite a virtually undetectable priming of the gB-CD8 response at acute times post-infection (Fig 22B). This suggests that the levels of protein generated in the context of the initial priming is insufficient to compete with all other viral antigens and primer a gB CD8 response. However, with LAP-driven continuous expression of gB peptide, $CD8^+$ T cells are subsequently primed during a time when there are few other antigens to compete. Remarkably, in the dual flank infection model, exogenous priming results in an efficiently retained gB-CD8 population in the TG. This suggests that the LAP promoter could be used to maintain a $CD8^+$ T cell population in the ganglia, but only when the T cells are efficiently primed[155].

We considered that there may be differences in the functionality of the ganglionic $CD8^+$ T cells retained by expression from the different promoters. Function and exhaustion are both influenced by chronicity and levels of antigen expression in the LCMV models[196]. In previous

studies with wild type HSV, gB-CD8s show a more functional phenotype and demonstrate better anti-viral effector properties than their non-gB-CD8 counterparts[77, 148, 155], as indicated by increased expression of the activation marker GzB and decreased expression of the exhaustion marker PD-1. We found that there was a global trend for increased GzB and reduced PD-1 on gB-CD8s generated by all gB promoter viruses (Fig 20). There were, however, a few minor differences. The gB CD8s retained by the CMVp virus show a higher level of PD-1 and lower level of GzB, which suggests they may have started to become exhausted due to more epitope expression within the TG. However, with all viruses the general trend is intriguingly similar, demonstrating that even with an apparent large difference among expression levels, the immunodominant gB-CD8s remain more activated and functional than their subdominant counterparts in the TG.

From our studies with the N- and C-terminal linked $gB_{498\text{-}505}$ peptide linked to mCherry in the UL41 gene, it is also clear that kinetic class is only one of a myriad of factors that determine $CD8^+$ T cell priming deficits in γ2 late genes. By creating a more stable protein to link gB peptide to, we saw somewhat different results. The N-terminally linked gB-mCherry expressed from the UL41 locus generated an intermediate gB-CD8 infiltrate at acute times, similar to what was seen for the gCp virus during acute infection, while the C-terminal version of this construct failed to prime gB-CD8s, despite higher levels of detectable $gB_{498\text{-}505}$ presentation *in vitro* (Fig 24 and 25). It would be telling to follow the gB-mCherry virus out to later time points to determine if these gB-CD8s are retained more efficiently as is seen in the gCp virus. It also is of note that N- or C-terminal positions of the peptides may be processed differently in APCs *in vivo*, despite the retained $gB_{494\text{-}509}$ processing sites surrounding the peptide [197].

Taken together, these data begin to paint a picture in which viral antigen expression kinetics play a role in shaping ganglionic $CD8^+$ T cell responses associated with HSV-1 latency. Not surprisingly, stronger lytic promoters can dictate the efficiency of priming of the effector $CD8^+$ T cell responses, but it also becomes apparent that promoter activity driving expression within the TG itself is important for retention of these responses. Furthermore, the fact that TG-resident/tissue-specific $CD8^+$ T cell responses associated with HSV latency do not necessarily reflect the splenic and systemic responses is not surprising. However, as latency progresses, viral gene expression significantly shapes the protective CD8 repertoire that patrols the TG and prevents reactivation.

6.0 VACCINATION STRATEGIES FOR PRIMING GANGLIONIC $GB_{498-505}$ $CD8^+$ T CELL RESPONSES UTILIZING AAV OR PRV VECTORS

Current evidence supports that a short burst of ganglionic replication follows initial infection with HSV-1, which contributes significantly to the latent viral load in the TG [198]. This is consistent with the detection of infectious virus at 2-4 dpi that we routinely observe in the TG, which is controlled by macrophages and γδ T cell-dependent expression of effector molecules such as IFNγ and TNFα by 6 dpi [101]. Given that protective $CD8^+$ T cell infiltrates in the TG are capable of mounting similar cytokine responses, expression of $gB_{498-505}$ in the TG and the establishment of a pre-existing $CD8^+$ T cell population prior to HSV-1 infection has been hypothesized to lessen this replicative burst and reduce the viral genomic load in the TG. Furthermore, superinfection with $gB_{498-505}$ expressing vectors after HSV-1 latency has been established may augment the infiltration and functionality of $CD8^+$ T cells. The vectors to be evaluated in this chapter include adeno-associated virus (AAV) and an attenuated pseudorabies virus (PRV).

Wild-type AAVs are replication defective viruses that need a helper virus to reproduce. This fact makes AAV one of the safest available viral vectors for gene delivery, although a limited amount of genetic material can be packaged. AAV transduced gene products can persist for weeks to months in long-lived cells such as neurons, which also adds to their potential[199]. AAV serotypes 2, 5 and 8 have been shown to be neurotrophic in some models, with some

serotypes having the ability to efficiently transduce dorsal root ganglia (DRG) from surface applications implying the ability to transduce sensory ganglia through neuronal axons [200-203]. This is important for our model of ocular infection, as there is an abundance of sensory nerve termini in the cornea.

PRV is an Alphaherpesvirus similar in structure to HSV-1, and which causes a naturally occurring infection of swine and bovines. PRV has been researched for decades as a model neurotropic Alphaherpesvirus, due to its ability to quickly and efficiently target and traverse axons in many model organisms[204-208]. This in part explains the severe infection of the nervous system observed in mice, rats, guinea-pigs, rabbits, and other mammals, in which a wild-type PRV infection is fatal. PRV strains lacking Thymidine Kinase (TK) gene expression, however, are unable to replicate efficiently in neurons, making them suitable as neurotrophic delivery vehicles for target gene expression[209]. TK- viruses are fully replication competent within epithelial tissues, with large inflammatory responses that are ideally suited to prime efficient memory $CD8^+$ T cell responses. To our knowledge, the use of PRV on mouse corneas to target TG neurons had not been attempted previously.

6.1 USING AAV TO TARGET TG NEURONS BY OCULAR INNOCULATION

To first test the ability of AAV to transduce TG neurons, we chose AAV2, 5, and 8 reporter constructs that express EGFP from the CAG promoter, a strong synthetic promoter designed to elicit very high persistent levels of target gene expression. B6 mice were ocularly treated with the AAV vectors in the same way HSV treatments were described earlier. We abrade the surface of the cornea to expose sensory nerve termini, then apply 1*10^10 genome

copies (gc) of AAV. Animals were examined at 2, 8, and 20 days post-inoculation and TG and cornea examined for reporter gene expression by both qPCR for EGFP, and tissues were mounted on slides and examined for EGFP by fluorescence microscopy.

In all AAV reporter constructs tested, no significant EGFP expression was observed within the TG, and similarly no EGFP mRNA was detectable by qPCR (data not shown). However within the cornea, large numbers of corneal stromal cells expressed EGFP, as determined by fluorescent microscopy of a whole corneal mount inoculated with AAV8-EGFP (Fig 26). Similar results were observed with AAV-2, albeit to a lesser extent, and no target gene expression with AAV5 was observed.

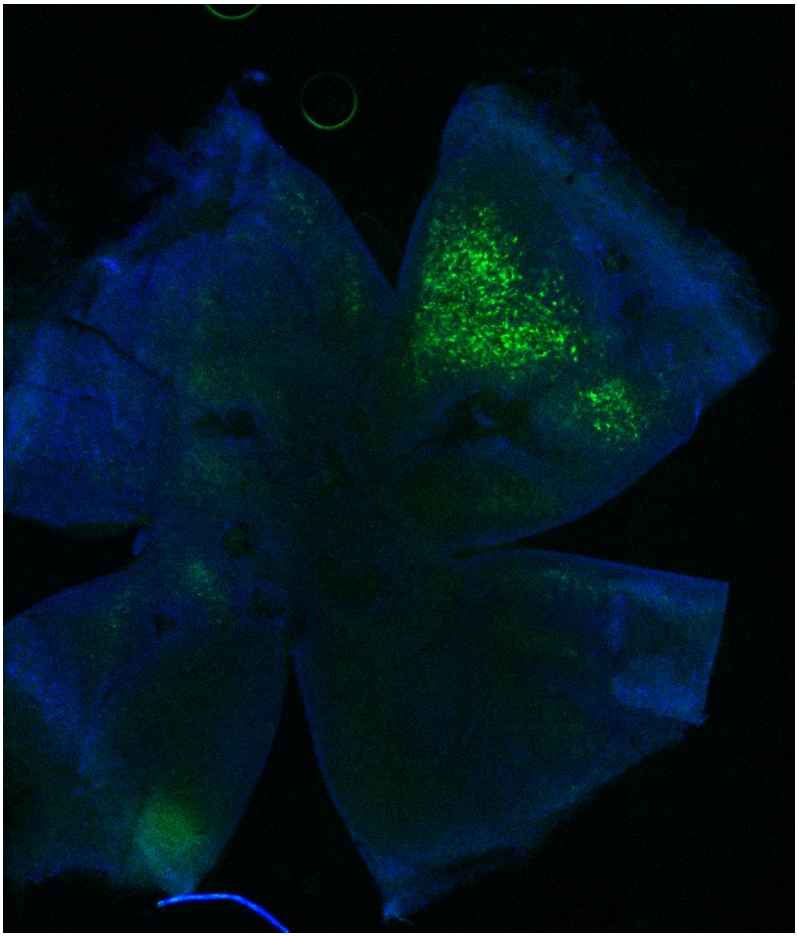

Figure 26. Whole corneal showing AAV8-EGFP target gene expression.

Anesthetized B6 mice were scarified and inoculated with 1*10^10 gc/eye with AAV8-EGFP. At 20 days after treatment, mice were sacrificed and whole-corneal mounts DAPI-stained and imaged for EGFP expression.

Targeting TG via sensory nerve endings from the cornea proved to be more difficult than was seen in skin-DRG models, which may in part be due to the neural-crest lineage of corneal stromal cells when comparted to skin [201-203, 210]. Given the lack of TG-neuron targeting, we did not proceed with generating an AAV that expresses $gB_{498\text{-}505}$, or developing an adjuvant strategy to induce $CD8^+$ T cell priming. It became clear from these data that we would benefit from the use of a strongly neurotropic virus for this model, and PRV was chosen for this reason.

6.2 DESIGNING PRV THAT EXPRESSES GB498-505

To reduce neuronal spread of PRV vectors, we first generated all PRV as TK knockout (PRV TK-) by inserting a cassette that consists of monomeric red fluorescent (mRFP, mRed) gene expressed from the TK promoter which disrupts the TK ORF. PRV that expresses the HSV-1 $gB_{498\text{-}505}$ peptides was generated in a similar fashion, with an additional PRV-gB or CMV promoter driving expression of $gB_{498\text{-}505}$ linked to EGFP (Fig 27).

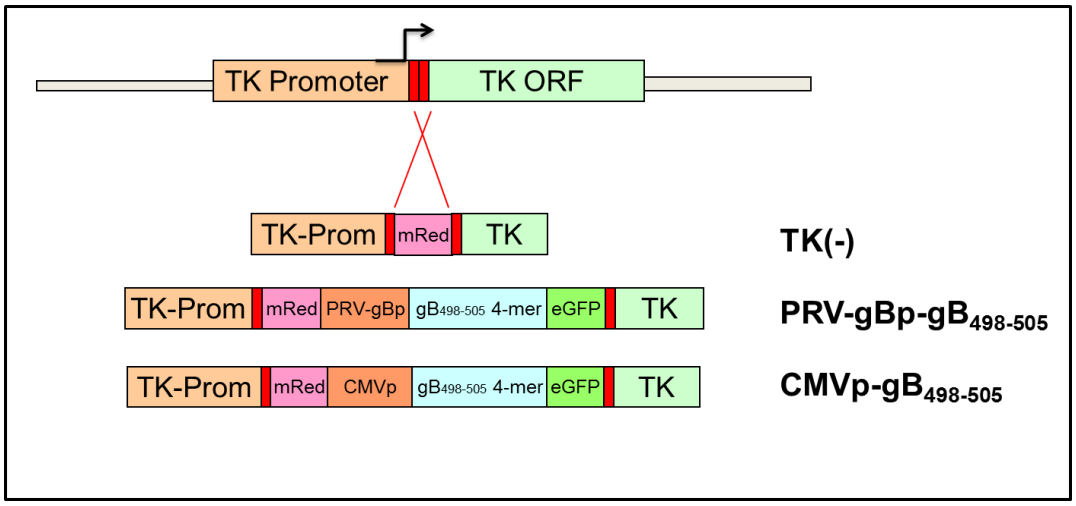

Figure 27. Schematic detailing construction of PRV expressing HSV-1 $gB_{498-505}$

6.3 PRIMING HSV-1 GB-$CD8^+$ T CELL RESPONSES WITH PRV-$GB_{498-505}$

PRV TK-. CMVp, or gBp were grown to high titer and confirmed by gB-CD8 T cell cocultures to express $gB_{498-505}$ that was readily detectable. B6 mice ocularly infected in a similar fashion to HSV studies carried out previously. At either acute (9 dpi) or latent (33 dpi), TG of mice were harvested and assessed by flow cytometry for $CD8^+$ T cell responses. Compared to WT HSV-1 at 9 dpi, PRV induced $CD8^+$ T cell responses nearly as large as WT HSV (Fig 28A). When $gB_{498-505}$ specific $CD8^+$ T cells were analyzed with tetramers, a large percentage of the PRV immune response was directed toward the $gB_{498-505}$ epitope, accounting for nearly a third of the total CD8 infiltrate (Fig 28B). This was surprising, given that PRV has its own array of virally encoded peptides that $CD8^+$ T cells can recognize. Of note, there is little-to-no overlap of $CD8^+$ T cell epitopes between wild-type HSV-1 and PRV, as demonstrated by sequence analysis, and by stimulation assays seen in Figure 11C, where the HSV-1 S1L-specific $CD8^+$ T cell

repertoire was not stimulated by PRV-$gB_{498\text{-}505}$ infected fibroblasts. By 33 dpi, there remained a large $CD8^+$ T cell infiltrate in the ganglia, of which almost half was $gB_{498\text{-}505}$-specific. This was a very promising result for the goal of priming an HSV-1 specific $CD8^+$ T cell response within the ganglia, but upon further analysis several problems arose that prevented use of PRV as a prophylactic HSV-1 vaccine, as described below.

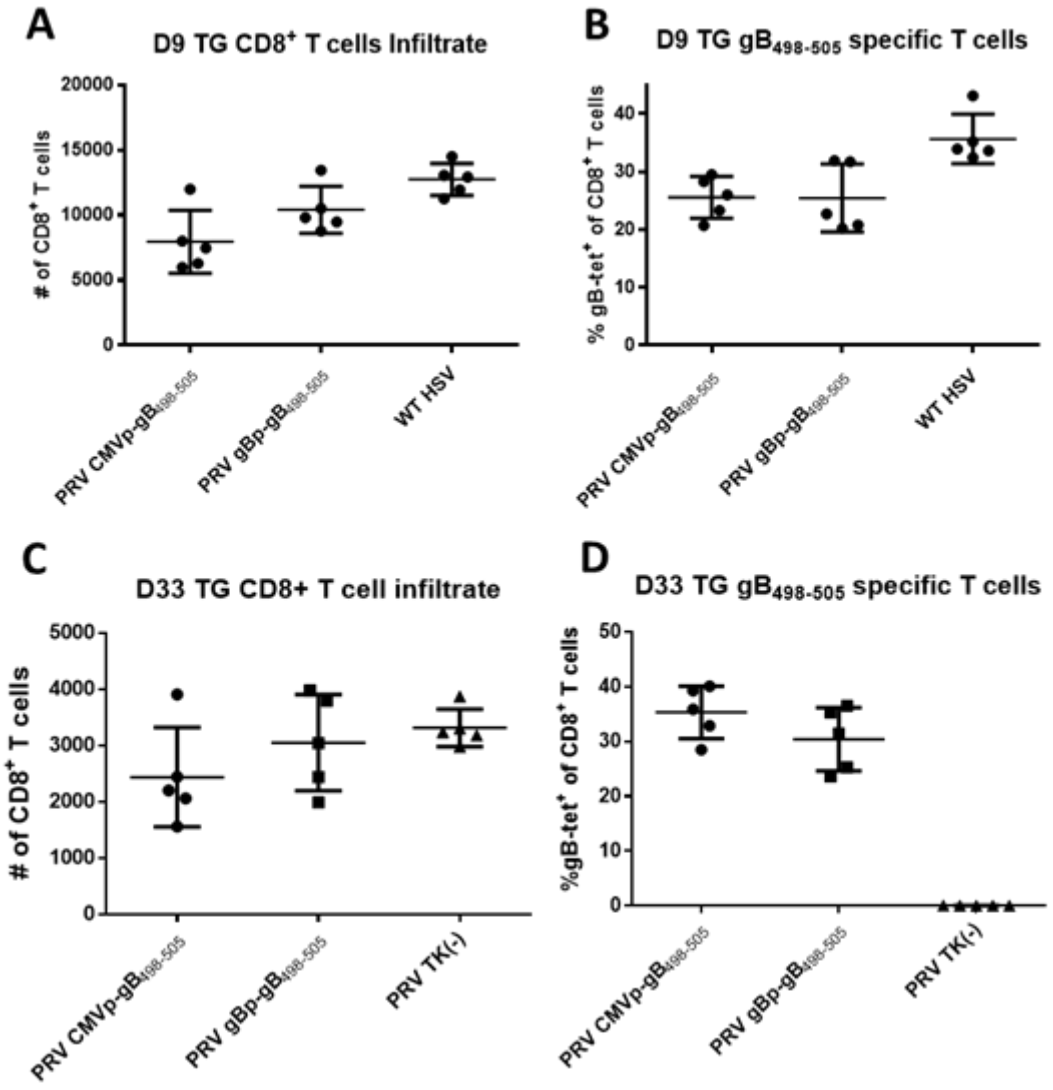

Figure 28. CD8$^+$ T cell responses to PRV vectors expressing HSV-1 gB498-505

Corneas of mice were infected with 1x10^5 PFU/eye of recombinant PRV vectors expressing gB$_{498-505}$ from the indicated promoter or WT HSV-1. At 9 dpi (near the peak of CD8$^+$ T cell infiltrate) or 33 dpi (viral latency), TG were dissociated into single cell suspensions and surface stained with antibodies to CD45, CD3, CD8, and with MHC-I gB$_{498-505}$ tetramer as detailed in Methods. Cells were subsequently analyzed at 9 dpi by flow cytometry and show **(A)** total CD8$^+$ T cells per TG and **(B)** the total percentage of gB$_{498-505}$ tetramer positive CD8$^+$ T cells in each TG also shown. Identical studies were carried out at 33 dpi showing **(C)** total CD8$^+$ T cells per TG and **(D)** the total percentage of gB$_{498-505}$ tetramer positive CD8$^+$ T cells.

6.4 OCULAR DISEASE IN PRV-INFECTED MICE

Between the acute and latent time points shown in the previous figure, it was observed that mice infected with TK- PRV began showing signs of severe HSK. When scored clinically for corneal sensation, almost all mice in PRV-infected groups had lost the blinking reflex usually observed when gently touching the corneal surface (Fig 29A). Accompanying the loss of corneal sensation was a severe keratitis, with very high opacity and blood vessel ingrowth into the inner cornea by 33 dpi (Fig 29B, C). By all appearances this disease is quite similar to a very pathogenic HSV-1 infection, which results in a similar phenotype. In the case of HSV-1, severe loss of corneal blink reflex as observed here is accompanied with a retraction of sensory nerve termini from the cornea, along with a subsequent ingrowth of sympathetic neurons that prevents sensory nerves from returning[211, 212]. This loss of sensory nerves and sensation contributes greatly to the keratitis disease phenotype, and may explain what is happening in our PRV model as well.

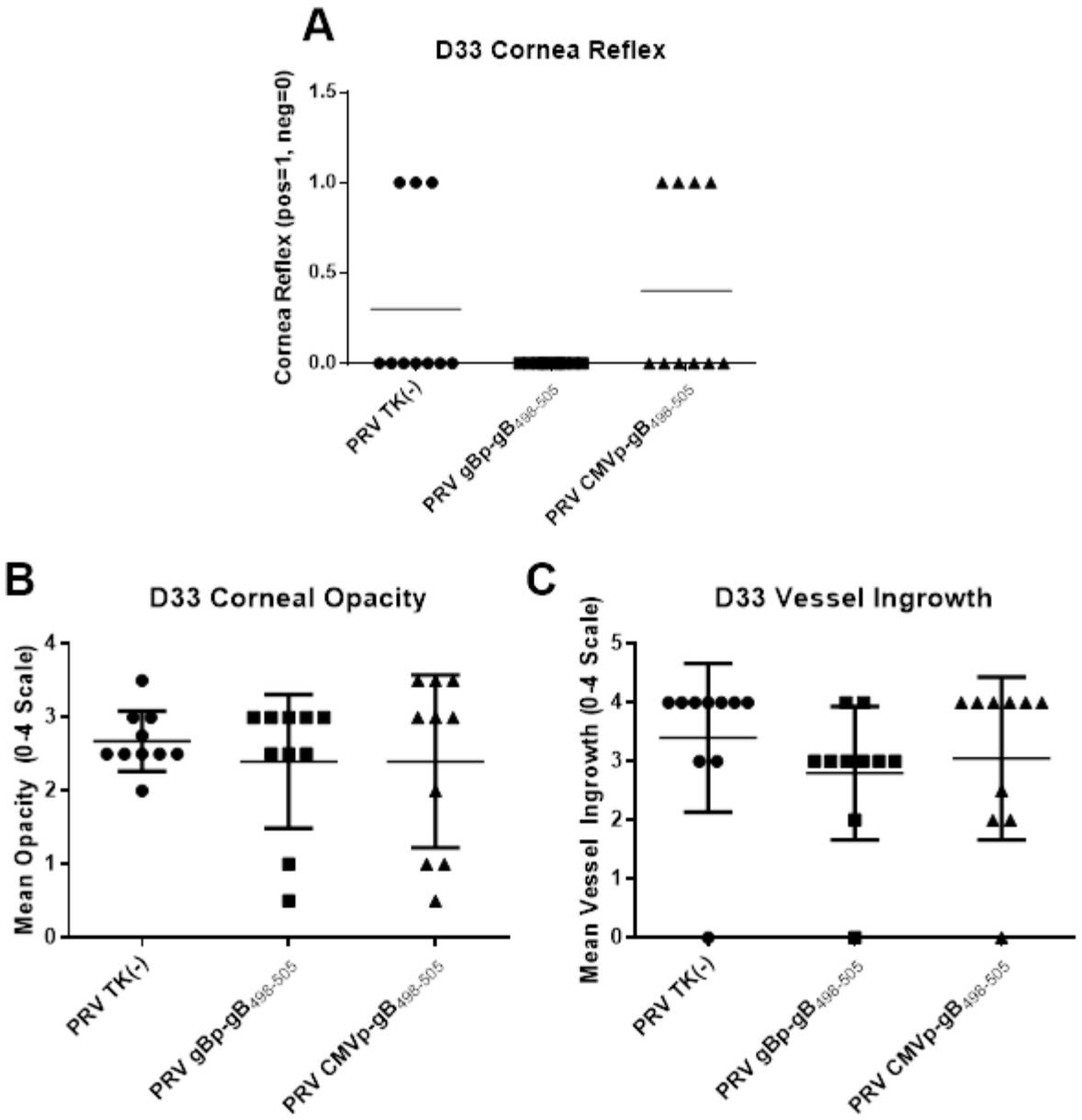

Figure 29. Corneal pathology in PRV infected mice

At 33 dpi, the corneas were examined for (A) corneal blink reflex, (B) corneal opacity as observed under slit-lamp microscopy and (C) degree of vascularization. Corneal reflex measured as a simple positive/negative ability to blink upon gently touching all quadrants of the cornea with a surgical spear. Corneal opacity is measured on a 0-4 scale for severity of opacity, as confirmed by two observers. Similarly, the severity of blood vessel ingrowth was measured on a 0-4 scale for vascularization extent across corneal quadrants by two observers.

To determine whether our PRV vectors were able to remain latent in the TG over the time measured, we performed qPCR for PRV glycoprotein H (gH) on DNA isolated from 9 or 33 dpi TG (Fig 30). At early time points, low levels of PRV genomes were readily detected in most samples, however at later times, no PRV genomes were detected. This suggests either clearance of viral DNA or death of infected neurons. Given the severity and rapid onset of the corneal disease, it seems likely that our PRV vector damaged or killed TG neurons innervating the cornea. A follow-up study looking for apoptotic markers within TG latently infected with PRV would allow us to address this question.

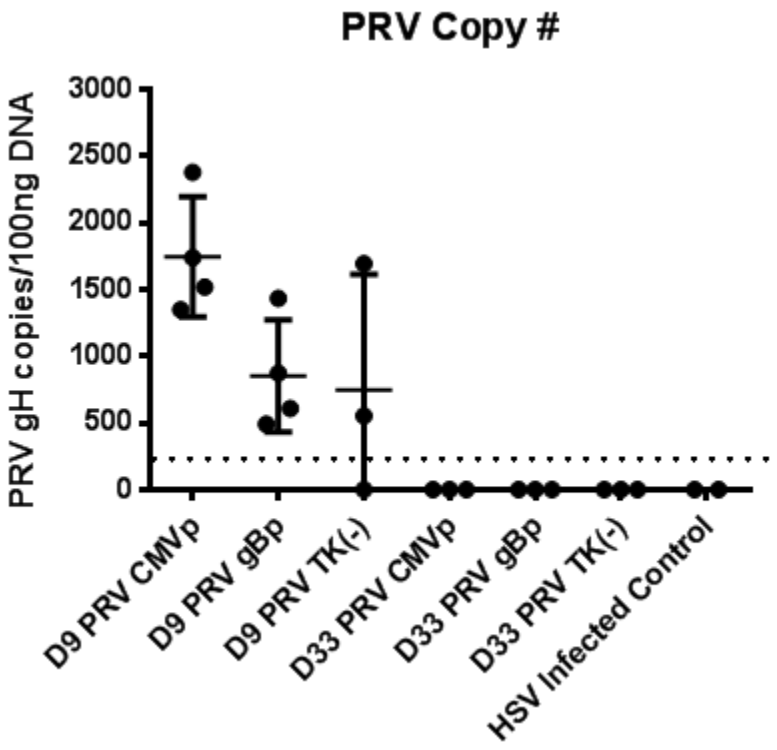

Figure 30. Genome copy numbers of PRV in infected TG at early and late times post infection

Genome copy number determined by qPCR in the TG of mice ocularly infected with 1x10^5 PFU of TK- PRV vectors expressing mRFP alone, or an mRFP cassette containing the HSV-1 epitope $gB_{498-505}$ expressed from either the PRV gB promoter, or the CMV promoter (n=3-4 mice per group). HSV infected control mice were infected with 1x10^5 PFU WT HSV-1 and treated identically. At 9 or 33 dpi, TGs were harvested, DNA isolated, and qPCR performed with primers specific for PRV gH. PRV BAC standard used as a positive control for detection, as well as calculations for viral copy number. Values are representative of the total copies per 100ng of TG DNA recovered. Dotted line indicates lower threshold of detection.

Given the potential therapeutic benefits of developing a ganglionic $CD8^+$ T cell vaccine, it is unfortunate that the strategies employed here were not more successful. While it was possible to generate a large HSV-specific CD8 response, the PRV vectors employed appear to be unsuitable for testing as prophylactic HSV-1 ganglionic T cell vaccines.

7.0 SUMMARY AND CONCLUSIONS

Most HSV-1 disease, including potentially blinding herpes stromal keratitis, results from sporadic reactivation of latent HSV-1 within sensory ganglia. Latently infected ganglia of humans and mice contain a persistent immune infiltrate of $CD4^+$ and $CD8^+$ T cells, with ganglionic $CD8^+$ T cells capable of blocking HSV-1 reactivation from *ex vivo* cultures of latently infected ganglia. The studies presented within this dissertation first describe the nature of a CD8+ T cell response directed to the S1L gB epitope mutant of HSV-1. We first demonstrate that the S1L mutation in gB generates a virus that is as fit as WT, but lacks the ability to be either primed or recognized by gB-CD8s. By ablating the immunodominant response that occurs in B6 mice, we were able to define the nature of the compensatory response. HSV-S1L infection primes an identically sized $CD8^+$ T cell response during both acute and latent infection, but the makeup of the subpopulations of antigen-specific T cells is very different from mice infected with WT virus.

At peak $CD8^+$ T cell response times post-infection, the TG-infiltrating $CD8^+$ T cell population in S1L shows a general increase in all subdominant epitope-specific CD8s that were previously identified[77]. By latency, when subdominant CD8+ T cell that recognize the 19 subdominant viral epitopes are generally exhausted and unresponsive to stimulation in WT infections, these same non-gB-CD8s are not only numerically enhanced, but show more function within latently infected ganglia. We also demonstrate by using a flank model of priming gB-

CD8s with WT coinfection, that gB-CD8s enter S1L infected ganglia, but are not retained in large numbers. This demonstrates that there is a strict requirement for antigen detection within the TG for maintaining memory $CD8^+$ T cell populations. It also suggests that the preferential retention of select RR1-, ICP8-, and UL28-specific $CD8^+$ T cells (shown in Figure 14) is in part due to ongoing MHC-I presentation of viral peptides and their detection during the establishment and/or maintenance of viral latency. Understanding the interplay between recognition of this viral protein, and how this shapes $CD8^+$ T cell effector function is vital to developing methods to maintain HSV-1 in its latent state and enhance blockade of late phase 1 reactivation events before they progress.

We next examined the effects of varying the promoter that drives $gB_{498\text{-}505}$ epitope expression to determine how viral promoter activity within the TG shapes the resident $CD8^+$ T cell populations. A panel of viruses that ectopically express this peptide from constitutive, immediate early, late, or latently active promoters was developed in HSV-1 S1L. We demonstrate that cells infected with these viruses effectively present $gB_{498\text{-}505}$ to gB-CD8s in fibroblast coculture experiments. Thus, all infected fibroblasts were able to activate as many gB-CD8s as in WT infection, by late timepoints. We also confirmed by this method that promoter activity followed the general kinetic trend expected, with early promoters activating gB-CD8s within four hours of infection, and some late promoters not being recognized until almost 24 hpi. These $gB_{498\text{-}505}$ promoter viruses allowed us to determine whether the immunodominance or number of $CD8^+$ T cells within latently infected TG can be altered by use of more active or earlier expressed viral promoters, and whether epitope expression from late or latently active promoters alter the development of the $CD8^+$ T cell response and ganglionic retention.

In all promoter viruses tested, equivalent numbers of $CD8^+$ T cells were seen in the TG throughout the acute and latent stages of infection. However, these viruses differed significantly in their ability to prime gB-CD8 responses in mice. Ectopic epitope expression from the gB promoter restored full gB-CD8 immunodominance. Expression from stronger constitutive, immediate early, and early promoters did not increase the level of immunodominance above that of WT HSV-1, suggesting a maximal level in this model had been reached. However, epitope expression from candidate viral γ2 gene promoters resulted in delayed or severely reduced priming efficiency of gB-CD8s, resulting in the compensatory $CD8^+$ T cell response of non-gB-CD8s previously described in the parental S1L virus. Epitope expression from the LAP failed to efficiently prime CD8s, with numbers not significantly different from S1L during the peak $CD8^+$ T cell infiltration. However, this virus could efficiently expand and retain a small population of gB-CD8s as other $CD8^+$ T cell populations were contracting, suggesting an increased level on ongoing recognition during the establishment of latency. These data are reminiscent of the RR1, ICP8, and UL28 specific memory $CD8^+$ T cell populations that become prominent during latency within the S1L virus due to preferential retention of these populations during the contraction phase.

We also tested the effects of peptide location and antigen stability within the context of the ability for a γ2 late gene to prime a $CD8^+$ T cell response. By using a stable mCherry-$gB_{498-505}$ expressing virus, we demonstrated that not only do the kinetics of expression alter the ability to prime efficient $CD8^+$ T cell responses, but so does the context of peptide location within the protein. Taken together, these data indicate that choice of viral promoters and context of peptide expression will influence the priming and ganglionic retention of $CD8^+$ T cell populations.

Given the ability of HSV-1 specific CD8s to remain within the latently infected tissue and monitor viral gene expression and reactivation, it would be very advantageous to establish an HSV-1 specific $CD8^+$ T cell population within the TG prior to the primary infection. To this end, we attempted to generate alternate viral vectors to prime $CD8^+$ T cell responses and deliver HSV-1 epitope to the ganglia. AAV would be an ideal method of delivery, as it is quite innocuous and nonpathogenic to the host, but targeting TG axonal termini by topical administration proved more difficult than expected. Conversely, an attenuated PRV vector was a potentially ideal choice for targeting sensory nerves within the cornea, and indeed PRV expressing $gB_{498\text{-}505}$ elicited a strong gB-CD8 response both systemically, and within the TG compartment. However, PRV had the unanticipated consequence of causing severe corneal disease— likely as a result of substantial damage to TG neurons, leading to loss of corneal innervation.

There are myriad factors within the latently infected ganglia that contribute to efficient $CD8^+$ T cell control of viral reactivation. In this work we demonstrate that there is ongoing $CD8^+$ T cell recognition within the ganglia that leads to preferential CD8 populations becoming dominant. This immunodominance is determined by a combination of host naïve T cell repertoire and selection, viral gene expression, and likely also competition between $CD8^+$ T cell populations within latently infected ganglia (possibly competition for antigen, cytokine, or costimulatory factors). By altering the amount and timing of antigen expression within the latently infected TG environment, we can partially control which memory T cell populations are present and functional. We propose that this work could lead to strategies to broaden and expand the functional $CD8^+$ T cell repertoire within latently infected sensory ganglia, which may reduce the incidence of HSV-1 reactivation and recurrent disease.

8.0 FUTURE DIRECTIONS

8.1 METHODS TO ENHANCE $CD8^+$ T CELL LATENCY MONITORING

Given the recent insights into how phase 1 "animation" leads to phase 2 progression of full lytic reactivation events in sensory ganglia, it becomes possible to think about how $CD8^+$ T cells could better monitor for and prevent reactivation. In the promoter virus studies discussed in Chapter 5, one obvious question was not addressed: Does earlier $CD8^+$ T cell recognition of viral targets better prevent progression to late phase 2 and full reactivation? Because the mouse model is a good latency model, but not an ideal reactivation model, it is difficult to answer this question *in vivo*. While it is possible to force mice to reactivate through the use of histone modifying chemical treatment, stress, or UV-light, there are many difficulties working with these models[59].

To further address this question, mice could be infected with the aforementioned constitutive, early, latently active, or late viral promoters driving the $gB_{498\text{-}505}$ to establish latent TG infections. Using the *ex vivo* reactivation approach, wherein latently TG are dissociated and cultured, with endogenous $CD8^+$ T cells depleted, and purified gB-CD8s added to the culture. Monitoring for reactivation events over time in the presence of gB-CD8s, should inform on the ability of CD8s to respond at late times in reactivation. As seen in Figure 9, gB-CD8s are not protective against the S1L virus, and require recognition of their cognate antigen to elicit effector

function. If gB-CD8s are deficient in responding to late genes, we would expect that they recognize late viral gene products, become activated, and initiate effector functions directed at TG neurons, yet the reactivation event may have progressed too far to stop by this time, and significant virus production would be detected in these cultures. Our hypothesis is that by the time γ2 viral gene products start to be expressed, HSV-1 α, β, and to some extent γ1, viral gene products will be expressed largely unchecked, leading to intracellular conditions that largely favor viral replication. Given the extensive immune evasion strategies employed by HSV-1, $CD8^+$ T cell responses at this late time may be fighting an uphill battle, and fail to effectively control release of infectious virus. This model is not perfect however, as it bypasses the necessity of the virus to undergo axonal transport from the TG to the surface as is necessary *in vivo*, and it is largely unknown whether $CD8^+$ T cells can block this vital transport step. Conversely, this same approach could be used to determine the effect that early and strong promoters have on $CD8^+$ T cell blockage of reactivation. If our hypothesis is true, and late antigen recognition is inefficient at blocking reactivation events, it would be advantageous to design future therapy strategies at targeting early viral genes.

As an alternative strategy to expressing antigen earlier, it may be advantageous to have antigen that is expressed more frequently during latency. IFNγ has been shown to be effective at reducing viral phase 1 gene expression and invoking a "quieter" latent state in viral lytic genes[142]. Therefore, provoking more frequent $CD8^+$ T cell responses directed at latently infected neurons may be highly advantageous to blocking progression to phase 2. To that end, we propose the use of chromatin insulating sequences, similar to those seen in the LAP virus presented in Chapter 5. By using better characterized and stronger chromatin insulating sequences, such as that identified in the β-globin locus in chickens[213], it may be possible to

enhance expression of peptide-expressing cassettes that will invoke $CD8^+$ T cell responses more often. A possible negative consequence to this, however, is the increased likelihood of exhausting TG-resident $CD8^+$ T cells, and a balance would need to be found. As intrinsic neuronal type 1 interferon responses also push the virus into quieter latency, it also may be possible to design recombinant HSV-1 that elicits stronger IFNα/β responses, which would bypass the need for constant $CD8^+$ T cell activation.

8.2 MECHANISM OF LATE GENE $CD8^+$ T CELL PRIMING DEFECT

Since a large number of HSV-1 encoded proteins are expressed as late genes, it would be useful to understand why they are disfavored as $CD8^+$ T cell targets. In Chapter 5, we showed that of the three γ2 late gene promoters selected, gCp failed to prime gB-CD8 responses efficiently, and UL38p and UL41p failed to prime gB-CD8 responses at all. As these viruses all had similar expression cassettes, with the $gB_{498\text{-}505}$ linked as a fusion to EGFP, the only variable is the amount and timing of antigen expression. This seemed to somewhat coincide with the later expression as determined by infected fibroblast cocultures. As discussed above, this defect in priming by late genes has been seen in other viral models. In vaccinia virus models of infection, viral genes expressed late are poor at priming $CD8^+$ T cells, and are physically sequestered within infected cells, and so are inefficiently processed and cross-presented[188, 189]. Indeed, in HSV-1 infections of DCs, there is a late-infection block of DC activation and maturation[214]. Expression of the viral UL41 gene product, the tegument protein referred to as the virion-host shutoff (vhs) gene, has been demonstrated to block DC activation, and their ability to activate naïve $CD8^+$ T cell populations[215, 216], with vhs-knockout viruses allowing DCs to retain

function [38]. Thus, it may be of future interest to determine whether vhs-knockout mutants could more efficiently prime $CD8^+$ T cell responses against late viral gene products in our model, as this may be beneficial in the design of effective vaccine vectors.

By use of a recombinant CRE-reporting mouse strain, such as the B6.Ai9(RCL-tdT), which express a bright fluorescent reporter (tdTomato) after CRE expression, it may also be possible to determine whether viral late genes are expressed in DCs within the context of early $CD8^+$ T cell priming. By creating a recombinant HSV-1 expressing a CRE-$gB_{498\text{-}505}$ fusion with a nuclear localization signal, under control of α, β, or γ2 promoters, we should be able to mark any cells that express (or take up) intact CRE-$gB_{498\text{-}505}$, and thus mark most cells that are capable of presenting the $gB_{498\text{-}505}$ epitope from the chosen promoter. Subsequent flow analysis on DLN of infected mice would determine the relative number of DC that take up viral antigen for processing, as well as characterize the subset of DC. If late genes are not expressed or processed in large numbers within the necessary DLN DC populations, this may explain the discrepancy between the amount of *in vitro* $CD8^+$ T cell recognition and the $CD8^+$ T cell priming defect observed *in vivo*.

8.3 ALTERNATIVE VIRAL VECTOR STRATEGIES TO PRIME GANGLIONIC $CD8^+$ T CELL RESPONSES

In order to design better strategies for eliciting HSV-1 specific TG-$CD8^+$ T cell responses prior to HSV-1 infection, we need to rethink the design of the vectors assessed in Chapter 6. AAV has rather limited coding capacity, but can accommodate several viral epitopes. The main issues with this vector are 1) the lack of neurotrophism in our model, and 2) the low

immunogenicity of AAV vectors. The first problem is a common one in the cornea, as we have subsequently engaged with several researchers (personal communication) unable to target corneal nerves with topically applied AAV vectors in mice. However, this issue can be overcome by using a skin model of HSV-1, where sensory termini present in the skin are known to be targeted by several AAV serotypes, and very similar $CD8^+$ T cell dynamics are seen within the DRG[200-203]. The second issue is also readily overcome by ensuring the use of an immunogenic transgene (linked to HSV-1 $CD8^+$ T cell epitopes) expressed from the AAV vector, which will elicit $CD8^+$ T cell responses within local DLN [217]. Whether these $CD8^+$ T cell responses are able to traffic to AAV transduced DRG neurons is not known and will need to be investigated.

The use of PRV as a potential therapeutic is also still a potential avenue of research, with the pathogenicity observed in mouse corneas necessitating a further PRV attenuation. The major viral transactivator in PRV, and only immediate early gene expressed, IE180, an attractive target to knock out. This would mirror many potential HSV-1 recombinant vaccine vector strategies in which ICP4 has been deleted, which yields highly attenuated viruses that are able to persist in latently infected cells[218]. IE180 is a highly toxic gene in cell culture, and successful deletion knockouts grown in conditionally expressing complementing cell lines have only recently been described [217]. This choice of viral vector would have many benefits, including: 1) not expressing viral genes that are toxic within infected neurons, thus likely reducing the loss of corneal sensory nerves and the disease as detailed previously. 2) the lack of a strong viral transactivator would prevent large amounts of antigen from expressing during PRV latency within TG neurons, thus reducing the likelihood of exhausting antiviral TG-resident CD8+ T cells. 3) Using PRV that lacks IE180 would reduce the likelihood that PRV inoculation would

transactivate HSV-1 gene expression in latently coinfected neurons. 4) PRV has no overlap with HSV-1 $CD8^+$ T cell epitopes, allowing us to methodically induce and study the efficacy of $CD8^+$ T cells that target HSV-1 genes at specific points in the viral life cycle (α, β, γ) for their ability to prevent the establishment of viral latency.

LIST OF WORKS

Treat, B. R., Bidula, S. M., Hendricks, R. L., & Kinchington, P. (2018) Manipulating promoters driving an Herpes Simplex Virus type 1 immunodominant CD8+ T cell epitope can influence the priming, development and ganglionic retention of the CD8+ T cell response. *(manuscript in preparation)*

Treat, B. R., Bidula, S. M., Ramachandran, S., Leger, A. J., Hendricks, R. L., & Kinchington, P. R. (2017). Influence of an immunodominant herpes simplex virus type 1 CD8 T cell epitope on the target hierarchy and function of subdominant CD8 T cells. PLOS Pathogens, 13(12). doi:10.1371/journal.ppat.1006732

Rowe, A M., Yun, H., **Treat, B. R**., Kinchington, P. R., & Hendricks, R. L. (2017). Subclinical Herpes Simplex Virus Type 1 Infections Provide Site-Specific Resistance to an Unrelated Pathogen. The Journal of Immunology, 198(4), 1706-1717. doi:10.4049/jimmunol.1601310

Korzeniewski, N., **Treat, B**. **R.**, & Duensing, S. (2011). The HPV-16 E7 oncoprotein induces centriole multiplication through deregulation of Polo-like kinase 4 expression. Molecular Cancer, 10(1), 61. doi:10.1186/1476-4598-10-61

BIBLIOGRAPHY

1. Beswick TS. The origin and the use of the word herpes. Medical history. 1962;6:214-32. Epub 1962/07/01. PubMed PMID: 13868599; PubMed Central PMCID: PMC1034725.
2. Pellet PE, Roizman B. The Family Herpesviridae: A Brief Introduction. In: Knipe DM, Howley PM, eds. Fields Virology. Vol. 6th edition. 6th ed. Philadelphia: Lippincott Williams & Wilkins; 2013.
3. Davison AJ. Overview of classification. In: Arvin A, Campadelli-Fiume G, Mocarski E, Moore PS, Roizman B, Whitley R, et al., editors. Human Herpesviruses: Biology, Therapy, and Immunoprophylaxis. Cambridge2007.
4. Davison AJ, Eberle R, Ehlers B, Hayward GS, McGeoch DJ, Minson AC, et al. The order Herpesvirales. Arch Virol. 2009;154(1):171-7. doi: 10.1007/s00705-008-0278-4. PubMed PMID: 19066710; PubMed Central PMCID: PMCPMC3552636.
5. Townsend CL, Forsgren M, Ahlfors K, Ivarsson SA, Tookey PA, Peckham CS. Long-term outcomes of congenital cytomegalovirus infection in Sweden and the United Kingdom. Clin Infect Dis. 2013;56(9):1232-9. doi: 10.1093/cid/cit018. PubMed PMID: 23334811; PubMed Central PMCID: PMCPMC3616516.
6. Boshoff C, Weiss R. AIDS-related malignancies. Nat Rev Cancer. 2002;2(5):373-82. doi: 10.1038/nrc797. PubMed PMID: 12044013.
7. Preston CM, Efstathiou S. Molecular basis of HSV latency and reactivation. 2007. Epub 2011/02/25. doi: NBK47421 [bookaccession]. PubMed PMID: 21348106.
8. Lee S, Ives AM, Bertke AS. Herpes Simplex Virus 1 Reactivates from Autonomic Ciliary Ganglia Independently from Sensory Trigeminal Ganglia To Cause Recurrent Ocular Disease. Journal of virology. 2015;89(16):8383-91. Epub 2015/06/05. doi: 10.1128/JVI.00468-15. PubMed PMID: 26041294; PubMed Central PMCID: PMC4524238.
9. Smith JS, Robinson NJ. Age-specific prevalence of infection with herpes simplex virus types 2 and 1: a global review. The Journal of infectious diseases. 2002;186 Suppl 1:S3-28. Epub 2002/09/28. doi: 10.1086/343739. PubMed PMID: 12353183.
10. Roizman B, Knipe DM, Whitley RJ. Herpes Simplex Viruses. In: Knipe DM, Howley PM, eds. Fields Virology. Vol. 6th edition. 6th ed. Philadelphia: Lippincott Williams & Wilkins; 2013.
11. Brazzale AG, Russell DB, Cunningham AL, Taylor J, McBride WJ. Seroprevalence of herpes simplex virus type 1 and type 2 among the Indigenous population of Cape York, Far North Queensland, Australia. Sexual health. 2010;7(4):453-9. Epub 2010/11/11. doi: 10.1071/SH09098. PubMed PMID: 21062586.
12. Mark KE, Wald A, Magaret AS, Selke S, Olin L, Huang ML, et al. Rapidly cleared episodes of herpes simplex virus reactivation in immunocompetent adults. The Journal of

infectious diseases. 2008;198(8):1141-9. Epub 2008/09/12. doi: 10.1086/591913. PubMed PMID: 18783315; PubMed Central PMCID: PMC2667115.
13. James SH, Kimberlin DW. Neonatal herpes simplex virus infection: epidemiology and treatment. Clin Perinatol. 2015;42(1):47-59, viii. doi: 10.1016/j.clp.2014.10.005. PubMed PMID: 25677996.
14. Farooq AV, Shukla D. Herpes simplex epithelial and stromal keratitis: an epidemiologic update. Surv Ophthalmol. 2012;57(5):448-62. doi: 10.1016/j.survophthal.2012.01.005. PubMed PMID: 22542912; PubMed Central PMCID: PMCPMC3652623.
15. Liesegang TJ. Herpes simplex virus epidemiology and ocular importance. Cornea. 2001;20(1):1-13. Epub 2001/02/24. PubMed PMID: 11188989.
16. Loret S, Guay G, Lippe R. Comprehensive characterization of extracellular herpes simplex virus type 1 virions. Journal of virology. 2008;82(17):8605-18. Epub 2008/07/04. doi: 10.1128/JVI.00904-08. PubMed PMID: 18596102; PubMed Central PMCID: PMC2519676.
17. Hayward GS, Ambinder R, Ciufo D, Hayward SD, LaFemina RL. Structural organization of human herpesvirus DNA molecules. J Invest Dermatol. 1984;83(1 Suppl):29s-41s. PubMed PMID: 6330219.
18. Strang BL, Stow ND. Circularization of the herpes simplex virus type 1 genome upon lytic infection. Journal of virology. 2005;79(19):12487-94. doi: 10.1128/JVI.79.19.12487-12494.2005. PubMed PMID: 16160176; PubMed Central PMCID: PMCPMC1211550.
19. Knipe DM, Howley PM. Fields virology. 6th ed. Philadelphia, PA: Wolters Kluwer/Lippincott Williams & Wilkins Health; 2013. 2 volumes p.
20. Shieh MT, WuDunn D, Montgomery RI, Esko JD, Spear PG. Cell surface receptors for herpes simplex virus are heparan sulfate proteoglycans. The Journal of cell biology. 1992;116(5):1273-81. Epub 1992/03/01. PubMed PMID: 1310996; PubMed Central PMCID: PMC2289355.
21. WuDunn D, Spear PG. Initial interaction of herpes simplex virus with cells is binding to heparan sulfate. Journal of virology. 1989;63(1):52-8. Epub 1989/01/01. PubMed PMID: 2535752; PubMed Central PMCID: PMC247656.
22. Herold BC, WuDunn D, Soltys N, Spear PG. Glycoprotein C of herpes simplex virus type 1 plays a principal role in the adsorption of virus to cells and in infectivity. Journal of virology. 1991;65(3):1090-8. PubMed PMID: 1847438; PubMed Central PMCID: PMCPMC239874.
23. Sears AE, McGwire BS, Roizman B. Infection of polarized MDCK cells with herpes simplex virus 1: two asymmetrically distributed cell receptors interact with different viral proteins. Proceedings of the National Academy of Sciences of the United States of America. 1991;88(12):5087-91. Epub 1991/06/15. PubMed PMID: 1647025; PubMed Central PMCID: PMC51816.
24. Tran LC, Kissner JM, Westerman LE, Sears AE. A herpes simplex virus 1 recombinant lacking the glycoprotein G coding sequences is defective in entry through apical surfaces of polarized epithelial cells in culture and in vivo. Proceedings of the National Academy of Sciences of the United States of America. 2000;97(4):1818-22. Epub 2000/03/04. doi: 10.1073/pnas.020510297. PubMed PMID: 10677539; PubMed Central PMCID: PMC26519.
25. Spear PG. Herpes simplex virus: receptors and ligands for cell entry. Cell Microbiol. 2004;6(5):401-10. doi: 10.1111/j.1462-5822.2004.00389.x. PubMed PMID: 15056211.

26. Spear PG, Longnecker R. Herpesvirus entry: an update. Journal of virology. 2003;77(19):10179-85. Epub 2003/09/13. PubMed PMID: 12970403; PubMed Central PMCID: PMC228481.
27. Subramanian RP, Geraghty RJ. Herpes simplex virus type 1 mediates fusion through a hemifusion intermediate by sequential activity of glycoproteins D, H, L, and B. Proceedings of the National Academy of Sciences of the United States of America. 2007;104(8):2903-8. Epub 2007/02/15. doi: 10.1073/pnas.0608374104. PubMed PMID: 17299053; PubMed Central PMCID: PMC1815279.
28. Fuller AO, Spear PG. Anti-glycoprotein D antibodies that permit adsorption but block infection by herpes simplex virus 1 prevent virion-cell fusion at the cell surface. Proc Natl Acad Sci U S A. 1987;84(15):5454-8. PubMed PMID: 3037552; PubMed Central PMCID: PMCPMC298876.
29. Nicola AV, McEvoy AM, Straus SE. Roles for endocytosis and low pH in herpes simplex virus entry into HeLa and Chinese hamster ovary cells. Journal of virology. 2003;77(9):5324-32. PubMed PMID: 12692234; PubMed Central PMCID: PMCPMC153978.
30. Karasneh GA, Shukla D. Herpes simplex virus infects most cell types in vitro: clues to its success. Virology journal. 2011;8:481. Epub 2011/10/28. doi: 10.1186/1743-422X-8-481. PubMed PMID: 22029482; PubMed Central PMCID: PMC3223518.
31. Dohner K, Wolfstein A, Prank U, Echeverri C, Dujardin D, Vallee R, et al. Function of dynein and dynactin in herpes simplex virus capsid transport. Molecular biology of the cell. 2002;13(8):2795-809. Epub 2002/08/16. doi: 10.1091/mbc.01-07-0348. PubMed PMID: 12181347; PubMed Central PMCID: PMC117943.
32. Sodeik B, Ebersold MW, Helenius A. Microtubule-mediated transport of incoming herpes simplex virus 1 capsids to the nucleus. J Cell Biol. 1997;136(5):1007-21. PubMed PMID: 9060466; PubMed Central PMCID: PMCPMC2132479.
33. Campbell ME, Palfreyman JW, Preston CM. Identification of herpes simplex virus DNA sequences which encode a trans-acting polypeptide responsible for stimulation of immediate early transcription. Journal of molecular biology. 1984;180(1):1-19. Epub 1984/11/25. PubMed PMID: 6096556.
34. Gerster T, Roeder RG. A herpesvirus trans-activating protein interacts with transcription factor OTF-1 and other cellular proteins. Proceedings of the National Academy of Sciences of the United States of America. 1988;85(17):6347-51. Epub 1988/09/01. PubMed PMID: 2842768; PubMed Central PMCID: PMC281967.
35. Stern S, Tanaka M, Herr W. The Oct-1 homoeodomain directs formation of a multiprotein-DNA complex with the HSV transactivator VP16. Nature. 1989;341(6243):624-30. Epub 1989/10/19. doi: 10.1038/341624a0. PubMed PMID: 2571937.
36. Wilson AC, LaMarco K, Peterson MG, Herr W. The VP16 accessory protein HCF is a family of polypeptides processed from a large precursor protein. Cell. 1993;74(1):115-25. Epub 1993/07/16. PubMed PMID: 8392914.
37. Kwong AD, Frenkel N. Herpes simplex virus-infected cells contain a function(s) that destabilizes both host and viral mRNAs. Proceedings of the National Academy of Sciences of the United States of America. 1987;84(7):1926-30. Epub 1987/04/01. PubMed PMID: 3031658; PubMed Central PMCID: PMC304554.
38. Smiley JR. Herpes simplex virus virion host shutoff protein: immune evasion mediated by a viral RNase? Journal of virology. 2004;78(3):1063-8. Epub 2004/01/15. PubMed PMID: 14722261; PubMed Central PMCID: PMC321390.

39. Field HJ, Wildy P. The pathogenicity of thymidine kinase-deficient mutants of herpes simplex virus in mice. The Journal of hygiene. 1978;81(2):267-77. Epub 1978/10/01. PubMed PMID: 212476; PubMed Central PMCID: PMC2129783.
40. Pyles RB, Sawtell NM, Thompson RL. Herpes simplex virus type 1 dUTPase mutants are attenuated for neurovirulence, neuroinvasiveness, and reactivation from latency. Journal of virology. 1992;66(11):6706-13. Epub 1992/11/01. PubMed PMID: 1328686; PubMed Central PMCID: PMC240166.
41. Hwang S, Kim KS, Flano E, Wu TT, Tong LM, Park AN, et al. Conserved herpesviral kinase promotes viral persistence by inhibiting the IRF-3-mediated type I interferon response. Cell host & microbe. 2009;5(2):166-78. Epub 2009/02/17. doi: 10.1016/j.chom.2008.12.013. PubMed PMID: 19218087; PubMed Central PMCID: PMC2749518.
42. Benetti L, Munger J, Roizman B. The herpes simplex virus 1 US3 protein kinase blocks caspase-dependent double cleavage and activation of the proapoptotic protein BAD. Journal of virology. 2003;77(11):6567-73. Epub 2003/05/14. PubMed PMID: 12743316; PubMed Central PMCID: PMC155029.
43. Leopardi R, Van Sant C, Roizman B. The herpes simplex virus 1 protein kinase US3 is required for protection from apoptosis induced by the virus. Proceedings of the National Academy of Sciences of the United States of America. 1997;94(15):7891-6. Epub 1997/07/22. PubMed PMID: 9223283; PubMed Central PMCID: PMC21525.
44. Everett RD. ICP0, a regulator of herpes simplex virus during lytic and latent infection. Bioessays. 2000;22(8):761-70. doi: 10.1002/1521-1878(200008)22:8<761::AID-BIES10>3.0.CO;2-A. PubMed PMID: 10918307.
45. Hagglund R, Roizman B. Role of ICP0 in the strategy of conquest of the host cell by herpes simplex virus 1. Journal of virology. 2004;78(5):2169-78. PubMed PMID: 14963113; PubMed Central PMCID: PMCPMC369245.
46. Gu H, Liang Y, Mandel G, Roizman B. Components of the REST/CoREST/histone deacetylase repressor complex are disrupted, modified, and translocated in HSV-1-infected cells. Proc Natl Acad Sci U S A. 2005;102(21):7571-6. doi: 10.1073/pnas.0502658102. PubMed PMID: 15897453; PubMed Central PMCID: PMCPMC1140450.
47. DeLuca NA, McCarthy AM, Schaffer PA. Isolation and characterization of deletion mutants of herpes simplex virus type 1 in the gene encoding immediate-early regulatory protein ICP4. Journal of virology. 1985;56(2):558-70. PubMed PMID: 2997476; PubMed Central PMCID: PMCPMC252613.
48. Watson RJ, Clements JB. A herpes simplex virus type 1 function continuously required for early and late virus RNA synthesis. Nature. 1980;285(5763):329-30. PubMed PMID: 6246451.
49. Fruh K, Ahn K, Djaballah H, Sempe P, van Endert PM, Tampe R, et al. A viral inhibitor of peptide transporters for antigen presentation. Nature. 1995;375(6530):415-8. doi: 10.1038/375415a0. PubMed PMID: 7760936.
50. Hill A, Jugovic P, York I, Russ G, Bennink J, Yewdell J, et al. Herpes simplex virus turns off the TAP to evade host immunity. Nature. 1995;375(6530):411-5. doi: 10.1038/375411a0. PubMed PMID: 7760935.
51. Mavromara-Nazos P, Roizman B. Activation of herpes simplex virus 1 gamma 2 genes by viral DNA replication. Virology. 1987;161(2):593-8. PubMed PMID: 2825424.

52. Honess RW, Roizman B. Regulation of herpesvirus macromolecular synthesis. I. Cascade regulation of the synthesis of three groups of viral proteins. Journal of virology. 1974;14(1):8-19. PubMed PMID: 4365321; PubMed Central PMCID: PMCPMC355471.
53. Mettenleiter TC. Herpesvirus assembly and egress. Journal of virology. 2002;76(4):1537-47. PubMed PMID: 11799148; PubMed Central PMCID: PMCPMC135924.
54. Herrera FJ, Triezenberg SJ. VP16-dependent association of chromatin-modifying coactivators and underrepresentation of histones at immediate-early gene promoters during herpes simplex virus infection. Journal of virology. 2004;78(18):9689-96. doi: 10.1128/JVI.78.18.9689-9696.2004. PubMed PMID: 15331701; PubMed Central PMCID: PMCPMC515004.
55. Smith G. Herpesvirus transport to the nervous system and back again. Annu Rev Microbiol. 2012;66:153-76. doi: 10.1146/annurev-micro-092611-150051. PubMed PMID: 22726218; PubMed Central PMCID: PMCPMC3882149.
56. Nicoll MP, Hann W, Shivkumar M, Harman LE, Connor V, Coleman HM, et al. The HSV-1 Latency-Associated Transcript Functions to Repress Latent Phase Lytic Gene Expression and Suppress Virus Reactivation from Latently Infected Neurons. PLoS pathogens. 2016;12(4):e1005539. doi: 10.1371/journal.ppat.1005539. PubMed PMID: 27055281; PubMed Central PMCID: PMCPMC4824392.
57. Bloom DC. HSV LAT and neuronal survival. Int Rev Immunol. 2004;23(1-2):187-98. PubMed PMID: 14690860.
58. Thompson RL, Sawtell NM. Herpes simplex virus type 1 latency-associated transcript gene promotes neuronal survival. Journal of virology. 2001;75(14):6660-75. doi: 10.1128/JVI.75.14.6660-6675.2001. PubMed PMID: 11413333; PubMed Central PMCID: PMCPMC114389.
59. Nicoll MP, Proenca JT, Efstathiou S. The molecular basis of herpes simplex virus latency. FEMS Microbiol Rev. 2012;36(3):684-705. doi: 10.1111/j.1574-6976.2011.00320.x. PubMed PMID: 22150699; PubMed Central PMCID: PMCPMC3492847.
60. Stevens JG, Wagner EK, Devi-Rao GB, Cook ML, Feldman LT. RNA complementary to a herpesvirus alpha gene mRNA is prominent in latently infected neurons. Science. 1987;235(4792):1056-9. PubMed PMID: 2434993.
61. Cliffe AR, Wilson AC. Restarting Lytic Gene Transcription at the Onset of Herpes Simplex Virus Reactivation. Journal of virology. 2017;91(2). doi: 10.1128/JVI.01419-16. PubMed PMID: 27807236; PubMed Central PMCID: PMCPMC5215350.
62. Kim JY, Mandarino A, Chao MV, Mohr I, Wilson AC. Transient reversal of episome silencing precedes VP16-dependent transcription during reactivation of latent HSV-1 in neurons. PLoS pathogens. 2012;8(2):e1002540. Epub 2012/03/03. doi: 10.1371/journal.ppat.1002540. PubMed PMID: 22383875; PubMed Central PMCID: PMC3285597.
63. Du T, Zhou G, Roizman B. HSV-1 gene expression from reactivated ganglia is disordered and concurrent with suppression of latency-associated transcript and miRNAs. Proc Natl Acad Sci U S A. 2011;108(46):18820-4. Epub 2011/11/09. doi: 1117203108 [pii]
10.1073/pnas.1117203108. PubMed PMID: 22065742; PubMed Central PMCID: PMC3219146.
64. Roizman B, Zhou G, Du T. Checkpoints in productive and latent infections with herpes simplex virus 1: conceptualization of the issues. Journal of neurovirology. 2011;17(6):512-7. Epub 2011/11/05. doi: 10.1007/s13365-011-0058-x. PubMed PMID: 22052379.
65. Harkness JM, Kader M, DeLuca NA. Transcription of the herpes simplex virus 1 genome during productive and quiescent infection of neuronal and nonneuronal cells. Journal of virology.

2014;88(12):6847-61. doi: 10.1128/JVI.00516-14. PubMed PMID: 24719411; PubMed Central PMCID: PMCPMC4054390.
66. Ma JZ, Russell TA, Spelman T, Carbone FR, Tscharke DC. Lytic gene expression is frequent in HSV-1 latent infection and correlates with the engagement of a cell-intrinsic transcriptional response. PLoS pathogens. 2014;10(7):e1004237. doi: 10.1371/journal.ppat.1004237. PubMed PMID: 25058429; PubMed Central PMCID: PMC4110040.
67. Russell TA, Tscharke DC. Lytic Promoters Express Protein during Herpes Simplex Virus Latency. PLoS pathogens. 2016;12(6):e1005729. Epub 2016/06/28. doi: 10.1371/journal.ppat.1005729. PubMed PMID: 27348812; PubMed Central PMCID: PMC4922595.
68. Khanna KM, Bonneau RH, Kinchington PR, Hendricks RL. Herpes simplex virus-specific memory CD8+ T cells are selectively activated and retained in latently infected sensory ganglia. Immunity. 2003;18(5):593-603. Epub 2003/05/20. doi: S1074761303001122 [pii]. PubMed PMID: 12753737; PubMed Central PMCID: PMC2871305.
69. Wilcox CL, Johnson EM, Jr. Nerve growth factor deprivation results in the reactivation of latent herpes simplex virus in vitro. Journal of virology. 1987;61(7):2311-5. PubMed PMID: 3035230; PubMed Central PMCID: PMCPMC283698.
70. Arthur JL, Scarpini CG, Connor V, Lachmann RH, Tolkovsky AM, Efstathiou S. Herpes simplex virus type 1 promoter activity during latency establishment, maintenance, and reactivation in primary dorsal root neurons in vitro. Journal of virology. 2001;75(8):3885-95. doi: 10.1128/JVI.75.8.3885-3895.2001. PubMed PMID: 11264377; PubMed Central PMCID: PMCPMC114879.
71. Stanberry LR, Kern ER, Richards JT, Overall JC, Jr. Recurrent genital herpes simplex virus infection in guinea pigs. Intervirology. 1985;24(4):226-31. Epub 1985/01/01. doi: 10.1159/000149647. PubMed PMID: 3000982.
72. Hill TJ, Field HJ, Blyth WA. Acute and recurrent infection with herpes simplex virus in the mouse: a model for studying latency and recurrent disease. The Journal of general virology. 1975;28(3):341-53. Epub 1975/09/01. doi: 10.1099/0022-1317-28-3-341. PubMed PMID: 170376.
73. Koelle DM, Wald A. Herpes simplex virus: the importance of asymptomatic shedding. The Journal of antimicrobial chemotherapy. 2000;45 Suppl T3:1-8. Epub 2000/06/16. PubMed PMID: 10855766.
74. Berman EJ, Hill JM. Spontaneous ocular shedding of HSV-1 in latently infected rabbits. Investigative ophthalmology & visual science. 1985;26(4):587-90. Epub 1985/04/01. PubMed PMID: 2984140.
75. Kumar M, Kaufman HE, Clement C, Bhattacharjee PS, Huq TS, Varnell ED, et al. Effect of high versus low oral doses of valacyclovir on herpes simplex virus-1 DNA shedding into tears of latently infected rabbits. Investigative ophthalmology & visual science. 2010;51(9):4703-6. Epub 2010/04/16. doi: 10.1167/iovs.09-4884. PubMed PMID: 20393107; PubMed Central PMCID: PMC2941183.
76. Cleary MA, Stern S, Tanaka M, Herr W. Differential positive control by Oct-1 and Oct-2: activation of a transcriptionally silent motif through Oct-1 and VP16 corecruitment. Genes & development. 1993;7(1):72-83. Epub 1993/01/01. PubMed PMID: 8422989.
77. St Leger AJ, Peters B, Sidney J, Sette A, Hendricks RL. Defining the herpes simplex virus-specific CD8+ T cell repertoire in C57BL/6 mice. J Immunol. 2011;186(7):3927-33. doi:

10.4049/jimmunol.1003735. PubMed PMID: 21357536; PubMed Central PMCID: PMC3308013.
78. Liu T, Khanna KM, Chen X, Fink DJ, Hendricks RL. CD8(+) T cells can block herpes simplex virus type 1 (HSV-1) reactivation from latency in sensory neurons. J Exp Med. 2000;191(9):1459-66. Epub 2000/05/03. PubMed PMID: 10790421; PubMed Central PMCID: PMC2213436.
79. Chew T, Taylor KE, Mossman KL. Innate and adaptive immune responses to herpes simplex virus. Viruses. 2009;1(3):979-1002. doi: 10.3390/v1030979. PubMed PMID: 21994578; PubMed Central PMCID: PMCPMC3185534.
80. Krug A, Luker GD, Barchet W, Leib DA, Akira S, Colonna M. Herpes simplex virus type 1 activates murine natural interferon-producing cells through toll-like receptor 9. Blood. 2004;103(4):1433-7. doi: 10.1182/blood-2003-08-2674. PubMed PMID: 14563635.
81. Herbst-Kralovetz M, Pyles R. Toll-like receptors, innate immunity and HSV pathogenesis. Herpes. 2006;13(2):37-41. PubMed PMID: 16895653.
82. Li H, Zhang J, Kumar A, Zheng M, Atherton SS, Yu FS. Herpes simplex virus 1 infection induces the expression of proinflammatory cytokines, interferons and TLR7 in human corneal epithelial cells. Immunology. 2006;117(2):167-76. doi: 10.1111/j.1365-2567.2005.02275.x. PubMed PMID: 16423052; PubMed Central PMCID: PMCPMC1782219.
83. Jin X, Qin Q, Chen W, Qu J. Expression of toll-like receptors in the healthy and herpes simplex virus-infected cornea. Cornea. 2007;26(7):847-52. doi: 10.1097/ICO.0b013e318093de1f. PubMed PMID: 17667620.
84. Lund J, Sato A, Akira S, Medzhitov R, Iwasaki A. Toll-like receptor 9-mediated recognition of Herpes simplex virus-2 by plasmacytoid dendritic cells. J Exp Med. 2003;198(3):513-20. doi: 10.1084/jem.20030162. PubMed PMID: 12900525; PubMed Central PMCID: PMCPMC2194085.
85. Ishikawa H, Ma Z, Barber GN. STING regulates intracellular DNA-mediated, type I interferon-dependent innate immunity. Nature. 2009;461(7265):788-92. doi: 10.1038/nature08476. PubMed PMID: 19776740; PubMed Central PMCID: PMCPMC4664154.
86. Unterholzner L, Keating SE, Baran M, Horan KA, Jensen SB, Sharma S, et al. IFI16 is an innate immune sensor for intracellular DNA. Nat Immunol. 2010;11(11):997-1004. doi: 10.1038/ni.1932. PubMed PMID: 20890285; PubMed Central PMCID: PMCPMC3142795.
87. Hendricks RL, Weber PC, Taylor JL, Koumbis A, Tumpey TM, Glorioso JC. Endogenously produced interferon alpha protects mice from herpes simplex virus type 1 corneal disease. J Gen Virol. 1991;72 (Pt 7):1601-10. doi: 10.1099/0022-1317-72-7-1601. PubMed PMID: 1649898.
88. Gu H, Zheng Y, Roizman B. Interaction of herpes simplex virus ICP0 with ND10 bodies: a sequential process of adhesion, fusion, and retention. Journal of virology. 2013;87(18):10244-54. doi: 10.1128/JVI.01487-13. PubMed PMID: 23864622; PubMed Central PMCID: PMCPMC3753982.
89. Jerome KR, Fox R, Chen Z, Sears AE, Lee H, Corey L. Herpes simplex virus inhibits apoptosis through the action of two genes, Us5 and Us3. Journal of virology. 1999;73(11):8950-7. PubMed PMID: 10516000; PubMed Central PMCID: PMCPMC112926.
90. He B, Gross M, Roizman B. The gamma(1)34.5 protein of herpes simplex virus 1 complexes with protein phosphatase 1alpha to dephosphorylate the alpha subunit of the eukaryotic translation initiation factor 2 and preclude the shutoff of protein synthesis by double-

stranded RNA-activated protein kinase. Proc Natl Acad Sci U S A. 1997;94(3):843-8. PubMed PMID: 9023344; PubMed Central PMCID: PMCPMC19601.
91. Daheshia M, Kanangat S, Rouse BT. Production of key molecules by ocular neutrophils early after herpetic infection of the cornea. Exp Eye Res. 1998;67(6):619-24. doi: 10.1006/exer.1998.0565. PubMed PMID: 9990326.
92. He J, Ichimura H, Iida T, Minami M, Kobayashi K, Kita M, et al. Kinetics of cytokine production in the cornea and trigeminal ganglion of C57BL/6 mice after corneal HSV-1 infection. J Interferon Cytokine Res. 1999;19(6):609-15. doi: 10.1089/107999099313749. PubMed PMID: 10433361.
93. Keadle TL, Usui N, Laycock KA, Miller JK, Pepose JS, Stuart PM. IL-1 and TNF-alpha are important factors in the pathogenesis of murine recurrent herpetic stromal keratitis. Invest Ophthalmol Vis Sci. 2000;41(1):96-102. PubMed PMID: 10634607.
94. Oakes JE, Monteiro CA, Cubitt CL, Lausch RN. Induction of interleukin-8 gene expression is associated with herpes simplex virus infection of human corneal keratocytes but not human corneal epithelial cells. Journal of virology. 1993;67(8):4777-84. PubMed PMID: 7687302; PubMed Central PMCID: PMCPMC237864.
95. Tumpey TM, Cheng H, Cook DN, Smithies O, Oakes JE, Lausch RN. Absence of macrophage inflammatory protein-1alpha prevents the development of blinding herpes stromal keratitis. Journal of virology. 1998;72(5):3705-10. PubMed PMID: 9557652; PubMed Central PMCID: PMCPMC109592.
96. Vollstedt S, Arnold S, Schwerdel C, Franchini M, Alber G, Di Santo JP, et al. Interplay between alpha/beta and gamma interferons with B, T, and natural killer cells in the defense against herpes simplex virus type 1. Journal of virology. 2004;78(8):3846-50. PubMed PMID: 15047800; PubMed Central PMCID: PMCPMC374284.
97. Carr DJ, Harle P, Gebhardt BM. The immune response to ocular herpes simplex virus type 1 infection. Exp Biol Med (Maywood). 2001;226(5):353-66. PubMed PMID: 11393165.
98. Tang Q, Hendricks RL. Interferon gamma regulates platelet endothelial cell adhesion molecule 1 expression and neutrophil infiltration into herpes simplex virus-infected mouse corneas. J Exp Med. 1996;184(4):1435-47. PubMed PMID: 8879215; PubMed Central PMCID: PMCPMC2192815.
99. Miyazaki D, Inoue Y, Araki-Sasaki K, Shimomura Y, Tano Y, Hayashi K. Neutrophil chemotaxis induced by corneal epithelial cells after herpes simplex virus type 1 infection. Curr Eye Res. 1998;17(7):687-93. PubMed PMID: 9678413.
100. Tumpey TM, Chen SH, Oakes JE, Lausch RN. Neutrophil-mediated suppression of virus replication after herpes simplex virus type 1 infection of the murine cornea. Journal of virology. 1996;70(2):898-904. Epub 1996/02/01. PubMed PMID: 8551629; PubMed Central PMCID: PMC189893.
101. Kodukula P, Liu T, Rooijen NV, Jager MJ, Hendricks RL. Macrophage control of herpes simplex virus type 1 replication in the peripheral nervous system. J Immunol. 1999;162(5):2895-905. Epub 1999/03/11. PubMed PMID: 10072539.
102. Liu T, Tang Q, Hendricks RL. Inflammatory infiltration of the trigeminal ganglion after herpes simplex virus type 1 corneal infection. Journal of virology. 1996;70(1):264-71. PubMed PMID: 8523535; PubMed Central PMCID: PMCPMC189813.
103. Sciammas R, Kodukula P, Tang Q, Hendricks RL, Bluestone JA. T cell receptor-gamma/delta cells protect mice from herpes simplex virus type 1-induced lethal encephalitis. J

Exp Med. 1997;185(11):1969-75. PubMed PMID: 9166426; PubMed Central PMCID: PMCPMC2196341.
104. Mori R, Minagawa H, Sakuma S, Mohri S, Watanabe T. Herpes simplex virus type 1 infection in mice with severe combined immunodeficiency (SCID). Advances in experimental medicine and biology. 1990;278:191-7. Epub 1990/01/01. PubMed PMID: 1705079.
105. Beland JL, Sobel RA, Adler H, Del-Pan NC, Rimm IJ. B cell-deficient mice have increased susceptibility to HSV-1 encephalomyelitis and mortality. Journal of neuroimmunology. 1999;94(1-2):122-6. Epub 1999/06/22. PubMed PMID: 10376944.
106. Mikloska Z, Sanna PP, Cunningham AL. Neutralizing antibodies inhibit axonal spread of herpes simplex virus type 1 to epidermal cells in vitro. Journal of virology. 1999;73(7):5934-44. PubMed PMID: 10364346; PubMed Central PMCID: PMCPMC112655.
107. Eing BR, Kuhn JE, Braun RW. Neutralizing activity of antibodies against the major herpes simplex virus type 1 glycoproteins. J Med Virol. 1989;27(1):59-65. PubMed PMID: 2466100.
108. Ghiasi H, Perng G, Nesburn AB, Wechsler SL. Either a CD4(+)or CD8(+)T cell function is sufficient for clearance of infectious virus from trigeminal ganglia and establishment of herpes simplex virus type 1 latency in mice. Microb Pathog. 1999;27(6):387-94. doi: 10.1006/mpat.1999.0314. PubMed PMID: 10588911.
109. Shimeld C, Whiteland JL, Nicholls SM, Grinfeld E, Easty DL, Gao H, et al. Immune cell infiltration and persistence in the mouse trigeminal ganglion after infection of the cornea with herpes simplex virus type 1. J Neuroimmunol. 1995;61(1):7-16. PubMed PMID: 7560014.
110. Frank GM, Lepisto AJ, Freeman ML, Sheridan BS, Cherpes TL, Hendricks RL. Early CD4(+) T cell help prevents partial CD8(+) T cell exhaustion and promotes maintenance of Herpes Simplex Virus 1 latency. J Immunol. 2010;184(1):277-86. Epub 2009/12/02. doi: 10.4049/jimmunol.0902373. PubMed PMID: 19949087; PubMed Central PMCID: PMC3298035.
111. Heiligenhaus A, Bauer D, Zheng M, Mrzyk S, Steuhl KP. CD4+ T-cell type 1 and type 2 cytokines in the HSV-1 infected cornea. Graefe's archive for clinical and experimental ophthalmology = Albrecht von Graefes Archiv fur klinische und experimentelle Ophthalmologie. 1999;237(5):399-406. Epub 1999/05/20. PubMed PMID: 10333107.
112. Keadle TL, Morris JL, Pepose JS, Stuart PM. CD4(+) and CD8(+) cells are key participants in the development of recurrent herpetic stromal keratitis in mice. Microbial pathogenesis. 2002;32(6):255-62. Epub 2002/07/26. PubMed PMID: 12137752.
113. St Leger AJ, Hendricks RL. CD8+ T cells patrol HSV-1-infected trigeminal ganglia and prevent viral reactivation. Journal of neurovirology. 2011;17(6):528-34. Epub 2011/12/14. doi: 10.1007/s13365-011-0062-1. PubMed PMID: 22161682.
114. Sheridan BS, Cherpes TL, Urban J, Kalinski P, Hendricks RL. Reevaluating the CD8 T-cell response to herpes simplex virus type 1: involvement of CD8 T cells reactive to subdominant epitopes. Journal of virology. 2009;83(5):2237-45. Epub 2008/12/17. doi: JVI.01699-08 [pii]
10.1128/JVI.01699-08. PubMed PMID: 19073721; PubMed Central PMCID: PMC2643732.
115. Joffre OP, Segura E, Savina A, Amigorena S. Cross-presentation by dendritic cells. Nat Rev Immunol. 2012;12(8):557-69. doi: 10.1038/nri3254. PubMed PMID: 22790179.
116. Ackerman AL, Cresswell P. Cellular mechanisms governing cross-presentation of exogenous antigens. Nat Immunol. 2004;5(7):678-84. doi: 10.1038/ni1082. PubMed PMID: 15224093.

117. Singh R, Cresswell P. Defective cross-presentation of viral antigens in GILT-free mice. Science. 2010;328(5984):1394-8. doi: 10.1126/science.1189176. PubMed PMID: 20538950; PubMed Central PMCID: PMCPMC2925227.
118. Whitney PG, Makhlouf C, MacLeod B, Ma JZ, Gressier E, Greyer M, et al. Effective Priming of Herpes Simplex Virus-Specific CD8(+) T Cells In Vivo Does Not Require Infected Dendritic Cells. Journal of virology. 2018;92(3). doi: 10.1128/JVI.01508-17. PubMed PMID: 29142130; PubMed Central PMCID: PMCPMC5774880.
119. Gurevich I, Feferman T, Milo I, Tal O, Golani O, Drexler I, et al. Active dissemination of cellular antigens by DCs facilitates CD8(+) T-cell priming in lymph nodes. Eur J Immunol. 2017;47(10):1802-18. doi: 10.1002/eji.201747042. PubMed PMID: 28872666.
120. Hildner K, Edelson BT, Purtha WE, Diamond M, Matsushita H, Kohyama M, et al. Batf3 deficiency reveals a critical role for CD8alpha+ dendritic cells in cytotoxic T cell immunity. Science. 2008;322(5904):1097-100. doi: 10.1126/science.1164206. PubMed PMID: 19008445; PubMed Central PMCID: PMCPMC2756611.
121. Hor JL, Whitney PG, Zaid A, Brooks AG, Heath WR, Mueller SN. Spatiotemporally Distinct Interactions with Dendritic Cell Subsets Facilitates CD4+ and CD8+ T Cell Activation to Localized Viral Infection. Immunity. 2015;43(3):554-65. doi: 10.1016/j.immuni.2015.07.020. PubMed PMID: 26297566.
122. Lin LC, Flesch IE, Tscharke DC. Immunodomination during peripheral vaccinia virus infection. PLoS pathogens. 2013;9(4):e1003329. doi: 10.1371/journal.ppat.1003329. PubMed PMID: 23633956; PubMed Central PMCID: PMCPMC3635974.
123. Samji T, Khanna KM. Understanding memory CD8(+) T cells. Immunol Lett. 2017;185:32-9. doi: 10.1016/j.imlet.2017.02.012. PubMed PMID: 28274794; PubMed Central PMCID: PMCPMC5508124.
124. Doherty PC, Hou S, Tripp RA. CD8+ T-cell memory to viruses. Curr Opin Immunol. 1994;6(4):545-52. PubMed PMID: 7946041.
125. Lau LL, Jamieson BD, Somasundaram T, Ahmed R. Cytotoxic T-cell memory without antigen. Nature. 1994;369(6482):648-52. doi: 10.1038/369648a0. PubMed PMID: 7516038.
126. Himmelein S, St Leger AJ, Knickelbein JE, Rowe A, Freeman ML, Hendricks RL. Circulating herpes simplex type 1 (HSV-1)-specific CD8+ T cells do not access HSV-1 latently infected trigeminal ganglia. Herpesviridae. 2011;2(1):5. doi: 10.1186/2042-4280-2-5. PubMed PMID: 21429183; PubMed Central PMCID: PMCPMC3070622.
127. Wherry EJ. T cell exhaustion. Nat Immunol. 2011;12(6):492-9. PubMed PMID: 21739672.
128. Radziewicz H, Ibegbu CC, Fernandez ML, Workowski KA, Obideen K, Wehbi M, et al. Liver-infiltrating lymphocytes in chronic human hepatitis C virus infection display an exhausted phenotype with high levels of PD-1 and low levels of CD127 expression. Journal of virology. 2007;81(6):2545-53. doi: 10.1128/JVI.02021-06. PubMed PMID: 17182670; PubMed Central PMCID: PMCPMC1865979.
129. Angelosanto JM, Blackburn SD, Crawford A, Wherry EJ. Progressive loss of memory T cell potential and commitment to exhaustion during chronic viral infection. Journal of virology. 2012;86(15):8161-70. doi: 10.1128/JVI.00889-12. PubMed PMID: 22623779; PubMed Central PMCID: PMCPMC3421680.
130. Day CL, Kaufmann DE, Kiepiela P, Brown JA, Moodley ES, Reddy S, et al. PD-1 expression on HIV-specific T cells is associated with T-cell exhaustion and disease progression. Nature. 2006;443(7109):350-4. doi: 10.1038/nature05115. PubMed PMID: 16921384.

131. Wherry EJ, Blattman JN, Murali-Krishna K, van der Most R, Ahmed R. Viral persistence alters CD8 T-cell immunodominance and tissue distribution and results in distinct stages of functional impairment. Journal of virology. 2003;77(8):4911-27. PubMed PMID: 12663797; PubMed Central PMCID: PMCPMC152117.
132. Erickson JJ, Rogers MC, Hastings AK, Tollefson SJ, Williams JV. Programmed death-1 impairs secondary effector lung CD8(+) T cells during respiratory virus reinfection. J Immunol. 2014;193(10):5108-17. doi: 10.4049/jimmunol.1302208. PubMed PMID: 25339663; PubMed Central PMCID: PMCPMC4225166.
133. Wherry EJ, Kurachi M. Molecular and cellular insights into T cell exhaustion. Nat Rev Immunol. 2015;15(8):486-99. doi: 10.1038/nri3862. PubMed PMID: 26205583; PubMed Central PMCID: PMCPMC4889009.
134. Jin HT, Anderson AC, Tan WG, West EE, Ha SJ, Araki K, et al. Cooperation of Tim-3 and PD-1 in CD8 T-cell exhaustion during chronic viral infection. Proc Natl Acad Sci U S A. 2010;107(33):14733-8. doi: 10.1073/pnas.1009731107. PubMed PMID: 20679213; PubMed Central PMCID: PMCPMC2930455.
135. Okazaki T, Okazaki IM, Wang J, Sugiura D, Nakaki F, Yoshida T, et al. PD-1 and LAG-3 inhibitory co-receptors act synergistically to prevent autoimmunity in mice. J Exp Med. 2011;208(2):395-407. doi: 10.1084/jem.20100466. PubMed PMID: 21300912; PubMed Central PMCID: PMCPMC3039848.
136. Mackay LK, Wakim L, van Vliet CJ, Jones CM, Mueller SN, Bannard O, et al. Maintenance of T cell function in the face of chronic antigen stimulation and repeated reactivation for a latent virus infection. J Immunol. 2012;188(5):2173-8. Epub 2012/01/25. doi: 10.4049/jimmunol.1102719. PubMed PMID: 22271651; PubMed Central PMCID: PMC3378511.
137. Decman V, Freeman ML, Kinchington PR, Hendricks RL. Immune control of HSV-1 latency. Viral immunology. 2005;18(3):466-73. Epub 2005/10/11. doi: 10.1089/vim.2005.18.466. PubMed PMID: 16212525.
138. Held K, Derfuss T. Control of HSV-1 latency in human trigeminal ganglia--current overview. Journal of neurovirology. 2011;17(6):518-27. Epub 2011/12/06. doi: 10.1007/s13365-011-0063-0. PubMed PMID: 22139603.
139. Held K, Eiglmeier I, Himmelein S, Sinicina I, Brandt T, Theil D, et al. Clonal expansions of CD8(+) T cells in latently HSV-1-infected human trigeminal ganglia. Journal of neurovirology. 2012;18(1):62-8. Epub 2011/12/15. doi: 10.1007/s13365-011-0067-9. PubMed PMID: 22167486.
140. Derfuss T, Arbusow V, Strupp M, Brandt T, Theil D. The presence of lytic HSV-1 transcripts and clonally expanded T cells with a memory effector phenotype in human sensory ganglia. Ann N Y Acad Sci. 2009;1164:300-4. Epub 2009/08/04. doi: NYAS03871 [pii]
10.1111/j.1749-6632.2009.03871.x. PubMed PMID: 19645915.
141. Knickelbein JE, Khanna KM, Yee MB, Baty CJ, Kinchington PR, Hendricks RL. Noncytotoxic lytic granule-mediated CD8+ T cell inhibition of HSV-1 reactivation from neuronal latency. Science. 2008;322(5899):268-71. Epub 2008/10/11. doi: 10.1126/science.1164164. PubMed PMID: 18845757; PubMed Central PMCID: PMC2680315.
142. Linderman JA, Kobayashi M, Rayannavar V, Fak JJ, Darnell RB, Chao MV, et al. Immune Escape via a Transient Gene Expression Program Enables Productive Replication of a Latent Pathogen. Cell Rep. 2017;18(5):1312-23. doi: 10.1016/j.celrep.2017.01.017. PubMed PMID: 28147283; PubMed Central PMCID: PMCPMC5340258.

143. Koyanagi N, Imai T, Shindo K, Sato A, Fujii W, Ichinohe T, et al. Herpes simplex virus-1 evasion of CD8+ T cell accumulation contributes to viral encephalitis. J Clin Invest. 2017;127(10):3784-95. doi: 10.1172/JCI92931. PubMed PMID: 28891812; PubMed Central PMCID: PMCPMC5617679.
144. Imai T, Koyanagi N, Ogawa R, Shindo K, Suenaga T, Sato A, et al. Us3 kinase encoded by herpes simplex virus 1 mediates downregulation of cell surface major histocompatibility complex class I and evasion of CD8+ T cells. PLoS One. 2013;8(8):e72050. doi: 10.1371/journal.pone.0072050. PubMed PMID: 23951282; PubMed Central PMCID: PMCPMC3741198.
145. York IA, Roop C, Andrews DW, Riddell SR, Graham FL, Johnson DC. A cytosolic herpes simplex virus protein inhibits antigen presentation to CD8+ T lymphocytes. Cell. 1994;77(4):525-35. PubMed PMID: 8187174.
146. Sheridan BS, Khanna KM, Frank GM, Hendricks RL. Latent Virus Influences the Generation and Maintenance of CD8+ T Cell Memory. J Immunol. 2006;177(12):8356-64.
147. St Leger AJ, Jeon S, Hendricks RL. Broadening the repertoire of functional herpes simplex virus type 1-specific CD8+ T cells reduces viral reactivation from latency in sensory ganglia. J Immunol. 2013;191(5):2258-65. doi: 10.4049/jimmunol.1300585. PubMed PMID: 23878317; PubMed Central PMCID: PMC3779892.
148. Jeon S, St Leger AJ, Cherpes TL, Sheridan BS, Hendricks RL. PD-L1/B7-H1 regulates the survival but not the function of CD8+ T cells in herpes simplex virus type 1 latently infected trigeminal ganglia. J Immunol. 2013;190(12):6277-86. Epub 2013/05/10. doi: 10.4049/jimmunol.1300582. PubMed PMID: 23656736; PubMed Central PMCID: PMC3679223.
149. Pretell J, Greenfield RS, Tevethia SS. Biology of simian virus 40 (SV40) transplantation antigen (TrAg). V In vitro demonstration of SV40 TrAg in SV40 infected nonpermissive mouse cells by the lymphocyte mediated cytotoxicity assay. Virology. 1979;97(1):32-41. PubMed PMID: 224580.
150. Bowen CD, Renner DW, Shreve JT, Tafuri Y, Payne KM, Dix RD, et al. Viral forensic genomics reveals the relatedness of classic herpes simplex virus strains KOS, KOS63, and KOS79. Virology. 2016;492:179-86. doi: 10.1016/j.virol.2016.02.013. PubMed PMID: 26950505.
151. Smith GA, Enquist LW. A self-recombining bacterial artificial chromosome and its application for analysis of herpesvirus pathogenesis. Proc Natl Acad Sci U S A. 2000;97(9):4873-8. Epub 2000/04/26. doi: 10.1073/pnas.080502497. PubMed PMID: 10781094; PubMed Central PMCID: PMC18325.
152. Tischer BK, von Einem J, Kaufer B, Osterrieder N. Two-step red-mediated recombination for versatile high-efficiency markerless DNA manipulation in Escherichia coli. BioTechniques. 2006;40(2):191-7. PubMed PMID: 16526409.
153. Ramachandran S, Davoli KA, Yee MB, Hendricks RL, Kinchington PR. Delaying the expression of herpes simplex virus type 1 glycoprotein B (gB) to a true late gene alters neurovirulence and inhibits the gB-CD8+ T-cell response in the trigeminal ganglion. Journal of virology. 2010;84(17):8811-20. Epub 2010/06/25. doi: JVI.00496-10 [pii]
10.1128/JVI.00496-10. PubMed PMID: 20573821; PubMed Central PMCID: PMC2919033.
154. Decman V, Kinchington PR, Harvey SA, Hendricks RL. Gamma interferon can block herpes simplex virus type 1 reactivation from latency, even in the presence of late gene

expression. Journal of virology. 2005;79(16):10339-47. doi: 10.1128/JVI.79.16.10339-10347.2005. PubMed PMID: 16051826; PubMed Central PMCID: PMCPMC1182646.
155. Treat BR, Bidula SM, Ramachandran S, St Leger AJ, Hendricks RL, Kinchington PR. Influence of an immunodominant herpes simplex virus type 1 CD8+ T cell epitope on the target hierarchy and function of subdominant CD8+ T cells. PLoS pathogens. 2017;13(12):e1006732. doi: 10.1371/journal.ppat.1006732. PubMed PMID: 29206240; PubMed Central PMCID: PMCPMC5736228.
156. Mueller SN, Heath W, McLain JD, Carbone FR, Jones CM. Characterization of two TCR transgenic mouse lines specific for herpes simplex virus. Immunol Cell Biol. 2002;80(2):156-63. doi: 10.1046/j.1440-1711.2002.01071.x. PubMed PMID: 11940116.
157. Freeman ML, Sheridan BS, Bonneau RH, Hendricks RL. Psychological Stress Compromises CD8+ T Cell Control of Latent Herpes Simplex Virus Type 1 Infections. J Immunol. 2007;179(1):322-8.
158. Yewdell JW. Confronting complexity: real-world immunodominance in antiviral CD8+ T cell responses. Immunity. 2006;25(4):533-43. Epub 2006/10/19. doi: S1074-7613(06)00439-0 [pii]
10.1016/j.immuni.2006.09.005. PubMed PMID: 17046682.
159. Rowe AM, St Leger AJ, Jeon S, Dhaliwal DK, Knickelbein JE, Hendricks RL. Herpes keratitis. Progress in retinal and eye research. 2013;32:88-101. doi: 10.1016/j.preteyeres.2012.08.002. PubMed PMID: 22944008; PubMed Central PMCID: PMC3529813.
160. Stock AT, Jones CM, Heath WR, Carbone FR. CTL response compensation for the loss of an immunodominant class I-restricted HSV-1 determinant. Immunol Cell Biol. 2006;84(6):543-50. Epub 2006/09/08. doi: ICB1469 [pii]
10.1111/j.1440-1711.2006.01469.x. PubMed PMID: 16956387.
161. Zhou X, Ramachandran S, Mann M, Popkin DL. Role of lymphocytic choriomeningitis virus (LCMV) in understanding viral immunology: past, present and future. Viruses. 2012;4(11):2650-69. Epub 2012/12/04. doi: v4112650 [pii]
10.3390/v4112650. PubMed PMID: 23202498; PubMed Central PMCID: PMC3509666.
162. van Velzen M, Jing L, Osterhaus AD, Sette A, Koelle DM, Verjans GM. Local CD4 and CD8 T-cell reactivity to HSV-1 antigens documents broad viral protein expression and immune competence in latently infected human trigeminal ganglia. PLoS pathogens. 2013;9(8):e1003547. Epub 2013/08/24. doi: 10.1371/journal.ppat.1003547. PubMed PMID: 23966859; PubMed Central PMCID: PMC3744444.
163. Holtappels R, Simon CO, Munks MW, Thomas D, Deegen P, Kuhnapfel B, et al. Subdominant CD8 T-cell epitopes account for protection against cytomegalovirus independent of immunodomination. Journal of virology. 2008;82(12):5781-96. Epub 2008/03/28. doi: 10.1128/JVI.00155-08. PubMed PMID: 18367531; PubMed Central PMCID: PMC2395166.
164. Kotturi MF, Scott I, Wolfe T, Peters B, Sidney J, Cheroutre H, et al. Naive precursor frequencies and MHC binding rather than the degree of epitope diversity shape CD8+ T cell immunodominance. J Immunol. 2008;181(3):2124-33. Epub 2008/07/22. PubMed PMID: 18641351; PubMed Central PMCID: PMC3319690.
165. Probst HC, Lagnel J, Kollias G, van den Broek M. Inducible transgenic mice reveal resting dendritic cells as potent inducers of CD8+ T cell tolerance. Immunity. 2003;18(5):713-20. Epub 2003/05/20. PubMed PMID: 12753747.

166. Mott KR, Gate D, Matundan HH, Ghiasi YN, Town T, Ghiasi H. CD8+ T Cells Play a Bystander Role in Mice Latently Infected with Herpes Simplex Virus 1. Journal of virology. 2016;90(10):5059-67. Epub 2016/03/11. doi: 10.1128/JVI.00255-16. PubMed PMID: 26962220; PubMed Central PMCID: PMC4859724.
167. Andreansky SS, Stambas J, Thomas PG, Xie W, Webby RJ, Doherty PC. Consequences of immunodominant epitope deletion for minor influenza virus-specific CD8+-T-cell responses. Journal of virology. 2005;79(7):4329-39. Epub 2005/03/16. doi: 10.1128/JVI.79.7.4329-4339.2005. PubMed PMID: 15767433; PubMed Central PMCID: PMC1061524.
168. Moskophidis D, Zinkernagel RM. Immunobiology of cytotoxic T-cell escape mutants of lymphocytic choriomeningitis virus. Journal of virology. 1995;69(4):2187-93. Epub 1995/04/01. PubMed PMID: 7533851; PubMed Central PMCID: PMC188887.
169. Weidt G, Utermohlen O, Heukeshoven J, Lehmann-Grube F, Deppert W. Relationship among immunodominance of single CD8+ T cell epitopes, virus load, and kinetics of primary antiviral CTL response. J Immunol. 1998;160(6):2923-31. Epub 1998/03/24. PubMed PMID: 9510196.
170. Wolpert EZ, Grufman P, Sandberg JK, Tegnesjo A, Karre K. Immunodominance in the CTL response against minor histocompatibility antigens: interference between responding T cells, rather than with presentation of epitopes. J Immunol. 1998;161(9):4499-505. Epub 1998/10/30. PubMed PMID: 9794374.
171. Kedl RM, Rees WA, Hildeman DA, Schaefer B, Mitchell T, Kappler J, et al. T cells compete for access to antigen-bearing antigen-presenting cells. J Exp Med. 2000;192(8):1105-13. Epub 2000/10/18. PubMed PMID: 11034600; PubMed Central PMCID: PMC2195874.
172. Farrington LA, Smith TA, Grey F, Hill AB, Snyder CM. Competition for antigen at the level of the APC is a major determinant of immunodominance during memory inflation in murine cytomegalovirus infection. J Immunol. 2013;190(7):3410-6. Epub 2013/03/05. doi: 10.4049/jimmunol.1203151. PubMed PMID: 23455500; PubMed Central PMCID: PMC3608834.
173. Borkner L, Sitnik KM, Dekhtiarenko I, Pulm AK, Tao R, Drexler I, et al. Immune Protection by a Cytomegalovirus Vaccine Vector Expressing a Single Low-Avidity Epitope. J Immunol. 2017;199(5):1737-47. Epub 2017/08/05. doi: 10.4049/jimmunol.1602115. PubMed PMID: 28768725.
174. Baur K, Brinkmann K, Schweneker M, Patzold J, Meisinger-Henschel C, Hermann J, et al. Immediate-early expression of a recombinant antigen by modified vaccinia virus ankara breaks the immunodominance of strong vector-specific B8R antigen in acute and memory CD8 T-cell responses. Journal of virology. 2010;84(17):8743-52. Epub 2010/06/12. doi: 10.1128/JVI.00604-10. PubMed PMID: 20538860; PubMed Central PMCID: PMC2919044.
175. Dekhtiarenko I, Jarvis MA, Ruzsics Z, Cicin-Sain L. The context of gene expression defines the immunodominance hierarchy of cytomegalovirus antigens. J Immunol. 2013;190(7):3399-409. Epub 2013/03/06. doi: 10.4049/jimmunol.1203173. PubMed PMID: 23460738.
176. Pudney VA, Leese AM, Rickinson AB, Hislop AD. CD8+ immunodominance among Epstein-Barr virus lytic cycle antigens directly reflects the efficiency of antigen presentation in lytically infected cells. J Exp Med. 2005;201(3):349-60. Epub 2005/02/03. doi: 10.1084/jem.20041542. PubMed PMID: 15684323; PubMed Central PMCID: PMC2213038.
177. Tewari K, Sacha J, Gao X, Suresh M. Effect of chronic viral infection on epitope selection, cytokine production, and surface phenotype of CD8 T cells and the role of IFN-gamma

receptor in immune regulation. J Immunol. 2004;172(3):1491-500. Epub 2004/01/22. PubMed PMID: 14734726.
178. Khan TN, Mooster JL, Kilgore AM, Osborn JF, Nolz JC. Local antigen in nonlymphoid tissue promotes resident memory CD8+ T cell formation during viral infection. J Exp Med. 2016;213(6):951-66. Epub 2016/05/25. doi: 10.1084/jem.20151855. PubMed PMID: 27217536; PubMed Central PMCID: PMC4886364.
179. Ramachandran S, Knickelbein JE, Ferko C, Hendricks RL, Kinchington PR. Development and pathogenic evaluation of recombinant herpes simplex virus type 1 expressing two fluorescent reporter genes from different lytic promoters. Virology. 2008;378(2):254-64. doi: 10.1016/j.virol.2008.05.034. PubMed PMID: 18619637; PubMed Central PMCID: PMCPMC2613845.
180. Sawtell NM, Thompson RL. De Novo Herpes Simplex Virus VP16 Expression Gates a Dynamic Programmatic Transition and Sets the Latent/Lytic Balance during Acute Infection in Trigeminal Ganglia. PLoS pathogens. 2016;12(9):e1005877. doi: 10.1371/journal.ppat.1005877. PubMed PMID: 27607440; PubMed Central PMCID: PMCPMC5015900.
181. Aguilar JS, Devi-Rao GV, Rice MK, Sunabe J, Ghazal P, Wagner EK. Quantitative comparison of the HSV-1 and HSV-2 transcriptomes using DNA microarray analysis. Virology. 2006;348(1):233-41. doi: 10.1016/j.virol.2005.12.036. PubMed PMID: 16448680.
182. Chen X, Schmidt MC, Goins WF, Glorioso JC. Two herpes simplex virus type 1 latency-active promoters differ in their contributions to latency-associated transcript expression during lytic and latent infections. Journal of virology. 1995;69(12):7899-908. PubMed PMID: 7494302; PubMed Central PMCID: PMCPMC189734.
183. Batchelor AH, O'Hare P. Regulation and cell-type-specific activity of a promoter located upstream of the latency-associated transcript of herpes simplex virus type 1. Journal of virology. 1990;64(7):3269-79. PubMed PMID: 2161941; PubMed Central PMCID: PMCPMC249552.
184. Dobson AT, Sederati F, Devi-Rao G, Flanagan WM, Farrell MJ, Stevens JG, et al. Identification of the latency-associated transcript promoter by expression of rabbit beta-globin mRNA in mouse sensory nerve ganglia latently infected with a recombinant herpes simplex virus. Journal of virology. 1989;63(9):3844-51. PubMed PMID: 2474674; PubMed Central PMCID: PMCPMC250978.
185. Mueller SN, Jones CM, Chen W, Kawaoka Y, Castrucci MR, Heath WR, et al. The early expression of glycoprotein B from herpes simplex virus can be detected by antigen-specific CD8+ T cells. Journal of virology. 2003;77(4):2445-51. Epub 2003/01/29. PubMed PMID: 12551982; PubMed Central PMCID: PMC141123.
186. Zhu J, Kang W, Marquart ME, Hill JM, Zheng X, Block TM, et al. Identification of a novel 0.7-kb polyadenylated transcript in the LAT promoter region of HSV-1 that is strain specific and may contribute to virulence. Virology. 1999;265(2):296-307. doi: 10.1006/viro.1999.0057. PubMed PMID: 10600601.
187. Kahan SM, Wherry EJ, Zajac AJ. T cell exhaustion during persistent viral infections. Virology. 2015;479-480:180-93. doi: 10.1016/j.virol.2014.12.033. PubMed PMID: 25620767; PubMed Central PMCID: PMCPMC4424083.
188. Kastenmuller W, Gasteiger G, Gronau JH, Baier R, Ljapoci R, Busch DH, et al. Cross-competition of CD8+ T cells shapes the immunodominance hierarchy during boost vaccination. J Exp Med. 2007;204(9):2187-98. doi: 10.1084/jem.20070489. PubMed PMID: 17709425; PubMed Central PMCID: PMCPMC2118691.

189. Tewalt EF, Grant JM, Granger EL, Palmer DC, Heuss ND, Gregerson DS, et al. Viral sequestration of antigen subverts cross presentation to CD8(+) T cells. PLoS pathogens. 2009;5(5):e1000457. doi: 10.1371/journal.ppat.1000457. PubMed PMID: 19478869; PubMed Central PMCID: PMCPMC2680035.
190. Halford WP, Schaffer PA. ICP0 is required for efficient reactivation of herpes simplex virus type 1 from neuronal latency. Journal of virology. 2001;75(7):3240-9. doi: 10.1128/JVI.75.7.3240-3249.2001. PubMed PMID: 11238850; PubMed Central PMCID: PMCPMC114117.
191. Eickhoff S, Brewitz A, Gerner MY, Klauschen F, Komander K, Hemmi H, et al. Robust Anti-viral Immunity Requires Multiple Distinct T Cell-Dendritic Cell Interactions. Cell. 2015;162(6):1322-37. Epub 2015/08/25. doi: 10.1016/j.cell.2015.08.004. PubMed PMID: 26296422; PubMed Central PMCID: PMC4567961.
192. Brewitz A, Eickhoff S, Dahling S, Quast T, Bedoui S, Kroczek RA, et al. CD8(+) T Cells Orchestrate pDC-XCR1(+) Dendritic Cell Spatial and Functional Cooperativity to Optimize Priming. Immunity. 2017;46(2):205-19. Epub 2017/02/14. doi: 10.1016/j.immuni.2017.01.003. PubMed PMID: 28190711; PubMed Central PMCID: PMC5362251.
193. Feldman LT, Ellison AR, Voytek CC, Yang L, Krause P, Margolis TP. Spontaneous molecular reactivation of herpes simplex virus type 1 latency in mice. Proc Natl Acad Sci U S A. 2002;99(2):978-83. doi: 10.1073/pnas.022301899. PubMed PMID: 11773630; PubMed Central PMCID: PMCPMC117416.
194. Kramer MF, Chen SH, Knipe DM, Coen DM. Accumulation of viral transcripts and DNA during establishment of latency by herpes simplex virus. Journal of virology. 1998;72(2):1177-85. PubMed PMID: 9445016; PubMed Central PMCID: PMCPMC124594.
195. Spivack JG, Fraser NW. Expression of herpes simplex virus type 1 latency-associated transcripts in the trigeminal ganglia of mice during acute infection and reactivation of latent infection. Journal of virology. 1988;62(5):1479-85. PubMed PMID: 2833602; PubMed Central PMCID: PMCPMC253171.
196. Probst HC, Tschannen K, Gallimore A, Martinic M, Basler M, Dumrese T, et al. Immunodominance of an antiviral cytotoxic T cell response is shaped by the kinetics of viral protein expression. J Immunol. 2003;171(10):5415-22. PubMed PMID: 14607945.
197. Blum JS, Wearsch PA, Cresswell P. Pathways of antigen processing. Annu Rev Immunol. 2013;31:443-73. doi: 10.1146/annurev-immunol-032712-095910. PubMed PMID: 23298205; PubMed Central PMCID: PMCPMC4026165.
198. Margolis TP, Sedarati F, Dobson AT, Feldman LT, Stevens JG. Pathways of viral gene expression during acute neuronal infection with HSV-1. Virology. 1992;189(1):150-60. PubMed PMID: 1604806.
199. Husain T, Passini MA, Parente MK, Fraser NW, Wolfe JH. Long-term AAV vector gene and protein expression in mouse brain from a small pan-cellular promoter is similar to neural cell promoters. Gene Ther. 2009;16(7):927-32. doi: 10.1038/gt.2009.52. PubMed PMID: 19458648; PubMed Central PMCID: PMCPMC5473363.
200. Watakabe A, Ohtsuka M, Kinoshita M, Takaji M, Isa K, Mizukami H, et al. Comparative analyses of adeno-associated viral vector serotypes 1, 2, 5, 8 and 9 in marmoset, mouse and macaque cerebral cortex. Neurosci Res. 2015;93:144-57. doi: 10.1016/j.neures.2014.09.002. PubMed PMID: 25240284.
201. Zheng H, Qiao C, Wang CH, Li J, Li J, Yuan Z, et al. Efficient retrograde transport of adeno-associated virus type 8 to spinal cord and dorsal root ganglion after vector delivery in

muscle. Hum Gene Ther. 2010;21(1):87-97. doi: 10.1089/hum.2009.131. PubMed PMID: 19719401; PubMed Central PMCID: PMCPMC2829464.
202. Jacques SJ, Ahmed Z, Forbes A, Douglas MR, Vigenswara V, Berry M, et al. AAV8(gfp) preferentially targets large diameter dorsal root ganglion neurones after both intra-dorsal root ganglion and intrathecal injection. Mol Cell Neurosci. 2012;49(4):464-74. doi: 10.1016/j.mcn.2012.03.002. PubMed PMID: 22425560.
203. Mason MR, Ehlert EM, Eggers R, Pool CW, Hermening S, Huseinovic A, et al. Comparison of AAV serotypes for gene delivery to dorsal root ganglion neurons. Mol Ther. 2010;18(4):715-24. doi: 10.1038/mt.2010.19. PubMed PMID: 20179682; PubMed Central PMCID: PMCPMC2862541.
204. Card JP, Enquist LW, Miller AD, Yates BJ. Differential tropism of pseudorabies virus for sensory neurons in the cat. Journal of neurovirology. 1997;3(1):49-61. PubMed PMID: 9147821.
205. Field HJ, Hill TJ. The pathogenesis of pseudorabies in mice: virus replication at the inoculation site and axonal uptake. J Gen Virol. 1975;26(1):145-8. doi: 10.1099/0022-1317-26-1-145. PubMed PMID: 164517.
206. Martin X, Dolivo M. Neuronal and transneuronal tracing in the trigeminal system of the rat using the herpes virus suis. Brain Res. 1983;273(2):253-76. PubMed PMID: 6311350.
207. Strack AM, Sawyer WB, Hughes JH, Platt KB, Loewy AD. A general pattern of CNS innervation of the sympathetic outflow demonstrated by transneuronal pseudorabies viral infections. Brain Res. 1989;491(1):156-62. PubMed PMID: 2569907.
208. Card JP, Rinaman L, Schwaber JS, Miselis RR, Whealy ME, Robbins AK, et al. Neurotropic properties of pseudorabies virus: uptake and transneuronal passage in the rat central nervous system. J Neurosci. 1990;10(6):1974-94. PubMed PMID: 2162388.
209. Tenser RB, Ressel SJ, Fralish FA, Jones JC. The role of pseudorabies virus thymidine kinase expression in trigeminal ganglion infection. J Gen Virol. 1983;64 (Pt 6):1369-73. doi: 10.1099/0022-1317-64-6-1369. PubMed PMID: 6304238.
210. Williams AL, Bohnsack BL. Neural crest derivatives in ocular development: discerning the eye of the storm. Birth Defects Res C Embryo Today. 2015;105(2):87-95. doi: 10.1002/bdrc.21095. PubMed PMID: 26043871; PubMed Central PMCID: PMCPMC5262495.
211. Yun H, Rowe AM, Lathrop KL, Harvey SA, Hendricks RL. Reversible nerve damage and corneal pathology in murine herpes simplex stromal keratitis. Journal of virology. 2014;88(14):7870-80. doi: 10.1128/JVI.01146-14. PubMed PMID: 24789786; PubMed Central PMCID: PMCPMC4097779.
212. Yun H, Lathrop KL, Hendricks RL. A Central Role for Sympathetic Nerves in Herpes Stromal Keratitis in Mice. Invest Ophthalmol Vis Sci. 2016;57(4):1749-56. doi: 10.1167/iovs.16-19183. PubMed PMID: 27070108; PubMed Central PMCID: PMCPMC4849540.
213. Chung JH, Bell AC, Felsenfeld G. Characterization of the chicken beta-globin insulator. Proc Natl Acad Sci U S A. 1997;94(2):575-80. PubMed PMID: 9012826; PubMed Central PMCID: PMCPMC19555.
214. Pollara G, Speidel K, Samady L, Rajpopat M, McGrath Y, Ledermann J, et al. Herpes simplex virus infection of dendritic cells: balance among activation, inhibition, and immunity. The Journal of infectious diseases. 2003;187(2):165-78. Epub 2003/01/29. doi: 10.1086/367675. PubMed PMID: 12552441.
215. Kruse M, Rosorius O, Kratzer F, Stelz G, Kuhnt C, Schuler G, et al. Mature dendritic cells infected with herpes simplex virus type 1 exhibit inhibited T-cell stimulatory capacity.

Journal of virology. 2000;74(15):7127-36. Epub 2000/07/11. PubMed PMID: 10888653; PubMed Central PMCID: PMC112231.
216. Cotter CR, Nguyen ML, Yount JS, Lopez CB, Blaho JA, Moran TM. The virion host shut-off (vhs) protein blocks a TLR-independent pathway of herpes simplex virus type 1 recognition in human and mouse dendritic cells. PLoS One. 2010;5(2):e8684. Epub 2010/02/23. doi: 10.1371/journal.pone.0008684. PubMed PMID: 20174621; PubMed Central PMCID: PMC2823768.
217. Carpentier M, Lorain S, Chappert P, Lalfer M, Hardet R, Urbain D, et al. Intrinsic transgene immunogenicity gears CD8(+) T-cell priming after rAAV-mediated muscle gene transfer. Mol Ther. 2015;23(4):697-706. doi: 10.1038/mt.2014.235. PubMed PMID: 25492560; PubMed Central PMCID: PMCPMC4395773.
218. Samaniego LA, Neiderhiser L, DeLuca NA. Persistence and expression of the herpes simplex virus genome in the absence of immediate-early proteins. Journal of virology. 1998;72(4):3307-20. PubMed PMID: 9525658; PubMed Central PMCID: PMCPMC109808.